UILU-ENG-2001-2002

CIVIL ENGINEERING STUDIES

Structural Research Series No. 632

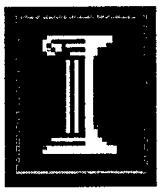

ISSN: 0069-4274

PB2001-107648

IDENTIFICATION OF DAMAGE IN STRUCTURAL SYSTEMS USING MODAL DATA

By

Thanyawat Pothisiri

and

Keith D. Hjelmstad

A report on research

Department of Civil Engineering
University of Illinois at Urbana-Champaign
Urbana, Illinois

April 2001

Identification of Damage in Structural Systems Using Modal Data

By

Thanyawat Pothisiri

and

Keith D. Hjelmstad

A report on research

Department of Civil Engineering
University of Illinois at Urbana–Champaign
Urbana, Illinois

April 2001

Thanyawat Pothisiri

and

Keith D. Hjelmstad

Department of Civil Engineering
University of Illinois at Urbana-Champaign
205 N. Mathews
Urbana, Illinois 61801
U.S.A.

Identification of Damage in Structural Systems Using Modal Data

Printed in the United States of America.
9 8 7 6 5 4 3 2 1

TABLE OF CONTENTS

LIST OF TABLES

LIST OF FIGURES

CHAPTER 1
INTRODUCTION

1.1 Introduction

Damage can occur in civil engineering structures either gradually from operational loading events during their service lives or abruptly from severe loading events during natural disasters. From a serviceability or a safety point of view, it is essential to inspect structures periodically for damaged components. Based on the obtained information of damage, important decisions can be made regarding the rehabilitation of the structure.

During the past few decades, many nondestructive evaluation methods have been developed to assess general integrity of structures that are suspected of damage. These methods can be viewed as either local or global. Local experimental methods are mainly designed for local investigation of structural components. The examples of these methods are visual inspection, ultrasonic or acoustic methods, magnetic field methods, radiographs, thermal field methods and eddy-current methods (Bray and Stanley 1989). Although these techniques are adequate for a detailed local examination, they require that the structural components be readily accessible and that the vicinity of the damage be known a priori. These methods tend to be cost prohibitive for large-scale civil engineering structures. Global methods that use forced structural response as a mean of nondestructively evaluating large structures have been viewed as a much more powerful alternative. Recently, this damage detection technique has drawn considerable attention in the literature (Doebling et al. 1996). The basic idea is that modal properties, such as natural frequencies and mode shapes, are functions of the physical properties of the structure; thus, changes in the physical properties or damage will cause changes in the modal properties. The main problem in global nondestructive evaluation is essentially how to use these changes to extract damage information from a structure. An effective damage identification scheme should be able to determine the damage locations as well as to assess the severity of damage to those parts of the structure.

To develop a useful global damage identification scheme, noise and sparseness of the measured modal data must be taken into account. Measurement noise is inevitable. If one does not

consider noise and its random nature, the damage evaluation algorithm may not provide accurate results. In addition to noise, spatial sparseness of measured modal response presents a main problem in developing a robust damage detection scheme. Most civil engineering structures require a large number of degrees of freedom in a finite element model due to their size and complexity, however, only a limited number of physical locations can be practically measured. It is cost prohibitive or impossible to measure modal displacements at every degree of freedom of the structure.

A robust damage detection scheme should be able to account for noise and sparseness of the measured structural response, to accurately identify multiple damage locations, and to provide some estimate of the severity of damage. The aim of this research is to develop such an algorithm for damage detection with sparse and noisy data and to evaluate the performance of that algorithm using a suite of benchmark numerical simulation problems.

1.2 Literature Review of Damage Identification Algorithms from Modal Response

The idea of using shifts in natural frequency to detect damage in a structural system was introduced in the literature in the late 1960s (Lifshitz and Rotem 1969). The observation that changes in structural properties cause changes in vibration frequencies was the impetus for using modal methods in damage identification. Early attempts were made to model damage mathematically, then the measured frequencies were compared to the predicted frequencies to determine damage (Vandiver 1975; Begg et al. 1976; Wojnarowski et al. 1977; Cawley and Adams 1979). Some researchers have tried to also calculate the damage parameters, e.g., crack length and/or location, from the frequency shift (Adams et al. 1978; Stubbs et al. 1990; Stubbs and Osegueda 1990a; 1990b). However, it is not clear that changes in modal frequencies alone can be used to identify more than the existence of damage in the structure.

In the early 1980s, the use of mode shape information for the location of structural damage was introduced in the literature (West 1984; Yuen 1985). Mode shape derivatives, such as curvature and modal strain energy have also been used to obtain spatial information about structural changes (Pandey et al. 1991; Stubbs et al. 1992; Chance et al. 1994; Dong et al. 1994). The use of mode shape information in addition to the modal frequencies has been shown to be very prom-

ising. Some researchers have used direct comparisons between the measured modal data of the damaged structure and the baseline structure to detect damage (Yuen 1985; Pandey et al. 1991; Yao et al. 1992). These direct methods can be used only in a global manner to identify the existence of damage in a structural system. Further, they cannot provide a quantitative measure of the severity of structural damage.

A popular alternative to the direct comparison methods is based on the perturbation of structural model matrices, such as mass, stiffness, and damping, to reproduce the measured modal response data. These methods solve for the updated matrices by forming a constrained optimization problem based on the structural equations of motion, the nominal model, and the measured data. Comparisons of the updated matrices to the original correlated matrices provide an indication of damage and can be used to quantify the location and extent of damage. Most of these algorithms detect damage by nodal perturbation of structural matrices (Chen and Garba 1988; Agbabian et al. 1991; Zimmerman and Kaouk 1992; Kim and Bartkowicz 1993); thus they have difficulties in defining a structural model due to problems with maintaining mass orthogonality and preserving load path. A more attractive approach is to update the element-level parameters rather than the nodal components of the structural matrices (Hajela and Soeiro 1990a; 1990b; Li and Smith 1994; Shin and Hjelmstad 1994; Doebling 1996). In this approach, damage can be assessed by examining changes in the estimated element parameters for a structural model. However, it may be difficult to justify how much change will indicate damage when measured data are noise-polluted.

Some research attempts have been made to introduce nonlinearity into structural systems as a result of damage (Lin and Ewins 1990; Krawczuk and Ostachowicz 1992; Manson et al. 1993). In this case, the initially linear-elastic structure is considered to behave in a nonlinear manner after the damage has been introduced. These methods are applicable to only the classes of problems where the structural nonlinearity can be incorporated into the structural model.

Another class of damage identification methods is the use of neural network methods to estimate and predict the location and extent of damage in the structure (Kudva et al. 1991; Wu et al. 1992; Manning 1994; Schwarz et al. 1996). Although the non-parametric nature of neural net-

works is useful for complex structures, an excessive amount of measured modal data from different damage cases is required to train the algorithm before it can be used for damage identification.

In summary, recent research attempts have been focused on damage evaluation schemes that use various system identification techniques to evaluate properties of structural models from the measured modal information. The main differences among these methods lie in the choice of the system identification method used to evaluate the structural properties and how damage is defined in the structural model. Still, it remains uncertain which method will perform best in global damage detection of real-life structures.

A number of challenges exist in the practical application of global damage detection using the measured modal response of a structure. The focuses of the present study are on incompleteness of the measured data and the presence of the measurement noise. In general, measurements obtained from a modal testing will be discrete and sparsely distributed over the spatial domain of the test structure. Furthermore, only the first few natural modes will be accessible through testing. In addition, measured data are generally polluted with random measurement errors. These measurement errors can dramatically affect the accuracy of the damage detection results.

A successful damage detection algorithm from the measured response of a structure requires that the measurement noise and the sparseness of data be taken into account. Almost all of the proposed algorithms in the literature failed to consider these crucial aspects in their developments. Shin and Hjelmstad (1994) are among the first few researchers to consider these aspects in developing their damage detection and assessment algorithm. They proposed the adaptive parameter grouping scheme to overcome the sparseness problem by grouping the element constitutive parameters hierarchically in a depth-first search to localize damage. A data perturbation scheme was proposed for an assessment of damage to account for noise in the measurements. The adaptive parameter-grouping scheme has been shown to be successful in dealing with noisy and sparse measured data. However, it has some drawbacks in lack of computational efficiency and can fail to detect multiple damage locations when damage is spatially isolated throughout the entire structure.

1.3 Objective and Scope

The objective of this research is to develop an efficient damage detection and assessment algorithm for structural systems using spatially sparse and noise-polluted modal response. We characterize a structural system by a parameterized finite-element model and we estimate the values of the system parameters using a least-squares minimization of the modal displacement residual. We infer damage from changes in the constitutive properties of elements in the finite element model of the structure. Based on the adaptive parameter-grouping scheme of Shin and Hjelmstad (1994), we propose a new parameter group-updating scheme that has enhanced capability of localizing multiple damage with sparse measurements. The proposed algorithm takes into account the solution multiplicity of the parameter estimation problem arising from using sparse and noisy data. A unified approach, based on the method of random starting points (Hjelmstad 1996) and the optimum sensitivity analysis (Araki and Hjelmstad 2000), for determining solution clustering is used to identify multiple solutions and to assess which of the solutions is the best one. This best solution provides the basis for deciding which parameter group should be subdivided in the parameter group-updating process. In addition, the selective near-optimal measurement set is used as input to the parameter estimation problem to reduce the effect of measurement errors. To account for the effect of noise on the parameter estimates, the data perturbation scheme of Shin and Hjelmstad (1994) is used to generate a Monte Carlo sample of parameter estimates, and damage is assessed by comparing the statistical distribution of the member parameters for the damaged and the associated baseline structure.

We demonstrate the use of the damage detection and assessment algorithm on two example structures: a planar bridge truss and a three-dimensional tower truss. Numerical simulation studies are employed to examine the capabilities of the algorithm in detecting and assessing damage. The numerical simulation procedure is selected over the real case study because our objective is to quantify the performance of the algorithm rather than to plainly illustrate its use. In the simulation process, the measured data are generated by adding proportional random errors to the analytical modal response of a finite-element model of the structure. This allows us to investigate different levels of noise in the measurements by simply varying the amplitude of the imposed random errors.

A number of assumptions have been adopted in the current study. First, a refined finite element model of the structure is defined. Second, the baseline or undamaged properties of the structure are given a priori. Third, the amplitude of noise in the measurements is known. Fourth, the mass of the structure does not change as a result of damage. Finally, damage is regarded as a drop in the stiffness parameter of the structural element, and hence nonlinearity effects are not taken into account.

The manuscript consists of six chapters and one appendix. Chapter 1 is an introduction. A number of research works in the area of global damage detection are briefly summarized in this chapter. Chapter 2 addresses the issues of structural modeling and estimation of system parameters from measured modal response. A new parameter estimation algorithm, based on the output error estimator of Banan and Hjelmstad (1993), is described. The proposed algorithm is adopted as the main tool for estimating structural parameters for the proposed damage detection scheme in Chapter 3. The random starting point scheme of Hjelmstad (1996) is adopted to take into account non-uniqueness of modal parameter estimation arising from using spatially sparse data. In addition, the optimum sensitivity method of Araki and Hjelmstad (2000) is presented to obtain sensitivities of the system parameters in the presence of measurement errors. A heuristic method to select a near-optimal subset of measurement locations is illustrated with a simple numerical example. In Chapter 3, a parameter group-updating scheme is developed to localize damage with sparse data taking into account the non-uniqueness problem of parameter estimation and the sentivity of parameter estimates to the measurement noise. Based on the statistical distributions of the system parameters, a new procedure for assessing the severity of damage is established. In Chapter 4, simulation studies are carried out for a two-dimensional bridge truss. A simulated single component of damage as well as multiple damage cases are investigated for different levels of simulated measurement noise. Through simulation studies, the procedure of detecting and assessing damage is illustrated. In Chapter 5, the damage detection and assessment algorithm is applied to a three-dimensional tower truss. The response of a constructed finite-element model of the tower structure in three spatial dimensions is expected to replicate the true behavior of the structure. Two damage scenarios with different levels of noise are considered in this chapter. Chapter 6 summarizes principal findings obtained from the current study and discusses future

research work. Appendix illustrates the application of the data perturbation scheme of Shin and Hjelmstad (1994) to obtain the sensitivity information for the clusters of solutions around the noise-free multiple solutions to a parameter estimation problem.

CHAPTER 2

STRUCTURAL MODELING AND PARAMETER ESTIMATION

2.1 Introduction

Large or complex structures present a particular challenge in detection of damage – a challenge that is not adequately addressed by local methods, which require a close proximity of the excitation and measurement to the damage site. Global methods, in which the entire structure is excited and the response is measured at certain places, are better suited to the task of locating damage in a complex structure. One such testing environment, usually referred to as modal testing, measures the natural frequencies and mode shapes of the structure using resonant forced vibration (Ewins 1984). Damage detection methods that make use of the measured mode shapes and natural frequencies are called modal methods (Hjelmstad and Shin 1996; Law et al. 1998; Kosmatka and Ricles 1999).

A successful global damage detection method using the measured modal response of a structure requires accurate characterization of the measurement information by the established structural model. In addition, proper inclusion of damage into the selected structural model is essential to simulating the true behavior of the damaged structure. In general, the choice of how damage is incorporated into the analytical model of a structure is inextricably linked to the selection of the model itself. In this chapter, the issues of structural modeling and definition of damage in the structural model are addressed. A new parameter estimation algorithm, using a symmetrized version of the error function of the output-error least squares estimator of Banan and Hjelmstad (1993), is proposed to improve computational efficiency of parameter estimation from measured modal response. The present algorithm will be adopted as the main tool for estimating structural parameters for the damage detection scheme in Chapter 3. The issue of uniqueness of solution to the parameter estimation problem arising from using sparse and noise-polluted measurements is discussed. A random starting point scheme (Hjelmstad 1996) is proposed to search for possible solutions and the optimum sensitivity method (Araki and Hjelmstad 2000) is used to evaluate the

sensitivity of multiple solutions to the measurement noise. To reduce the effect of measurement noise on the estimated parameters, a heuristic method is presented to select a near-optimal subset of degrees of freedom with measurement information as input to the parameter estimation problem. A numerical example is provided to illustrate the method and examine the performance of the proposed algorithm.

2.2 Structural Modeling and Definition of Damage

Damage in a civil engineering structure is typically referred to localized deterioration of some components of the structure. This deterioration can be a complete loss of function in the parts or a degradation of stiffness or mass properties of the structure to some level. In order to assess the severity of damage in a structural system, a qualitative measure of damage in the structural model must be defined.

Mathematically, damage can be defined either in the parameter domain or in the model structure domain. In the model structure domain, explicit modifications are made to the structural model to account for damage. For example, the number of degrees of freedom of the finite element model can be increased by regarding damage as an extra element, the type of damping used in the structural model can be modified after damage, or the structural behavior can be changed from linear to non-linear as a result of damage. These approaches are not well suited to the damage detection problem in large or complex structures due to the difficulties in modifying the structural model. Further, they are limited to only a few classes of problems where the analytical model of the structure can be directly modified to account for damage. On the other hand, in the parameter domain damage can be regarded as changes of the structural model parameters, such as a reduction in stiffness, an increase or a decrease in inertia, and a modification to the damping coefficients. Because no modification to the structural model is required for this approach, it is more attractive to the task of global damage detection.

The selection of an appropriate parameter estimation algorithm is also of equal importance to how damage is regarded in the structural model. The parameterization of the structural model is implicitly determined by the parameter estimation method used to evaluate the structural parameters from the measured response of the structure. Generally, a parameter estimation algo-

rithm identifies properties of a structure from the measured data either by estimating the components of the structural matrices associated with the structural degrees of freedom or by estimating the element constitutive parameters of the model structure. Since damage is commonly associated with the structural element behavior, the latter approach is more attractive because changes in the estimated parameters are often a direct indication of damage.

Let us assume that a structure can be characterized by a linear finite element model with N_d degrees of freedom. The modal response of the structure is determined by the contribution of the element constitutive parameters in the stiffness matrix **K** and the material density properties composing the mass matrix **M**, respectively. The linear stiffness **K** of the structure is parameterized by N_p constitutive parameters **x**, each of which can change as a result of damage. We assume that the mass **M** of the structure does not change during the damage process and can be viewed as constant. Damage can be inferred from a drop in an element constitutive parameter value between two time-separated inferences as shown in Figure 2.1. From this notion of damage, the baseline properties of the structure can be regarded as a set of parameters associated with an undamaged or a lesser damaged state of the structure. In the current study we assume that the baseline values of parameters are known in advance (for example, from a previous application of this same procedure).

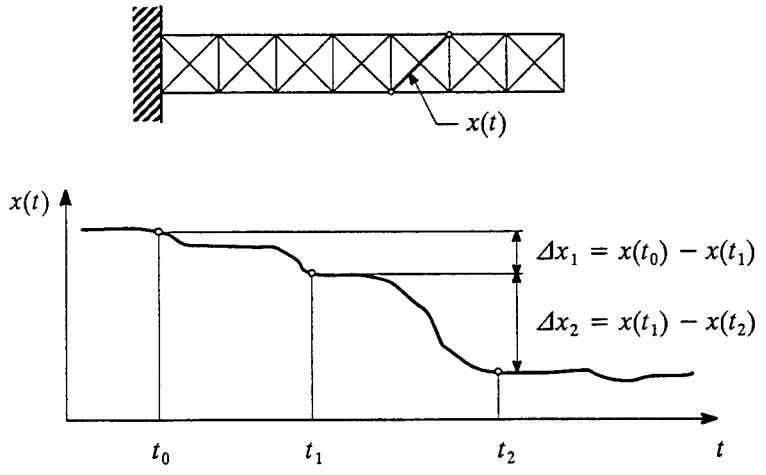

Figure 2.1 The definition of damage as a drop in element constitutive paramater value.

The truss elements in Figure 2.1 is usually modeled with a single stiffness parameter (i.e., the axial stiffness). A drop in the axial stiffness parameter of a truss element directly indicates damage in the element. However, the situation can be complicated for other types of structural elements with multiple modes of deformation. It may be important to represent each mode of deformation separately using multiple stiffness parameters since it is not clear which mode of behavior of a structural element governs the structural response of a damaged structure. In the literature, some researchers determine damage as a reduction in the value of a selected dominant parameter in the structural element, while others detect damage by investigating the changes of all available parameters. Shin and Hjelmstad (1994) observed from simulation studies that the use of the flexural stiffness parameter in a Timoshenko beam element to represent damage produced a more reliable damage detection result than using the shear stiffness parameter. Based on the results of their study, it was concluded that a single dominant stiffness parameter can be used to accurately identify damage in a structural member. The key task is to decide which parameter, of all the available ones, will best represent damage in the structural model. This aspect of the problem is not included in the scope of the present study.

2.3 A Parameter Grouping Scheme

The number of unknown constitutive parameters in a parameterized finite element model of a large or complex structure can be large compared to the available measured information. One approach to reduce the number of unknowns is to use the substructuring method (Lim 1990; Natke 1989). However, there are several drawbacks to this approach; for example, a substructure must be a connected region of the structure, and the subregion stiffness may comprise stiffnesses of varying characters. An alternative approach is to group similar parameters together without changing the finite element model of the structure (Hjelmstad et al. 1990). This technique has the merit of curing the two problems of the substructure method. In addition, the parameter grouping approach is better suited for civil engineering structures whose models are typically composed of a limited number of different element types, and thus can be parameterized by a small number of parameter groups.

Let us assume herein that each of the elements in the structural model can be assigned to one of the parameter groups $\{\Omega_1, \Omega_2, ..., \Omega_{N_g}\}$ where N_g is the number of different parameter groups in the model. Let us further assume that a group of elements Ω_k can be characterized by a set of stiffness parameters $\mathbf{x}_k = \{x_1^k, x_2^k, ..., x_{N_k}^k\}$ such that the subset of parameters associated with element $m \in \Omega_k$ are $\mathbf{x}_k$. The set of parameters $\mathbf{x}_k$ contains N_k parameters. The parameter x_i^k is the ith parameter in group Ω_k. This representation accomodates the possibility of multiple stiffness parameters in each structural element (e.g., Young's modulus and Poisson's ratio for linear elastic solid, the bending and shear stiffness for beams). It should be noted that each parameter group can comprise only the structural elements of the same type.

Based on the parameter grouping scheme, the linear stiffness matrix of the model can be written as (Shin and Hjelmstad 1994)

$$\mathbf{K}(\mathbf{x}) = \mathbf{K}_o + \sum_{k=1}^{N_g} \sum_{m \in \Omega_k} \mathbf{K}_m(\mathbf{x}_k) \tag{2.1}$$

where $\mathbf{K}_o$ is the fixed part of the stiffness matrix associated with elements having parameters with known values and $\mathbf{K}_m(\mathbf{x}_k)$ is the stiffness matrix of element m having parameters from the group Ω_k. The element stiffness matrix can often be decomposed as

$$\mathbf{K}_m(\mathbf{x}_k) = \sum_{i=1}^{N_k} f_i^m(\mathbf{x}_k)\mathbf{G}_i^m \tag{2.2}$$

where $f_i^m(\mathbf{x})$ is the (possibly nonlinear) constitutive parameter function, and $\mathbf{G}_i^m$ is the kernel matrix for the ith stiffness type of element m. The element kernel matrices essentially contain the geometrical information of the structural element, and are independent of the element constitutive parameters.

The total number of stiffness parameters N_p in the structural model can be computed as

$$N_p = \sum_{k=1}^{N_g} N_k \tag{2.3}$$

where, as mentioned earlier, N_k is the number of different stiffness types for the kth parameter group, which depends on the type of elements comprising that group.

2.4 Parameter Estimation from Measured Modal Response

One of the key issues in the development of the current damage detection algorithm is the selection of the parameter estimation scheme from the measured modal response of a structure. In this section, we derive a symmetrized version of the error function of the output-error least squares estimator of Banan and Hjelmstad (1993) to improve computational efficiency of modal parameter estimation. The output error estimator is chosen among other methods because of its ability to handle spatially sparse data sets without sacrificing computional efficiency. In addition, the output error estimator has an acceptable amount of bias for a wide range of measurement noise. The output error estimator is cast as the following least-squares optimization problem

$$\underset{\mathbf{x} \in \Re^{N_p}}{\text{Minimize}} \quad J(\mathbf{x}) = \frac{1}{2}\sum_{i=1}^{N_m} \delta_i \| \mathbf{e}_i(\mathbf{x}) \|^2 \tag{2.4}$$

where δ_i is the weight factor for the ith modal case and N_m is the number of modes with measured natural frequencies and mode shapes. This problem is often solved as a constrained minimization with bounding values on the parameters. Different estimators can be defined within the context of least-squares by using different definitions of the error term $\mathbf{e}_i(\mathbf{x})$, which represents either the force imbalance or displacement residual. In the current study, the output error $\mathbf{e}_i(\mathbf{x})$ is defined as the difference between the measured and equivalent modal displacements at the sampling locations. Free undamped vibrational response of a structure gives rise to the generalized eigenvalue problem

$$\mathbf{K}(\mathbf{x})\boldsymbol{\phi}_i = \lambda_i \mathbf{M}\boldsymbol{\phi}_i \tag{2.5}$$

in which λ_i and $\boldsymbol{\phi}_i$ represent the eigenvalue (the square of the natural frequency) and the eigenvector (mode shape) for the ith vibration mode.

Let us assume that the first N_m natural frequencies and natural modes can be obtained from a modal test. For each mode, we assume that the frequency is measured accurately and that the mode shape is sampled at certain discrete locations. We assume that these measurement locations correspond with degrees of freedom of the finite element model of the structure. In particular, we define the set of degrees of freedom associated with measurement locations on the test struc-

ture as $\hat{\aleph}$ and we define the set of remaining degrees of freedom as $\overline{\aleph}$. Moreover, we denote the number of measured and unmeasured degrees of freedom as $\hat{N}_d$ and $\overline{N}_d$, respectively. As such, we can partition the measured eigenvector and the structural system matrices based on these two sets. To wit, we reorder and partition the ith eigenvector as

$$\tilde{\boldsymbol{\phi}}_i \equiv \mathbf{P}\boldsymbol{\phi}_i = \begin{bmatrix} \hat{\boldsymbol{\phi}}_i \\ \overline{\boldsymbol{\phi}}_i \end{bmatrix} \tag{2.6}$$

where $\mathbf{P}$ is a column permutation of the identity matrix, $\hat{\boldsymbol{\phi}}_i$ and $\overline{\boldsymbol{\phi}}_i$ are the submatrices of the eigenvector components associated with the measured and unmeasured degrees of freedom, respectively. In addition, the structural matrices can be reordered as

$$\tilde{\mathbf{K}} \equiv \mathbf{P}\mathbf{K}\mathbf{P}^{\mathrm{T}}; \text{ and } \tilde{\mathbf{M}} \equiv \mathbf{P}\mathbf{M}\mathbf{P}^{\mathrm{T}} \tag{2.7}$$

Let us partition the reordered mass matrix as follows

$$\tilde{\mathbf{M}} = \begin{bmatrix} \tilde{\mathbf{M}}_{11} & \tilde{\mathbf{M}}_{12} \\ \tilde{\mathbf{M}}_{21} & \tilde{\mathbf{M}}_{22} \end{bmatrix} \tag{2.8}$$

where $\tilde{\mathbf{M}}_{i1}$ is the portion of the mass matrix associated with the measured degrees of freedom of the structural model and $\tilde{\mathbf{M}}_{i2}$ is the part associated with unmeasured degrees of freedom. We define the partitioned mass matrices as

$$\overline{\mathbf{M}} \equiv \begin{bmatrix} \mathbf{0} & \tilde{\mathbf{M}}_{12} \\ \tilde{\mathbf{M}}_{21} & \tilde{\mathbf{M}}_{22} \end{bmatrix}; \text{ and } \hat{\mathbf{M}} \equiv \begin{bmatrix} \tilde{\mathbf{M}}_{11} \\ \mathbf{0} \end{bmatrix} \tag{2.9}$$

With the above definitions, we introduce the matrix $\mathbf{B}_i(\mathbf{x}) \equiv \tilde{\mathbf{K}}(\mathbf{x}) - \lambda_i\overline{\mathbf{M}}$. A straightforward manipulation of equation (2.5) yields the equivalent expression

$$\mathbf{B}_i(\mathbf{x})\tilde{\boldsymbol{\phi}}_i = \lambda_i\hat{\mathbf{M}}\hat{\boldsymbol{\phi}}_i \tag{2.10}$$

The right hand side of the above equation involves only the measured response $\hat{\boldsymbol{\phi}}_i$ rather than a complete response vector. Also, it should be noted that the proposed $\mathbf{B}_i(\mathbf{x})$ is symmetric, which

is different from the definition of Banan and Hjelmstad (1993). With these definitions, a measure of error for the output error estimator can be defined as

$$\mathbf{e}_i(\mathbf{x}) \equiv \hat{\boldsymbol{\phi}}_i - \lambda_i \mathbf{Q}\mathbf{B}_i^{-1}(\mathbf{x})\hat{\mathbf{M}}\hat{\boldsymbol{\phi}}_i \tag{2.11}$$

where the boolean matrix $\mathbf{Q}$ extracts the components of the response vector associated with measured degrees of freedom from the complete eigenvector by the relationship of $\hat{\boldsymbol{\phi}}_i = \mathbf{Q}\boldsymbol{\phi}_i$.

For the above parameter estimation problem, an index of identifiability can be defined as

$$\beta \equiv \frac{N_m \hat{N}_d}{N_p} \tag{2.12}$$

This index represents the ratio of available data to the unknowns. The parameter estimates are completely unreliable if $\beta < 1$. The parameter estimation is possible if $\beta \geq 1$. The chance that the estimates will be reliable increases with the value of β. The constrained least-squares problem (2.4) can be solved using a recursive quadratic programming algorithm. The computations can be based on the Gauss-Newton approximation of the Hessian of the objective to avoid computing second derivatives of the error function $\mathbf{e}_i(\mathbf{x})$. The implementation of the algorithm is described in detail by Banan and Hjelmstad (1993).

Conventional parameter estimation schemes using a simple minimization of equation (2.4) can give rise to non-uniqueness of solutions when the measured data are spatially sparse and noise-polluted. The technique of regularization has been employed to overcome the problem of non-uniqueness of solution to the parameter estimation problem from measured data (Ge and Soong 1998; Yeo et al. 2000). In the regularization technique, the original error function is modified by adding a positive definite regularization function. The relative magnitude of the regularization function to the primary error function is adjusted by the regularization factor, which must be determined during the minimization process for a consistent regularization effect. In general, the regularization function represents a penalty term for limiting the values of the estimated parameters to lie in the vicinities of certain nominal parameters. This method assumes that the desired parameters are close to the nominal parameters, and that there are no spurious solutions in the neighborhood of the correct solution. For many applications this assumption is not tenable,

for example, in damage detection problems one cannot assume that the parameters of the damaged model are necessarily closed to the values of the baseline parameters.

2.5 Non-uniqueness of Modal Parameter Estimation

The structural parameter estimation from measured modal response using an output error least-squares estimator can give rise to multiple solutions if the data are spatially sparse (Hjelmstad 1996). Generally, the data are called sparse if the measurement locations are few, $\hat{N}_d/N_d \ll 1$, if the number of measured modes is few, $N_m/N_d \ll 1$, or if both are few, $N_m\hat{N}_d/N_d^2 \ll 1$ (Hjelmstad and Shin 1997). The extra solutions in the parameter estimation problem are local minima of the parameter estimation objective function and are probably extraneous. The existence of multiple solutions to the parameter estimation problem complicates the damage detection process since successful isolation of damaged elements depends upon identifying the correct solution from among the many choices. Ignoring the possibility of solution multiplicity leads either to erroneous damage locations or else the algorithm fails to converge at all.

In the literature, only a few articles have been devoted to the question of uniqueness of solution in the structural parameter estimation problem. Some of the proposed algorithms address the problem of uniqueness by finding the solution nearest to a set of nominal model parameters. Such methods assume that the desired parameters are close to the nominal parameters, and that there are no spurious solutions in the neighborhood of the correct solution. These assumptions are not tenable for global damage detection since the parameter estimates of the damaged structural model are not necessarily close to the values of the parameters associated with the baseline structure. One approach to the non-uniqueness problem is to use a random starting point scheme in conjunction with the objective minimization algorithm to find all of the multiple minima of the parameter estimation problem (Hjelmstad 1996). With a sufficiently large sample of starting points, one can assess the multiplicity of solutions with confidence.

Hjelmstad (1996) observed that for noise-free simulated measurements the correct solution can generally be distinguished from the extraneous solutions by a considerably larger and deeper basin of attraction, which is indicated by a larger fraction of solutions attracted from the random starting points and a lower average value of the objective function. The situation is more compli-

cated for noise-polluted data, where parameter estimates are scattered due to noise. The identified multiple solutions exhibit different levels of sensitivity to random noise for different patterns of measurement. Further, the sensitivity of the parameter estimates to noise in the data depends upon the number and density of solutions to the parameter estimation problem. Nevertheless, the study showed that there is a clear connection between multiple solutions associated with noise-free data and the distinct clusters of results with noisy data.

In the following sections, we present a general framework for using an error sensitivity analysis of parameter estimates to improve the outcome of parameter estimation from measured modal response. In particular, we show how the random starting point method can be used to generate populations of parameter estimates for a given parameter estimation problem and how clustering of the population can be used to identify the correct solution to the parameter estimation problem. Based on the study of Hjelmstad (1996), the correct solution is identified using the value of the parameter estimation objective function associated with the mean of the parameter estimates for each solution cluster. The method generalizes well to problems for which visualization tools are not useful (i.e., any problem with more than two or three parameters). A heuristic method is presented to reduce the effect of the measurement noise on the parameter estimation results by selecting a subset of degrees of freedom with measurement information to be used as input to the parameter estimation problem. The eigenvalues of the covariance matrix of parameter estimates associated with the identified solution are used to determine which measurement location should be dropped at each level of the measurement selection process. The proposed algorithm will later be incorporated into the damage detection and assessment scheme in Chapter 3.

2.5.1 Identification of Multiple Solutions

The solution of the parameter estimation problem (2.4) depends upon the topography of the objective function $J(\mathbf{x})$. When the measured data are spatially sparse, the objective function is usually nonlinear and multiple minima are possible. Each local minimum represents a candidate solution to the parameter estimation problem. The final outcome of the iterative parameter estimation process depends on the initial guess of parameters $\mathbf{x}^0$ that must be specified to start the iteration. Each starting point converges to the minimum within its basin of attraction (that is the

definition of the basin of attraction). The situation is illustrated in Figure 2.2 for a three-dimensional parameter space. In this illustration, we assume that there are two solutions, $\mathbf{x}_A$ and $\mathbf{x}_B$. From the seven starting points $\{\mathbf{x}_1^0, \mathbf{x}_2^0, ..., \mathbf{x}_7^0\}$, five of them converge to one or the other of the two solutions while starting points $\mathbf{x}_2^0$ and $\mathbf{x}_5^0$ get bound at the constraints $x_3 = 0$ and $x_2 = x_2^U$, respectively. Also, in the illustration the shaded area inside the rectangular paralellepiped represents a feasible domain of the parameter estimates determined by the lower bounds $\{x_1^L, x_2^L, x_3^L\}$ and the upper bounds $\{x_1^U, x_2^U, x_3^U\}$, respectively. These bounds must be selected properly in order for the parameter estimates to make any physical sense. Often, parameter values can be set to zero as natural lower bounds. The upper bounds, however, must be selected so that they provide sufficiently large domain for possible solutions to the parameter estimation problem.

Since it is impossible to know in advance the number of solutions for equation (2.4) and their distribution, we need an algorithm that can extract as much useful information as possible from our parameter estimation problem. We implemented the random starting point scheme proposed by Hjelmstad (1996). The idea of creating random points on an x-y plane is extrapolated to an N_p-dimensional parameter space to accommodate a general N_p-parameter model. In the current algorithm, a sample of N_r random starting points $\{\mathbf{x}_1^0, \mathbf{x}_2^0, ..., \mathbf{x}_{N_r}^0\}$ is generated. Each of these

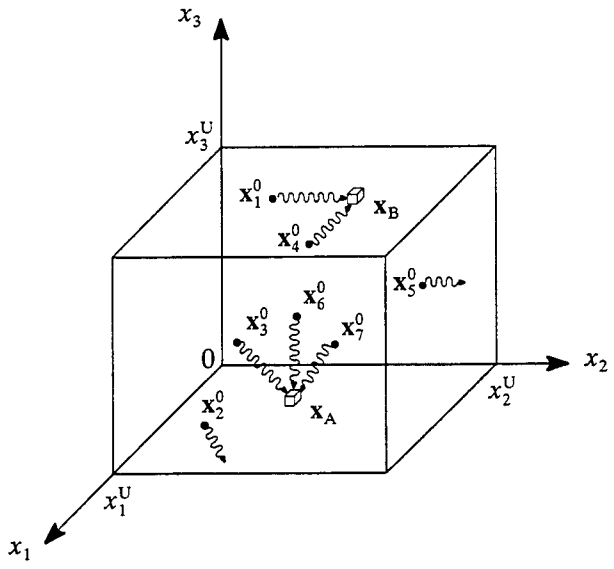

Figure 2.2 The result of parameter estimation from different starting points.

starting points will converge to a solution that is a member of a subset of all possible solutions to the parameter estimation problem. To assess the multiplicity of solutions with confidence, one must use a sufficiently large sample of starting points.

In this study we assume prior knowledge of the baseline structural model. In addition, we accept the notion of damage as a reduction of parameter values from the baseline values. As such, we will select our starting points from within a bounded region centered at the point associated with the known baseline parameters, $\hat{\mathbf{x}}^*$. In particular, to avoid starting from points that are likely to get stuck at bounding constraints, the ith starting point is chosen to lie within a hyper-ellipsoid centered at $\hat{\mathbf{x}}^*$. To wit, let $\mathbf{x}_i^0$ denotes the ith starting point in the N_p-dimensional parameter space. The ith starting point is allowed into the sample only if

$$(\mathbf{x}_i^0 - \hat{\mathbf{x}}^*)^T \mathbf{A} (\mathbf{x}_i^0 - \hat{\mathbf{x}}^*) \leqslant 1 \tag{2.13}$$

where $\mathbf{A}$ denotes a scaling matrix, which is defined as $\mathbf{A} \equiv \text{diag}[1/\hat{x}_1^{*2} \quad 1/\hat{x}_2^{*2} \quad \ldots \quad 1/\hat{x}_{N_p}^{*2}]$. The idea of restricting the starting parameter values is shown schematically for a three-dimensional parameter space in Figure 2.3 where $\hat{x}_1^*$, $\hat{x}_2^*$, and $\hat{x}_3^*$ are the three components of the vector of baseline parameters. In this figure, the shaded area inside the rectangular paralellepiped bounded at $\{x_1^U, x_2^U, x_3^U\}$ represents the feasible domain of the parameter estimates.

2.5.2 Measurement Error Sensitivity Analysis of Multiple Solutions

The multiplicity of solutions in modal parameter estimation is further complicated by the presence of noise in the measured data. Typically, different sets of noisy measurements will yield different outcomes of parameter estimation due to the effect of noise on the topography of the objective function $J(\mathbf{x})$. To account for the sensitivity of system parameters due to noise, Shin and Hjelmstad (1994) adopted a data perturbation scheme to generate a Monte Carlo sample of parameter estimates by adding a random perturbation with known statistical properties to the measured data. To wit, the jth component of the perturbed eigenvector is calculated from the jth component of the ith measured eigenvector as

$$\tilde{\phi}_{ij} = \hat{\phi}_{ij}(1 + \alpha \eta_{ij}) \tag{2.14}$$

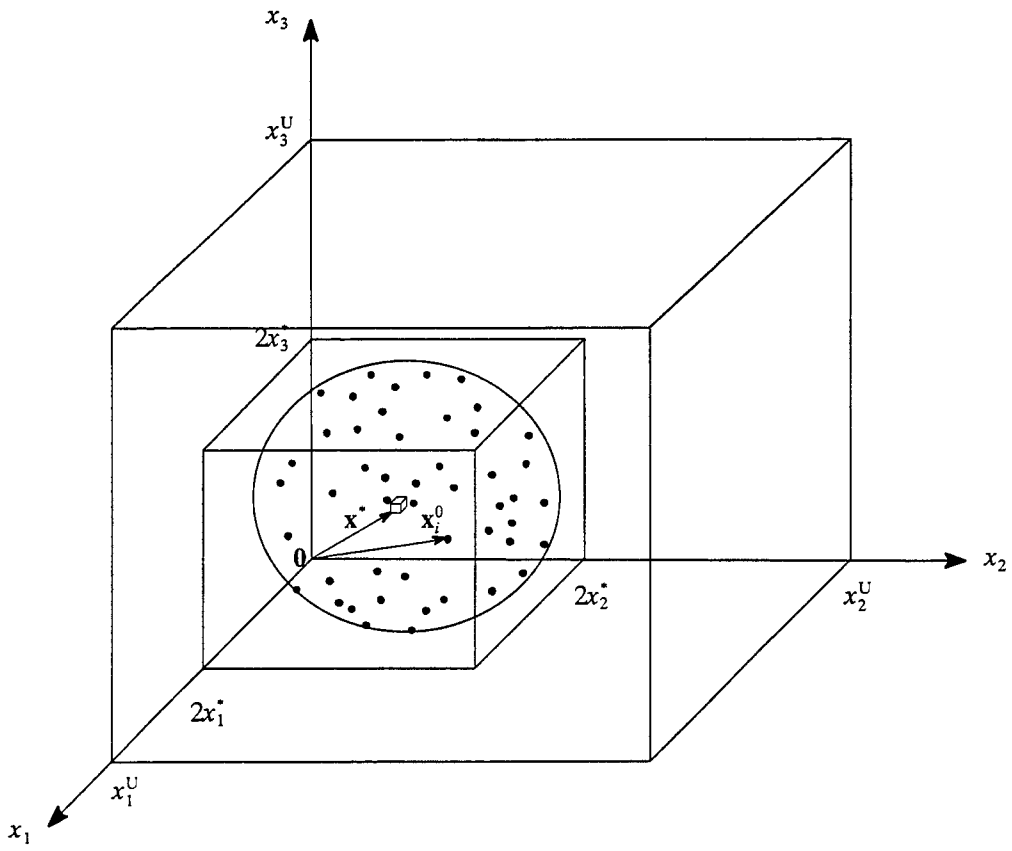

Figure 2.3 The schematic representation of the simulated random starting points.

where η_{ij} is a uniform random variate in the range $[-1, 1]$. The noise amplitude α can be varied to study the sensitivity of parameter estimates to noise in the measured data. It should be noted that the data perturbation scheme can be applied to obtain the sensitivity information for each of the multiple solutions identified from the random starting point scheme by using the individual solution as a fixed starting point for each perturbed data set. In addition, since each perturbation iteration requires one execution of the parameter estimation algorithm, the Monte Carlo approach can be computationally intensive as the number of perturbation iterations becomes large. A numerical example in which the Monte Carlo method is applied to simulate the sensitivity of noise-free solutions to the measurement noise is shown in Appendix.

In the Monte Carlo method, once a sample of solution points has been created using the random starting point and the data perturbation schemes, the correct solution must be identified

based upon the available solutions in the sample. In general, each of these solution points will be clustered in the vicinities of the noise-free solutions as shown in Figure 2.4 for a three-dimensional parameter space. In this figure we assume that four solution points $\{\mathbf{x}_A, \mathbf{x}_B, \mathbf{x}_C, \mathbf{x}_D\}$ have been identified from the random starting points. The groups of solutions essentially represent clustering of local minima of the perturbed objective functions. The distribution of the solution points within each clustered location indicates the sensitivity of a local minimum of the objective function $J(\mathbf{x})$ due to the random perturbation. As such, each individual cluster can be regarded as a set of perturbed solutions to the parameter estimation problem.

In general, the correct set, or cluster, of solutions can be distinguished from the extraneous ones by a considerably larger and deeper basin of attraction. The latter condition is indicated by a lower averaged objective function. A precise set of parameter estimates is the one that is insensitive to noise and is indicated by the compactness of the cluster. For a simple structural model with two or three parameters, the measure of compactness can be obtained directly from the plot of the solution points on a three-dimensional parameter space. However, this is not the case for an N_p-parameter model where such a plot is not feasible. As such, a mathematical description of a cluster is required.

One can use the statistical properties of the solutions inside a cluster to identify its shape. For example, the mean and standard deviation can be used to measure bias and spread of the solutions

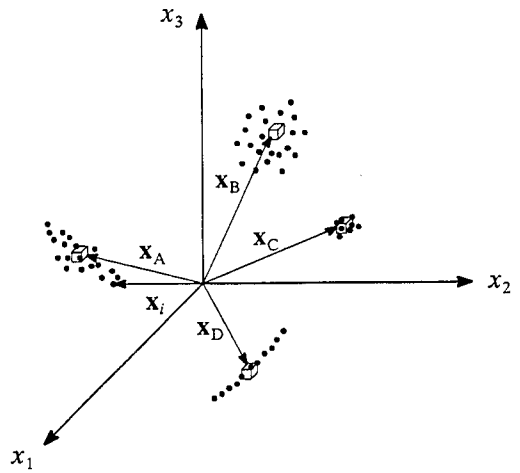

Figure 2.4 Noisy solution points in three-dimensional parameter space.

due to the data perturbation, respectively. However, as illustrated in Figure 2.5 for a two-parameter case, the standard deviation may not provide sufficient information to identify the correct shape of a cluster. On the other hand, the eigenvalues of the covariance matrix of the estimated parameters provide a more accurate basis for estimating the appearance of a cluster. The covariance matrix of parameters for cluster A can be computed as

$$\mathbf{R}^{x_A} = \left\{ \frac{1}{N_A} \sum_{i=1}^{N_A} \mathbf{x}_i \otimes \mathbf{x}_i \right\} - \frac{1}{N_A} \sum_{i=1}^{N_A} \mathbf{x}_i \otimes \frac{1}{N_A} \sum_{i=1}^{N_A} \mathbf{x}_i \tag{2.15}$$

where N_A is the number of solutions belonging to the cluster A and $\otimes$ indicates the tensor product. In general, the parameter estimates are accurate if the eigenvalues of the covariance matrix are small.

As previously mentioned, the Monte Carlo method is computationally expensive because the nonlinear optimization process is repeated many times. Alternatively, one can obtain the sensitivity of parameter estimates to random perturbation by using the optimum sensitivity approach (Araki and Hjelmstad 2000). In this method, the mean and covariance of system parameters are estimated using the optimum sensitivity derivatives, which can be computed by direct differentiation of the Kuhn-Tucker optimality criterion. As such, the method is computationally effiencient compared with the Monte Carlo approach. In addition, this approach is generally more efficient than the finite difference approach used by Sanayei et al. (1992), and does not require the

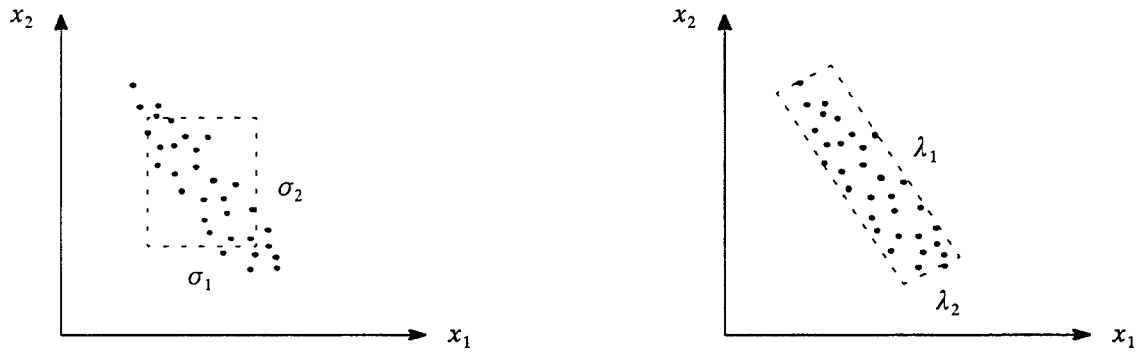

Figure 2.5 Two different statistical descriptions of a cluster. σ_i, Standard deviations; λ_i, eigenvalues.

assessment of numerical errors. However, the optimum sensitivity method may be unreliable when the system output-system parameters relation is highly nonlinear, in which case the Monte Carlo method is more robust. In the current study, we implement the optimum sensitivity method to determine the sensitivity of the parameter estimation solutions with respect to the data perturbation scheme.

Let us define a measurement vector of mode shapes as $\hat{\mathbf{\Phi}}^{\mathrm{T}} \equiv \{\hat{\phi}_1^{\mathrm{T}}, \hat{\phi}_2^{\mathrm{T}}, ..., \hat{\phi}_{N_m}^{\mathrm{T}}\}$ such that $\hat{\Phi}_k$ denotes the kth component of the vector $\hat{\mathbf{\Phi}}$ in which $k = 1, 2, ..., N_m\hat{N}_d$. Based on the perturbation method (Liu et al. 1986; Papadimitriou et al. 1997), let the mean and covariance of the perturbed measurements be computed as

$$\hat{\mathbf{\Phi}} \equiv E[\tilde{\mathbf{\Phi}}] \tag{2.16}$$

$$\mathbf{R}^{\Phi} \equiv E[(\tilde{\mathbf{\Phi}} - \hat{\mathbf{\Phi}}) \otimes (\tilde{\mathbf{\Phi}} - \hat{\mathbf{\Phi}})] \tag{2.17}$$

where $\tilde{\mathbf{\Phi}}$ represents a perturbed vector of the measured mode shapes. For a certain solution $\mathbf{x}_{\mathrm{A}}$ formerly determined using the random starting points, we can estimate the mean $\bar{\mathbf{x}}_{\mathrm{A}}$ and covariance $\mathbf{R}^{x_{\mathrm{A}}}$ of parameter estimates due to the measurement perturbation using the following approximation (Araki and Hjelmstad 2000)

$$\bar{\mathbf{x}}_{\mathrm{A}} \equiv E[\mathbf{x}_{\mathrm{A}}(\tilde{\mathbf{\Phi}})] \approx \mathbf{x}_{\mathrm{A}}(\hat{\mathbf{\Phi}}) + \frac{1}{2}\sum_{k=1}^{N_m\hat{N}_d}\sum_{l=1}^{N_m\hat{N}_d} \mathbf{x}_{\mathrm{A},kl}(\hat{\mathbf{\Phi}})R_{kl}^{\Phi} \tag{2.18}$$

$$\mathbf{R}^{x_{\mathrm{A}}} \equiv E[(\mathbf{x}_{\mathrm{A}}(\tilde{\mathbf{\Phi}}) - \bar{\mathbf{x}}_{\mathrm{A}}(\tilde{\mathbf{\Phi}})) \otimes (\mathbf{x}_{\mathrm{A}}(\tilde{\mathbf{\Phi}}) - \bar{\mathbf{x}}_{\mathrm{A}}(\tilde{\mathbf{\Phi}}))] \tag{2.19}$$

$$\approx \sum_{k=1}^{N_m\hat{N}_d}\sum_{l=1}^{N_m\hat{N}_d} \mathbf{x}_{\mathrm{A},k}(\hat{\mathbf{\Phi}}) \otimes \mathbf{x}_{\mathrm{A},l}(\hat{\mathbf{\Phi}})R_{kl}^{\Phi}$$

In the above equations, the first and second-order optimum sensitivity derivatives are indicated by $\mathbf{x}_{\mathrm{A},k} \equiv \partial\mathbf{x}_{\mathrm{A}}/\partial\hat{\Phi}_k$ and $\mathbf{x}_{\mathrm{A},kl} \equiv \partial^2\mathbf{x}_{\mathrm{A}}/\partial\hat{\Phi}_k\partial\hat{\Phi}_l$, respectively. These derivatives can be obtained by solving systems of linear equations consisting of the gradient terms of the error function $\mathbf{e}_i(\mathbf{x})$ as defined in equation (2.11). If the random perturbation of amplitude a is determined in accord with equation (2.14), equations (2.18) and (2.19) can be rewritten as

$$\bar{\mathbf{x}}_{\mathrm{A}}(\alpha) = \mathbf{x}_{\mathrm{A}}(\hat{\boldsymbol{\Phi}}) + \frac{\alpha^2}{6}\sum_{k=1}^{N_m\hat{N}_d} \mathbf{x}_{\mathrm{A},kk}(\hat{\boldsymbol{\Phi}})\hat{\Phi}_k^2 \tag{2.20}$$

$$\mathbf{R}^{x_A}(\alpha) = \frac{\alpha^2}{3}\sum_{k=1}^{N_m\hat{N}_d} \mathbf{x}_{\mathrm{A},k}(\hat{\boldsymbol{\Phi}}) \otimes \mathbf{x}_{\mathrm{A},k}(\hat{\boldsymbol{\Phi}})\hat{\Phi}_k^2 \tag{2.21}$$

The calculation of mean and covariance of parameter estimates associated with the individual solution can be repeated for each of the clusters around the noise-free multiple solutions previously identified from the random starting point scheme. Nevertheless, we focus our attention on the correct set, or cluster, of solutions to the parameter estimation problem that corresponds to the cluster of global minima of the objective function $J(\mathbf{x})$ as defined in equation (2.4). In particular, we calculate the objective function $J(\bar{\mathbf{x}})$ that corresponds to the mean of parameter estimates $\bar{\mathbf{x}}$ with respect to the random perturbation for each solution cluster. The mean of the global minima $\bar{\mathbf{x}}^{**}$ can be obtained as the set of parameters $\bar{\mathbf{x}}$ associated with the minimum $J(\bar{\mathbf{x}})$.

2.5.3 Selection of Measurement Locations for Error Reduction

Spatial location of measurements and the level of noise in the measured data can dramatically affect the accuracy of parameter estimation (see, for example, Sanayei et al. 1992; Hjelmstad 1996). By using the measurements at a certain subset of model degrees of freedom, one can limit error in the parameter estimates due to the measurement noise. A number of heuristic methods have been proposed in the literature to select a near-optimal set of noise-polluted measurement locations. These methods were originally used in the context of selecting the sensor and actuator locations to control the dynamic response of the structure (Skelton and Delorenzo 1983; Haftka and Adelman 1985; Kammer 1991). Sanayei et al. (1992) introduced the use of Delorenzo's method in selecting the subsets of noisy force and displacement measurements to reduce the error in the static parameter estimation prior to the nondestructive testing. Error sensitivity analysis was used to determine the smallest subset of applied force and measured displacement degrees of freedom that causes small errors in the identified parameters. In particular, the largest element of the error sensitivity matrix of parameter estimates identified by the finite difference method was used as an index for comparison between different set of measurements. This approach requires extra computations of the input-output error relationship to guarantee the improvement

of the results using the selected measurement locations. In addition, the method is limited to the case of a pretest simulation study in which one must select the near-optimal sensor location *before* measurements are made (i.e., it is not applicable in selection of the measurement set that reduces error in the parameter estimates *after* the measurements are obtained).

A heuristic method, which makes use of the error sensitivity analysis of Section 2.5.2, is described herein to select a near-optimal subset of the noisy measurement locations. The method takes into account the possibility of solution multiplicity of the modal parameter estimation problem. Unlike the finite difference approach of Sanayei et al. (1992), Monte Carlo simulations are not required to establish the input-output error relationships of the identified parameters in the present method. Moreover, the algorithm provides a natural basis for the parameter grouping scheme of Section 2.3. It should be noted that the identified subset of measurement locations is not guaranteed to minimize the error in the parameter estimates. Selection of the best subset of measurements requires an exhaustive search of different combinations of the measured degrees of freedoms and, hence, the process can be computationally intensive. The present method is aimed to assist in the selection of a near-optimal subset of the measurement locations that causes a relatively small error in the parameter estimation results.

Let us suppose that a set of measurement locations $\hat{\mathbf{\Phi}}_o$ is given as known information. One can find a set of multiple solutions to the parameter estimation problem of (2.4) corresponding to $\hat{\mathbf{\Phi}}_o$ from which the mean of the global optima $\bar{\mathbf{x}}^{**}(\hat{\mathbf{\Phi}}_o)$ can be identified. In general, the mean of the global optima is associated with the minimum value of $J(\bar{\mathbf{x}})$ as described in the previous section. Moreover, the eigenvalues of the covariance matrix of parameter estimates $\mathbf{R}^{x^{**}}$, evaluated from equation (2.21), can be used to determine the sensitivity of $\bar{\mathbf{x}}^{**}$ to the random perturbation. As mentioned earlier, the estimated parameters are expected to be accurate when these eigenvalues are small. In the current algorithm, we use the value of objective function and we sum the squares of the eigenvalues of the covariance matrix associated with the cluster of global minima to measure the accuracy and the sensitivity of the parameter estimation results, respectively. In particular, we devise a search scheme to find a set of measured locations that minimizes $J(\bar{\mathbf{x}}^{**})$ as well as the sum of the squares of the eigenvalues of $\mathbf{R}^{x^{**}}$.

The selection of the near-optimal subset of measurement locations can be described as an integer programming process as illustrated in Figure 2.6. In the illustration, the GPE (global parameter estimation) algorithm indicates the process of finding the mean of the global minima of the parameter estimation objective function using the random starting point scheme and the optimum sensitivity analysis. In addition, the sum of the squares of the covariance matrix of parameters $\mathbf{x}$ is defined as $s \equiv \sum_{i=1}^{N_p} \lambda_i^2(\mathbf{R}^x)$. It should be noted that when a measurement location is dropped, the mode shape information at the dropped location is disregarded for all measured modes.

The proposed algorithm provides explicit information on the sensitivity of parameter estimates as well as the objective function to the expected level of measurement noise for each of the measurement patterns investigated. The value of the objective function is used to guarantee the improvement in the values of the parameter estimates. Hence, there is no computational burden of re-examining the parameter estimation results for the selected subset of measurements.

1. Initialization

   1.*a*. Set $i = 0$, $\hat{\mathbf{\Phi}}_i = \hat{\mathbf{\Phi}}_o$ is given data.
   1.*b*. Compute $\bar{\mathbf{x}}_o^{**}$ by GPE algorithm.
   1.*c*. Compute $J_o = J(\bar{\mathbf{x}}_o^{**}, \hat{\mathbf{\Phi}}_o)$, $\mathbf{R}_o = \mathbf{R}^{\bar{\mathbf{x}}_o^{**}}(\hat{\mathbf{\Phi}}_o)$, $s_o = \sum_{i=1}^{N_p} \lambda_i^2(\mathbf{R}_o)$.

2. Measurement selection process

   2.*a*. If insufficient data remains, **EXIT**.
   2.*b*. Do $j = 1,..., \hat{N}_d$
      2.*b.i*. Set $J_{\min} = J_o$, $j_{\min} = 0$.
      2.*b.ii*. Create $\hat{\mathbf{\Phi}}_i^{(j)}$ by dropping the jth entry in $\hat{\mathbf{\Phi}}_i$ for all modes.
      2.*b.iii*. Solve for $\bar{\mathbf{x}}_j^{**}$ by GPE algorithm.
      2.*b.iv*. Compute $J_i^{(j)} = J(\bar{\mathbf{x}}_j^{**}, \hat{\mathbf{\Phi}}_i^{(j)})$, $\mathbf{R}_i^{(j)} = \mathbf{R}^{\bar{\mathbf{x}}_o^{**}}(\hat{\mathbf{\Phi}}_i^{(j)})$, $s_i^{(j)} = \sum_{i=1}^{N_p} \lambda_i^2(\mathbf{R}_i^{(j)})$.
      2.*b.v*. If $J_i^{(j)} < J_{\min}$ then $j_{\min} = j$.
   2.*c*. Set $\hat{\mathbf{\Phi}}_{i+1} \Leftarrow \hat{\mathbf{\Phi}}_i^{(j_{\min})}$, $J_{i+1} = J_i^{(j_{\min})}$, $s_{i+1} = s_i^{(j_{\min})}$.
   2.*d*. Test convergence.
      If $J_{i+1} > J_i$ or $s_{i+1} > s_i$ then **EXIT**
   2.*e*. Set $\hat{N}_d = \hat{N}_d - 1$.
   2.*f*. Go to 2.*a*.

Figure 2.6 Algorithm for selection of the near-optimal subset of measurement locations.

Nevertheless, the system output-system parameter relationship can become highly nonlinear when the level of uncertainty in the measurement is excessive or when the measured data are extremely sparse in which case the sensitivity analysis using the Monte Carlo approach will give better results.

In practice, the proposed strategy for finding the near-optimal set of measurement locations can be used either in a pretest simulation study prior to a nondestructive testing or to reduce error of the parameter estimation results for a given data set. In the case where a single noisy data set is given, the algorithm will search for the near-optimal set of measurements that produces small errors in the parameter estimates for the model structure. In the pretest simulation study, however, finding the near-optimal measurement *sets* is more useful than finding the near-optimal measurement *set* because there are usually many factors that affect the selection of the sensor locations other than those considered in this study (e.g., feasibility of the required number of sensors, accessibility of the sensor locations). In that case, Monte Carlo simulations can be used to create a sample of noisy measurements for the nominal model of the structure after which the near-optimal measurement sets can be obtained for each of the simulated noisy measurements.

2.6 A Numerical Example

In this section, we examine the performance of the present algorithm through a simulation study. The example structure is the six-story shear building with fixed base as shown in Figure 2.7. The structural model has six degrees of freedom, the horizontal translations at the story levels, from which all of them are initially measured as illustrated in the figure. The structure is parameterized with six parameters, $\mathbf{x} = \{x_1, x_2, ..., x_6\}^T$. The stiffness of the ith story is given by $k_i = x_i k$. The nominal properties of the structure is chosen such that $k_0/m_0 = 1.2$ /sec^2. Let us assume that the actual parameters associated with the current conditions of the structure are $\hat{\mathbf{x}} = \{2.0, 2.0, 2.0, 1.0, 1.0, 1.0\}^T$. Note that the prior knowledge of the actual values of parameters is not required in the current algorithm; these values are mainly used to illustrate the results of the simulation study and are regarded as unknowns in the estimation of structural parameters. In the current study, we assume that the baseline paramaters associated with the initial structure are given as $\mathbf{x}^* = \{3.0, 3.0, 2.0, 2.0, 1.0, 1.0\}^T$. The specified values of baseline parameters are

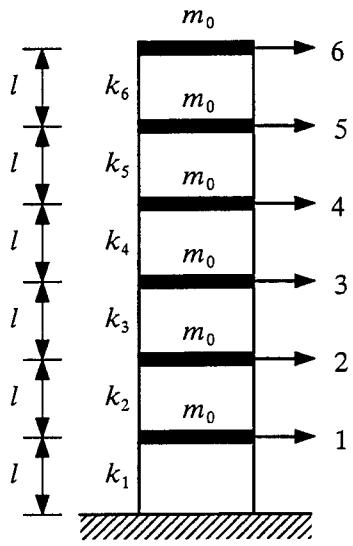

Figure 2.7 The six-degree-of-freedom shear building.

used in the random starting point scheme to identify the multiple solutions to the parameter estimation problem for each pattern of measurements investigated. These values can be selected to be different from the above set without significantly changing the results of the simulation study. The current sets of parameters might reflect a damage scenario in which $\{x_1, x_2\}$ and x_4 have decreased by 33% and 50%, respectively.

The results from a free vibrational analysis of the current structural model are shown in Table 2.1 where the ith mode shape ϕ_i is scaled such that $\phi_i^T \mathbf{M} \phi_i = 1$. From this table, the natural frequencies and mode shapes of all six modes are taken as our a priori known database. As such, the measurement vector can be written as $\hat{\mathbf{\Phi}}^T = \{\hat{\phi}_1^T, \hat{\phi}_2^T, ..., \hat{\phi}_6^T\}$. To study the effect of measurement noise, we generate noisy measurement data by adding uniform random variates with known statistical properties to the noise-free data. To wit, we calculate the kth component of the lth noisy measurement vector from the kth component of the computed noise-free measurement vector as

$$\tilde{\Phi}_{kl} = \hat{\Phi}_k(1 + \varepsilon\zeta_{kl}) \tag{2.22}$$

where ζ_{kl} is a uniform random variate in the range $[-1, 1]$. The amplitude ε will be used in our study to quantify the level of noise in the measurement. Throughout the study we will assume

Table 2.1 Noise-free data from free vibrational analysis of the current structure.

	1st Mode	2nd Mode	3rd Mode	4th Mode	5th Mode	6th Mode
Natural Frequency (Hz)	0.05350	0.14050	0.22465	0.30364	0.34424	0.45008
Mode Shape						
Level 1	0.03263	-0.09481	-0.10439	0.12439	-0.18499	-0.17133
Level 2	0.06373	-0.15884	-0.12212	0.06013	-0.00938	0.22824
Level 3	0.09183	-0.17129	-0.03847	-0.09533	0.18452	-0.13273
Level 4	0.13937	-0.08495	0.19270	-0.11710	-0.14704	0.02988
Level 5	0.17380	0.05656	0.10393	0.21631	0.09464	-0.00666
Level 6	0.19186	0.16133	-0.15740	-0.10639	-0.03265	0.00118

that the natural frequencies can be measured with negligible error and are considered to be noise-free.

During the measurement selection process in the algorithm, different patterns of measurements are used as input to the parameter estimation problem. Each case that we examine will be designated by the degrees of freedom which are measured, for example, the measurement case 12-4-6 uses modal displacements at levels 1, 2, 4 and 6 and does not use measurements at levels 3 and 5. In any measurement case, all of the six available modes will always be used as our measured information.

In the current simulation study, we generate 100 noisy data sets based upon the noise-free data from Table 2.1 in accord with equation (2.22) using three levels of noise: $\varepsilon = 5\%$, 10% and 20%, respectively. Each of the simulated noisy data sets are used as input for the initial measurement case from which the algorithm is performed to selectively eliminate the measured degrees of freedom until the near-optimal set of measurement locations is obtained. As such, the algorithm will converge to different subsets of measurement locations for different noisy data sets. For a certain noisy measurement case during the elimination process, we use 100 random starting points to identify multiple solutions to the parameter estimation problem. The mean of the global minima $\bar{\mathbf{x}}^{*}$ can be located using the optimum sensitivity analysis as described previously. Consequently, we can compute the mean of the parameter estimates and the sum of the squares of the

eigenvalues of the covariance matrix associated with the cluster of the global minima in accord with equations (2.20) and (2.21), respectively. Note that the amplitude of perturbation α in these equations should be selected as the same as the level of noise present in the measured data. In the present simulations, we assume the prior knowledge of the level of uncertainty in the measurement. Thus, the amplitudes of perturbation can be selected as $\alpha = 0.05, 0.1$ and 0.2 to characterize the bias and scatter of parameter estimates for the 5%, 10% and 20% noisy measurement cases, respectively.

Several measures of identification error are used to compare the parameter estimation results of the initial and the identified patterns of measurements. To wit, we compute the average of $\bar{\mathbf{x}}^{**}$ for a specified pattern of measurements based upon a certain subset of the simulated noisy database as

$$\bar{\bar{\mathbf{x}}}^{**} = \frac{1}{N_t}\sum_{t=1}^{N_t} \bar{\mathbf{x}}_t^{**} \tag{2.23}$$

where $\bar{\mathbf{x}}_t^{**}$ denotes the parameter estimates associated with the mean of the global minima for the tth noisy measurement set of the N_t simulated data sets under consideration. With the definition of $\bar{\bar{\mathbf{x}}}^{**}$, the average root quadratic bias (RQB) can be defined as

$$RQB = \frac{\| \bar{\bar{\mathbf{x}}}^{**} - \hat{\mathbf{x}} \|}{N_p \| \hat{\mathbf{x}} \|} \tag{2.24}$$

in which $\hat{\mathbf{x}}$ are the actual parameters for the current structural model and N_p is the number of estimated parameters as defined by equation (2.3). The quadratic bias is a measure of the distance between the expected value of the estimates $\bar{\bar{\mathbf{x}}}^{**}$ and the actual parameters $\hat{\mathbf{x}}$. To measure the scatter of the parameter estimates with respect to the actual parameters, we use the average root mean square error (RMS), which is given by

$$RMS = \frac{\left[\frac{1}{N_t}\sum_{t=1}^{N_t} \| \bar{\mathbf{x}}_t^{**} - \hat{\mathbf{x}} \|^2\right]^{\frac{1}{2}}}{N_p \| \hat{\mathbf{x}} \|}. \tag{2.25}$$

Notice that both RQB and RMS are normalized with respect to the norm of actual parameters.

The results of an error sensitivity analysis for the case of complete measurements (123456) are shown in Figure 2.8. In the figure, the values of the stiffness parameters obtained from equation (2.18) are plotted with respect to 100 noisy data sets for different levels of measurement noise. It should be noted that the solution to the parameter estimation problem for the complete measurement case is unique for each particular noisy data set and, hence, the multiplicity of solution can be disregarded. It is observed that the majority of the parameter estimates are quite far from the actual values. There is a tendency for the parameter estimation algorithm to overestimate. The variation of the parameter estimates is likely to increase with the level of noise in the measurements. The case with 20% noise level shows the greatest scatter and bias of the parameter estimation results.

The subsets of the near-optimal measurement locations obtained by the algorithm using different noisy data sets are shown in Table 2.2. The table reports the subsets of measurement locations and the corresponding fractions of the 100 noisy data sets that the algorithm converged for different levels of noise. For example, a fraction of 0.14 of the 5% noisy data sets for the measurement case 123-56 indicates that the algorithm converged to this set of measurements for a total of 14 data sets (out of a sample of generated 100 data sets with 5% noise). Let us examine a selected pattern of measurements 1----- with 10% noise in Table 2.2. We can plot the sum of the squares of the eigenvalues of the covariance matrix for parameter estimates associated with different sequences of measurement locations during the elimination process as shown in Figure 2.9. In this figure, λ_i denotes the ith eigenvalue of the covariance matrix. One can see that the sum of the squares of the eigenvalues decreases exponentially during the measurement selection process for each of the simulated noise trials. The reduction of the eigenvalues of the covariance matrix indicates that the outcome of the parameter estimation problem corresponding to the identified measurement locations are less sensitive to noise.

The identification errors of the parameter estimation results as defined by equations (2.25) and (2.26) for the complete measurement case and the identified subsets of measurement locations from Table 2.2 are illustrated in Figure 2.10. In the illustration, Case 0 denotes the complete measurement case. The average root quadratic bias (*RQB*) and the average root mean square error (*RMS*) are calculated based on the noisy data sets that converged to each particular measurement

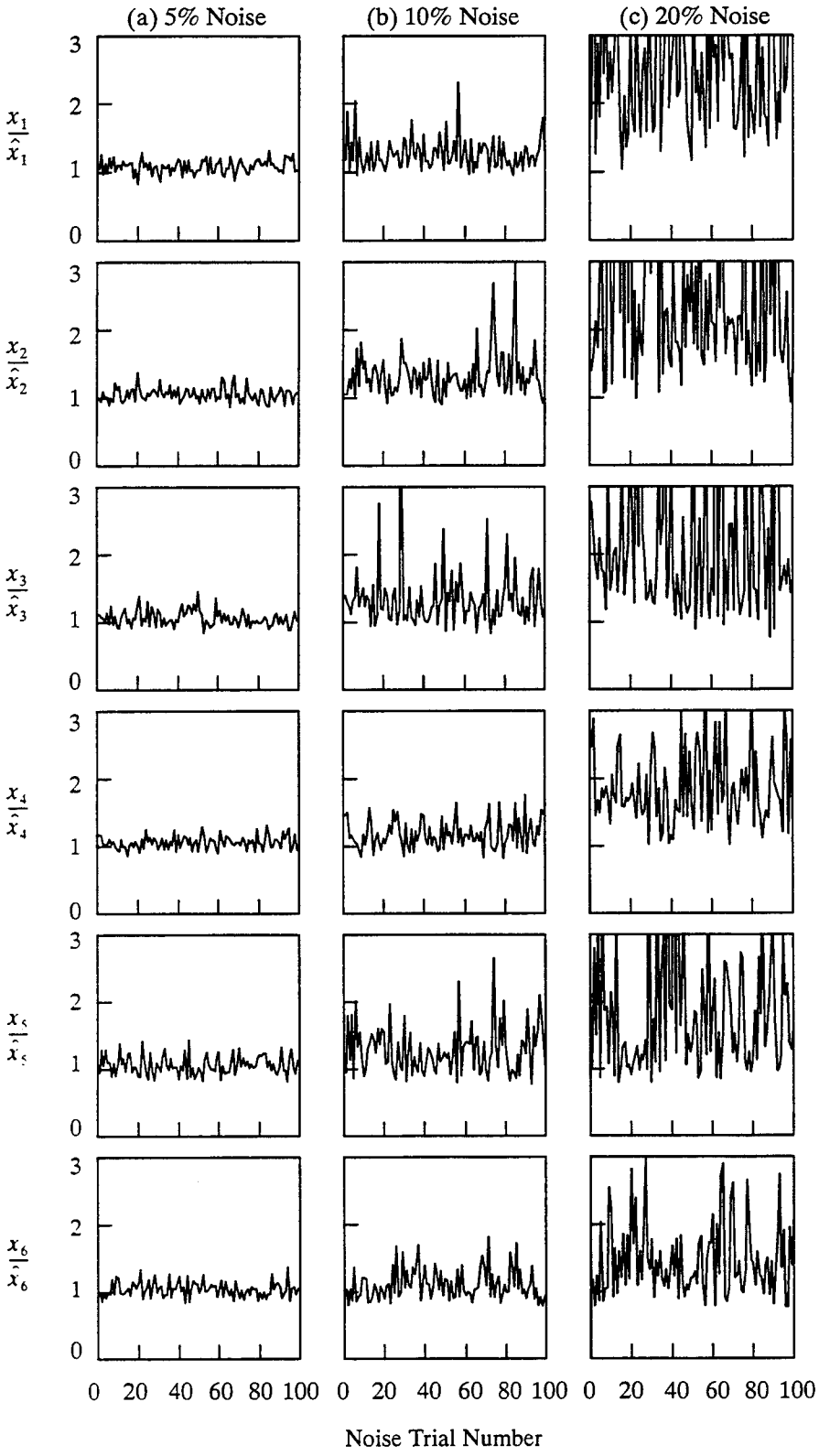

Figure 2.8 Variation of the parameter estimates with respect to different noisy data sets using complete measurements with three levels of noise.

Table 2.2 Fraction of 100 noisy data sets converging to different patterns of measurements for 5%, 10%, and 20% level of measurement noise.

5% Noise			10% Noise			20% Noise		
Case number	Measured d.o.f.s	Fraction	Case number	Measured d.o.f.s	Fraction	Case number	Measured d.o.f.s	Fraction
1	123-56	0.14	1	1-----	0.22	1	1-----	0.19
2	1-----	0.14	2	123-56	0.15	2	123-56	0.17
3	--3---	0.11	3	--3---	0.09	3	--3---	0.14
4	-23-5-	0.07	4	12--5-	0.08	4	-23-5-	0.12
5	-2----	0.07	5	-23-5-	0.08	5	12--5-	0.07
6	---4-6	0.06	6	-2----	0.05	6	-2----	0.06
7	12--5-	0.05	7	1--4-6	0.04	7	12-4--	0.04
8	--34-6	0.05	8	12----	0.04	8	1-345-	0.03
9	1-34-6	0.04	9	---4--	0.04	9	---4--	0.03
10	12----	0.04	10	12-45-	0.03	10	--34-6	0.02
11	1--4-6	0.03	11	-234-6	0.03	11	1--4--	0.02
12	12-4--	0.03	12	12-4--	0.03	12	--3-5-	0.02
13	---4--	0.03	13	----5-	0.02	13	----5-	0.02
14	123-5-	0.02	14	1234--	0.01	14	123-5-	0.01
15	12-45-	0.02	15	123-5-	0.01	15	123--6	0.01
16	1-345-	0.02	16	1-345-	0.01	16	1-34-6	0.01
17	1--45-	0.02	17	1-34-6	0.01	17	-234-6	0.01
18	1--4--	0.02	18	-2345-	0.01	18	1--4-6	0.01
19	12-4-6	0.01	19	-23-56	0.01	19	12----	0.01
20	1-3-56	0.01	20	1-3--6	0.01	20	1----6	0.01
21	-234-6	0.01	21	--34-6	0.01			
22	-2-45-	0.01	22	--3-5-	0.01			
			23	---4-6	0.01			

case. It is observed that all measurement cases reported in Table 2.2 perform well for all levels of noise as indicated by the lower values of *RMS* and *RQB* compared to the complete measurements. The measurement case 1----- shows the least identification errors for all levels of noise. Nevertheless, there is a tendency for different noisy data sets to converge to different subsets of measured locations. As such, one cannot rely on a fixed subset of degrees of freedom to work well for all cases of noisy measurements.

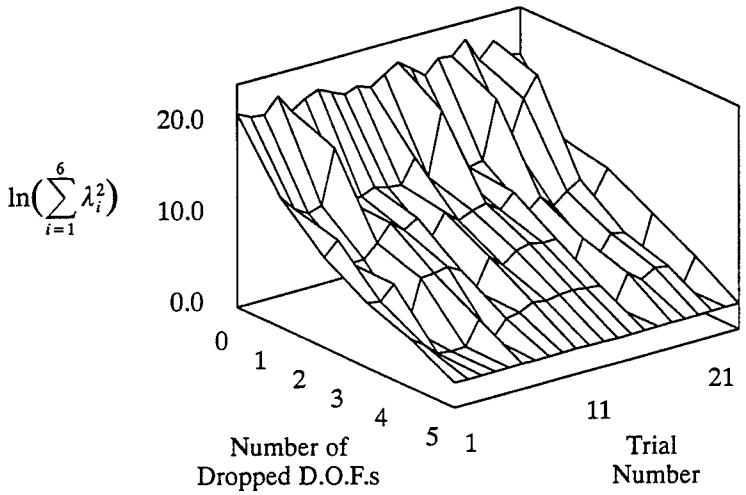

Figure 2.9 Sensitivity of the parameter estimates during the measurement selection process for each noisy data set with 10% level of noise that converged to the measurement case 1-----.

The heuristic method presented does not guarantee that the selected subset of degrees of freedom is optimal. However, the method assists in the selection of a subset of measured noisy degrees of freedom that cause a relatively small errors in the parameter estimates and greatly reduces the computational burden of the selection of the best degrees of freedom for parameter estimation that would otherwise require an exhaustive search of every possible combinations of the measured degrees of freedom. Although the selected subset of degrees of freedom may not be the optimal set, it can be regarded as a near-optimal set that allows a successful parameter estimation with small identification errors.

2.7 Summary

The key element of most damage detection algorithms is the estimation of the system parameters from measured response. For large and complex structures, sparsity of measured data is often unavoidable since only a limit number of model degrees of freedom of the structures can be measured. In general, parameter estimation from the measured modal response of a structure can give rise to multiple solutions if the data are spatially sparse. The extra solutions of the parameter estimation problem are local minima of the objective function and are probably extraneous. Ignoring the possibility of solution multiplicity can lead to erroneous parameter estimation results.

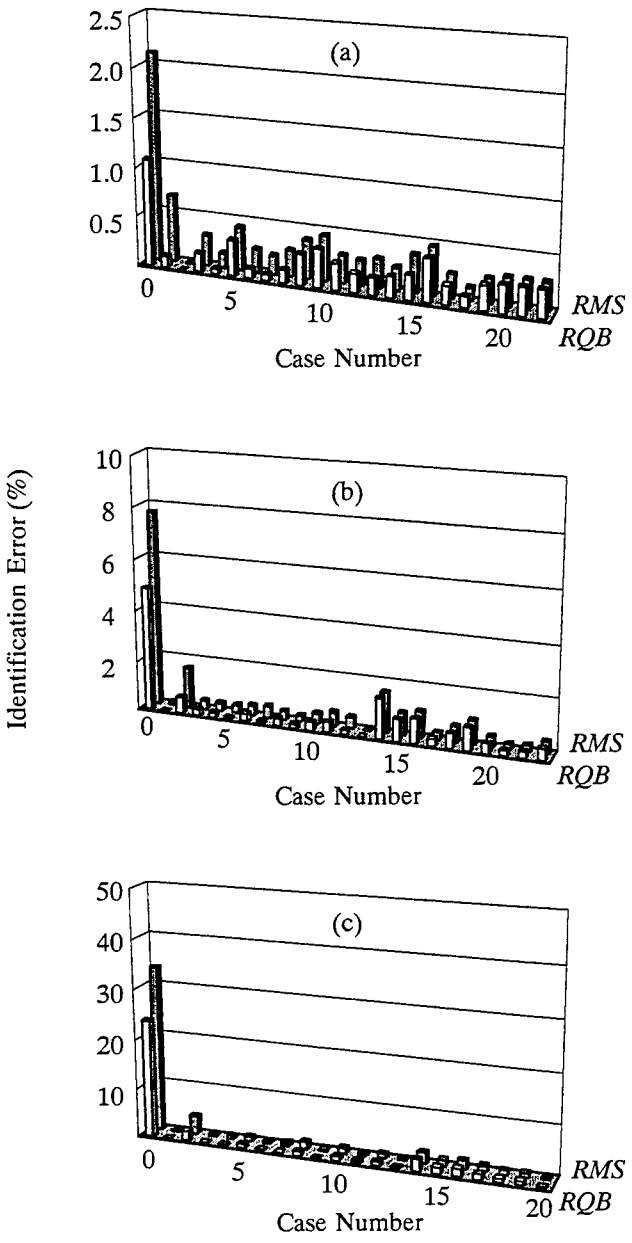

Figure 2.10 The identification errors of the parameter estimates for the complete measurement case (Case 0) and the identified subsets of measurement locations from Table 2.2 using three different levels of noise: (a) $\varepsilon = 5\%$, (b) $\varepsilon = 10\%$, and (c) $\varepsilon = 20\%$.

The success of a parameter estimation method depends on the behavior of the algorithm in the presence of measurement errors. With a selected subset of measurement locations, one can limit the error in the parameter estimation results. We have presented a general framework of an

error sensitivity analysis to obtain a near-optimal subset of measured degrees of freedom that can improve the parameter estimation results. We have employed the method of random starting points to locate the solutions to the parameter estimation problem. In addition, the optimum sensitivity method was used to extract the sensitivity information of each individual solution after which the global minimum of the parameter estimation objective function can be identified.

We have illustrated through a simple example that the data perturbation scheme and the optimum sensitivity analysis can be used to select noisy subsets of measurement locations that will produce small errors in the parameter estimates. The algorithm performed well in the illustrated example for a wide range of noise. Monte Carlo simulations are not required to establish the input-output error relationships of the identified parameters. With a single set of noisy data, the algorithm will search for a near-optimal subset of measurement locations that yields an improved set of parameter estimates with lower sensitivities to the measurement noise. In addition, the algorithm provides a natural basis for the parameter grouping scheme.

Based on the results of this chapter, we conclude that the measurement selection process is essential to a successful parameter estimation and damage assessment from measured modal response. The current approach can be used to select the near-optimal sensor location before the measurements are made or select the measurement set that reduces error in the parameter estimates after the measurements are obtained. Although we have not considered the effect of modal sparsity on the parameter estimates in the current study, it is possible to incorporate the selection of measured modes as input to the parameter estimation problem without significant modifications.

CHAPTER 3

DAMAGE DETECTION AND ASSESSMENT

3.1 Introduction

Global damage detection methods based upon measured natural modes and frequencies of a structure have gained considerable attention in the past few decades. Among the recent developments, the parameter estimation technique has proved effective as a tool to detect damage in structural systems (see, for example, Hajela and Soeiro 1990b; Agbabian et al. 1991; Hjelmstad et al. 1995). Damage detection methods based upon parameter estimation often require that the structure be represented by a parameterized finite element model and that the values of the system parameters be estimated using a least-squares minimization of either the force residual or displacement residual of the vibration eigenvalue problem. Generally, the number of elements in the model far exceeds the amount of data available for parameter estimation. Consequently, grouping similar elements together and associating each group of elements with a certain set of constitutive parameters are essential to these methods. This process is generally known as parameter grouping (Hjelmstad et al. 1992). The problem with parameter grouping is that one does not know in advance how to group the parameters. Ideally, one wishes to isolate damaged elements from undamaged elements and, hence, the parameter grouping must eventually reflect this division. However, the damaged elements are not known in advance. The first part of a global damage detection algorithm involves the determination of the best parameter grouping and hence the isolation of damaged elements.

Structural parameter estimation algorithms generally do not have unique solutions when the data are spatially sparse (Hjelmstad 1996). Further, the sensitivity of the parameter estimates to noise in the measured data depends upon the number and density of solutions to the parameter estimation problem. The existence of multiple solutions to the parameter estimation problem complicates the parameter grouping process because there are many potential groupings that turn out to be misleading. Successful isolation of damaged elements depends upon identifying the cor-

rect solution from among the many choices. In addition, measured data are generally polluted with random measurement errors. These measurement errors can dramatically affect the accuracy of the parameter estimates. Selection of a near-optimal subset of measurements to reduce uncertainty of the parameter estimates due to measurement noise is essential for a robust damage detection algorithm (Sanayei et al. 1992).

In this chapter we formulate a practical approach for global damage detection from incomplete and noise-polluted modal response of a structure. We propose a new parameter group-updating scheme, based upon the adaptive parameter grouping algorithm of Shin and Hjelmstad (1994), that has enhanced capability of finding multiple damage locations. The non-uniqueness of the parameter estimation solutions arising from using sparse and noisy data is acknowledged and treated by the algorithm. A unified approach, based on the methods described in Chapter 2, for determining solution clustering is used to find multiple solutions, improve the estimate of the parameter, and to assess which of the solutions is the best one. This best solution provides the basis for deciding which parameter group should be subdivided at each level of the damage localization algorithm. The method presented in Chapter 2 is employed for selection of the near-optimal measurement set to reduce error in the parameter estimates. New error functions are introduced to use the method of selective near-optimal measurement set in conjunction with the parameter group-updating scheme. To account for the uncertainty of parameter estimates, we assess damage by comparing the statistical distribution of the Monte Carlo sample of the element parameters for the damaged and undamaged structures. With the proposed damage assessment scheme, the probability of damage for a structural element can be computed for each specified level of damage.

3.2 Damage Localization

In this section, the method for isolation of damaged regions from undamaged parts of the structure based on limited measurement information is described. In particular, we propose a new parameter group-updating scheme to localize damage in a systematic manner with sparse data based on the parameter grouping scheme of Shin and Hjelmstad (1994). The present algorithm is aimed to improve computational efficiency as well as the ability to localize multiple damage

locations in a structural system, which are major drawbacks of the adaptive parameter grouping scheme. In the current algorithm, the parameter estimation method described in Chapter 2 is adopted as the main tool for estimating structural parameters at each step of the damage localization process. The non-uniqueness of solutions to the parameter estimation scheme is accounted for by the algorithm.

3.2.1 A Parameter Group-Updating Scheme

The adaptive parameter grouping scheme (Shin and Hjelmstad 1994) localizes damaged parts in the structural model by sequentially subdividing parameter groups. The candidate group for subdivision is the one that results in the greatest drop in the value of the objective function $J(\mathbf{x})$ as defined in equation (2.4). This approach is based on the observation that the value of the objective function decreases significantly when the damaged elements are grouped separately from undamaged elements. Natke (1989) and Natke and Cempel (1991) suggested a similar scheme that selects the best candidate group for subdivision as a group with the largest deviation of the value of the group parameter from the baseline value. This approach is not attractive when a comparable amount of noise is present in the measured data because the deviation of the value of the group parameter often represents noise rather than damage.

In the adaptive parameter group-updating scheme, the parameter group is subdivided consecutively as shown schematically in Figure 3.1. Starting with the baseline grouping, the algorithm finds the best candidate group for subdivision at each level of grouping that results in the greatest drop in $J(\mathbf{x})$. For example, group 1B at level 1 is subdivided because the subdivision of group 1B gives a smaller value of $J(\mathbf{x})$ than group 1A. The process repeats until group 4B at level 4 that contains a single element is split off. To assure that all damaged elements are detected, the algorithm has to work back up the grouping tree to explore the remaining branches of possible parameter groupings. Thus, if group 1A in the illustration presumably contains another damaged element, the algorithm will not be able to find it until groups 2B, 3A and 4A have been thoroughly investigated. In general, the number of different parameter groupings that require further investigation increases tremendously when the locations of damage in a structure are isolated. Hence, the algorithm is not computationally efficient for detecting spatially isolated damage locations.

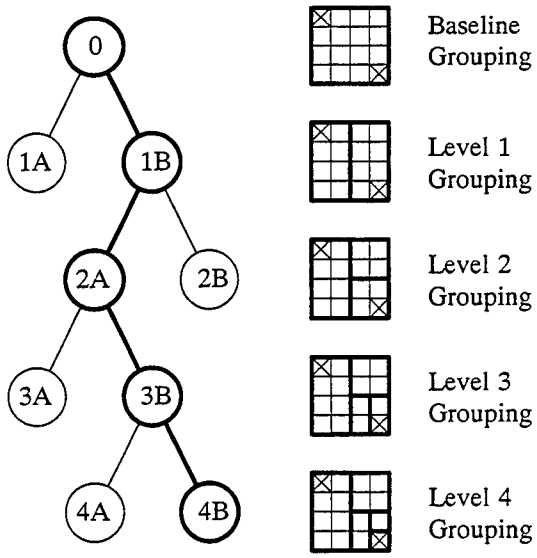

Figure 3.1 Parameter group subdivision for the adaptive parameter group-updating scheme.

To localize multiple damage more efficiently, we present a new parameter group-updating scheme as follows. Let us denote the initial baseline grouping as the grouping that contains the original parameter groups (i.e., the groups that are assigned in accord with the baseline or undamaged structural model). Further, let the updated baseline grouping represent the parameter grouping that is modified from the initial baseline grouping by including the parameter groups of the isolated elements identified from the localization process. We denote the parameter grouping at the ith stage of the parameter group-updating algorithm as $\mathbf{\Omega}_i = \{\Omega_1^i, \Omega_2^i, ..., \Omega_{N_g^i}^i\}$ where N_g^i is the number of parameter groups at subdivision stage i. The next level of grouping $\mathbf{\Omega}_{i+1}$ is determined from $\mathbf{\Omega}_i$ by subdividing one of the parameter groups in accord with a specified criterion based upon the value of the grouping index $\tilde{J}$ (that will be defined later on) associated with each parameter grouping. In particular, we select the best candidate group for subdivision as the one that results in the greatest drop in the value of $\tilde{J}$ after the group subdivision. Moreover, since several damaged regions with different levels of severity can coexist within the structural system, the subdivision must be continued until all of the damaged elements are isolated.

The proposed damage localization scheme is organized as a depth-first search as shown schematically in Figure 3.2. In the illustration, the baseline group 00 in the initial baseline grouping

is divided into two groups, 01A and 01B, respectively. These two newly created groups are then subdivided. The subdivision of group 01B yields a greater decrease in the value of the grouping index than group 01A and, hence, group 01B is selected as the candidate for further subdivision. The algorithm repeats until group 04B, which contains a single damage element, is isolated. At this point, the updated baseline group 10 is formed by eliminating the isolated elements (groups 04A and 04B) from the original baseline group. Note that the isolated elements are disregarded from any further subdivision. The updated baseline group is then subdivided into groups 11A and 11B, and group 11A is selected as the candidate for subdivision at the next level of grouping. The subdivision process continues until another damaged part in group 14A of the structural model is isolated. It can be seen that the backing up process of the adaptive parameter grouping scheme is eliminated by updating the baseline parameter grouping. This technique improves the ability of the algorithm in detecting multiple damage locations.

It is important to know when to terminate the group-updating process. Clearly, one would like to stop the algorithm as soon as all damage locations are detected. From simulation studies, it is evident that once all of the potentially damaged elements are completely isolated, the values of the parameter estimates for the updated baseline parameter groups of the current structure vary

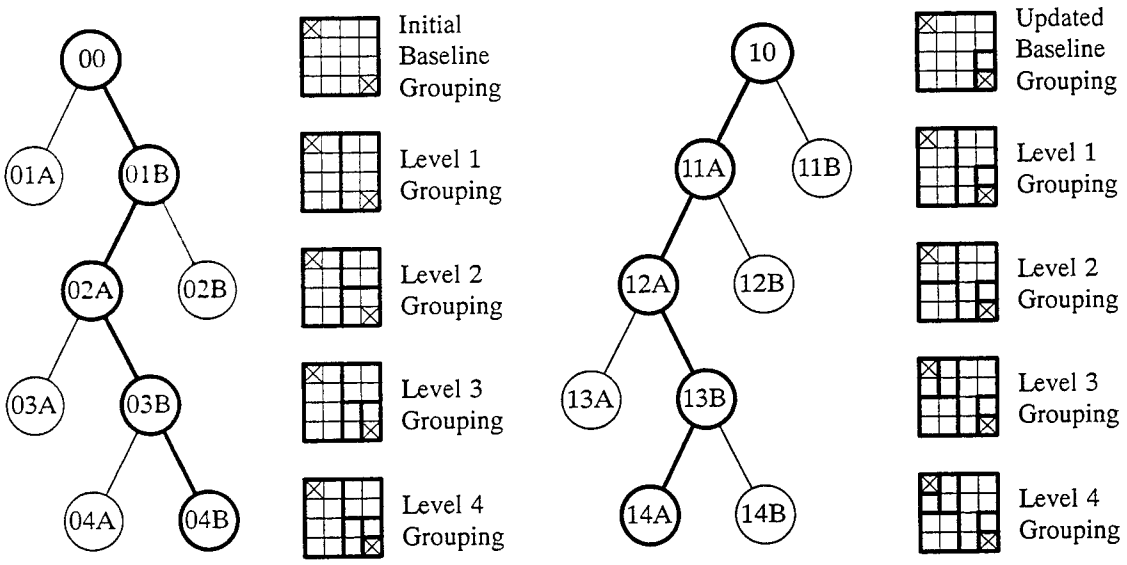

Figure 3.2 Sequential parameter group subdivision for initial and updated baseline grouping.

within a certain limit from the corresponding parameter values obtained from the baseline structure with the same parameter grouping and locations of measurements. If the measured data are noise-free, the comparison between the values of the system parameters for the baseline structure and the current structure can be made directly. When the measured data are noise-polluted, the uncertainty of parameter estimates due to error in the measurements must be taken into account.

In the current algorithm the statistical indices (i.e., mean and standard deviation) of the estimated parameters for the baseline and the current structures are used to account for the effect of noise in the measurements. Suppose that the values of the parameter estimates are obtained by using exactly the same conditions (i.e., parameter grouping and location of measurements) as input to the parameter estimation problem for both the current structure and the associated baseline structure. The deviation of the parameter estimates can be assessed by comparing the two statistical indices of the system parameters obtained from the sensitivity analysis of parameter estimates for the baseline and the current structure. The situation is illustrated in Figure 3.3 where each of the system parameters are assumed to be statistically distributed with certain probability density. In the illustration, $\bar{x}_o$ denotes the mean of the parameter estimates for an updated baseline parameter group in the current structure; and $\bar{x}_o^*$ denotes the mean of the parameter estimates for the same parameter group in the associated baseline structure. The group-updating process is terminated if the deviation of the system parameters for each updated baseline parameter group satisfies the following criterion:

$$\Delta x_o \leqslant \sigma_o + \sigma_o^* \tag{3.1}$$

where $\Delta x_o \equiv |\bar{x}_o^* - \bar{x}_o|$ is the deviation of the value of the mean of the group parameters for the current structure from the baseline structure; σ_o is the standard deviation of the group parameters for the current structure; and σ_o^* is the standard deviation of the group parameters for the associated baseline structure. The definition of Δx_o in the above equation implies that the termination criterion is also satisfied even when the value of $\bar{x}_o$ is larger than $\bar{x}_o^*$.

3.2.2 A New Criterion for Parameter Group-Updating

In the current damage detection algorithm the near-optimal set of measurement locations must be selected as input to the parameter estimation problem at each step of the parameter

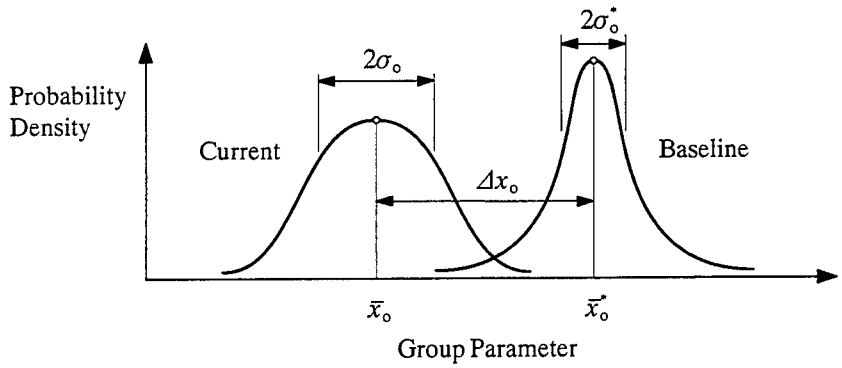

Figure 3.3 Assessment of the parameter estimates for the updated baseline parameter group.

group-updating process. Different sets of measurement locations may be selected for different parameter groupings. Since the value of the objective function $J(\mathbf{x})$ calculated based on equation (2.4) shows a comparable bias towards the set of measurements with fewer model degrees of freedom, it does not provide a fair basis of comparison for selection of the best parameter groupings. We propose a grouping index $\tilde{J}$ to measure the quality of each parameter grouping in the parameter group-updating scheme. The grouping index is defined as

$$\tilde{J} \equiv \gamma \tilde{J}_{\mathrm{I}} + (1 - \gamma)\tilde{J}_{\mathrm{II}} \tag{3.2}$$

where $\gamma \in [0, 1]$ is the weight factor for the components of the grouping index; $\tilde{J}_{\mathrm{I}}$ and $\tilde{J}_{\mathrm{II}}$ are defined, respectively, as

$$\tilde{J}_{\mathrm{I}} \equiv \frac{1}{N_m} \sum_{i=1}^{N_m} \left(\frac{\lambda_i^{\mathrm{M}} - \lambda_i^{\mathrm{C}}}{\lambda_i^{\mathrm{M}}} \right)^2 \tag{3.3}$$

$$\tilde{J}_{\mathrm{II}} \equiv \frac{1}{N_m} \sum_{i=1}^{N_m} \| \hat{\boldsymbol{\phi}}_i^{\mathrm{M}} - \rho_i \hat{\boldsymbol{\phi}}_i^{\mathrm{C}} \| \tag{3.4}$$

where λ_i and $\hat{\boldsymbol{\phi}}_i$ are the ith eigenvalue and eigenvector for the first N_m modes of the structure. The superscripts M and C represent the measured and the computed quantities, respectively. The measured response of the structure is assumed to be available from the modal testing. The computed eigenvalue λ_i^{C} and eigenvector $\hat{\boldsymbol{\phi}}_i^{\mathrm{C}}$ can be obtained from a free-vibration eigenvalue analysis of the finite element model of the structure parameterized with the set of parameter estimates

that has been identified as the mean of the global minima to the parameter estimation problem corresponding to the current parameter grouping. As described in the previous section, the mean of the global minima of the parameter estimation objective function can be located by using the GPE algorithm. Note that we define the norm quantity in equation (3.4) as

$$\| \hat{\phi} \| \equiv \hat{\phi}^T \hat{\mathbf{M}} \hat{\phi} \tag{3.5}$$

in which $\hat{\phi}$ is the measured response vector of dimensions $\hat{N}_d \times 1$; and $\hat{\mathbf{M}}$ is the symmetric partitioned mass matrix as defined in Chapter 2. In addition, the scalar ρ_i in equation (3.4) serves as a scaling factor that scales the components of $\hat{\phi}_i^C$ to the same level of magnitude as $\hat{\phi}_i^M$. The scaling factor ρ_i is derived by differentiating equation (3.4) and set to zero, which leads us to

$$\rho_i = \frac{\hat{\phi}_i^{M^T} \hat{\mathbf{M}} \hat{\phi}_i^C}{\hat{\phi}_i^{C^T} \hat{\mathbf{M}} \hat{\phi}_i^C} \tag{3.6}$$

This equation is valid when the ith measured mode shape is scaled such that $\hat{\phi}_i^{M^T} \hat{\mathbf{M}} \hat{\phi}_i^M = 1$. It can be seen that the weight factor γ in equation (3.2) essentially indicates whether $\tilde{J}_I$ or $\tilde{J}_{II}$ dominates the comparison between different parameter groupings. In the current study, an equal weight is assigned to $\tilde{J}_I$ and $\tilde{J}_{II}$, i.e., we set $\gamma = 0.5$. Note that each parameter grouping is generally selected regardless of the topology and geometry of the finite element model of the structure; it is possible that the values of the parameter estimates for certain group parameters are unnecessarily large due to the effect of the boundary conditions of the structural model on the parameter estimation problem. The stiffness parameters for the group of elements which is located near a fixed boundary are usually overestimated. One approach to such a problem is by imposing an upper limit on the values of the system parameters used to calculate λ_i^C and $\hat{\phi}_i^C$ in equations (3.3) and (3.4) at the baseline values to ensure a reasonable calculation of the grouping index.

3.2.3 Solution Multiplicity and Error Reduction for Sparse and Noisy Data

The proposed damage detection scheme requires that the parameters of the structural model be estimated for a fixed grouping at each stage of the localization process by solving the parameter estimation problem (2.4). It was shown in the previous chapter that this parameter estimation

problem can have multiple solutions when the measured data are spatially sparse. The multiplicity of solutions to the parameter estimation problem complicates the parameter grouping process since one must identify the correct solution to be used for calculation of the grouping index. Ignoring the possibility of solution multiplicity leads either to erroneous damage locations or else the algorithm fails to converge at all.

The non-uniqueness problem of modal parameter estimation is further complicated by the presence of measurement errors. A single set of noise-polluted data can lead to a biased result of parameter estimation. The effect of noise on the topography of the objective function is evident from the study of the sensitivity of parameter estimates when the simulated noise-free data are subjected to a random perturbation (Hjelmstad 1996). The accuracy of the parameter estimates is significantly affected by the measurement locations used as input to the parameter estimation problem (Sanayei et al. 1992; Hjelmstad 1996). In the current study, we adopt the optimum sensitivity method described in Chapter 2 to examine the sensitivity of parameter estimates due to a random perturbation at each stage of the damage localization process. In addition, we use the integer programming process presented in Chapter 2 to select the near-optimal subset of measurement locations as input to the parameter estimation problem for each of the parameter groupings examined during the parameter group-updating process. Note that the current approach is different from the approaches of Cobb and Liebst (1997) and Shi et al. (2000) that prioritize measurement locations according to their ability to localize structural damage based on the eigenvector sensitivity analysis with respect to changes in the structural parameters at the element level.

A certain set of different parameter groupings must be investigated at each stage of damage localization. The parameter estimation problem for a particular parameter grouping can be solved using the objective minimization algorithm in conjunction with the random starting point scheme. In addition, the near-optimal set of measurement locations can be selected as input to the parameter estimation problem. With the procedures described in Chapter 2, the parameter estimates associated with the mean of the global minima, $\bar{\mathbf{x}}^{**}$, that corresponds to the near-optimal measurement set can be identified. These parameter estimates represent the best solution to the parameter estimation problem for the specified parameter grouping based upon the available measurement information. The value of the grouping index for this best solution $\tilde{J}(\bar{\mathbf{x}}^{**})$, as calcu-

lated in accord with equation (3.2), can be used to compare with the values obtained from the competing parameter groupings in the set. The parameter grouping with the smallest $\tilde{J}(\bar{\mathbf{x}}^{**})$ is selected as the candidate for further investigation. Note that the measurement selection process to reduce errors in the parameter estimates is crucial to the parameter group-updating process since these errors can significantly affect selection of the candidate parameter grouping.

The schematic representation of the use of the parameter group-updating algorithm to localize damage in a structure using sparse and noisy measured modal response is illustrated in Figure 3.4. In the illustration, the GPE algorithm indicates the identification of the mean of the global minima of the parameter estimation problem for a certain subset of measurement locations and a fixed parameter grouping through the use of the random starting point scheme and the optimum sensitivity method.

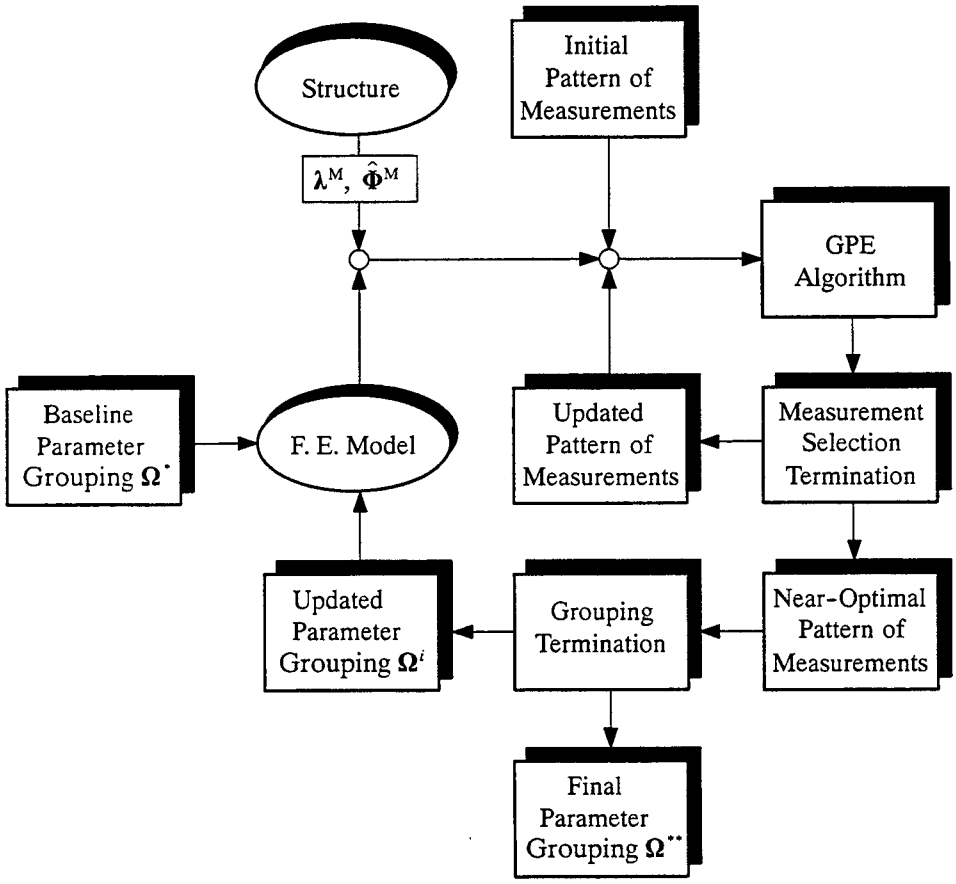

Figure 3.4 Schematic representation of damage localization process.

3.2.4 Damage Localization: Implementation

The damage localization process with the use of the proposed parameter group-updating scheme is summarized in Figure 3.5. In step 1, the given baseline parameter grouping Ω^* is used as the initial parameter grouping for an established finite-element model of the investigated structural system. The values of the initial group parameters $\mathbf{x}^{(0)}$ can be estimated using the GPE algorithm and the measurement selection process as described in the previous section. Step 2 describes the termination criterion of the parameter group-updating algorithm in which the value of the mean of the parameter estimates for each of the updated baseline parameter groups of the current structure is compared with the value of the mean of the estimated parameters for the same parameter groups of the baseline structure using the same test conditions. Based on equation (3.1), the localization process is terminated when the deviation of the values of the mean of the system parameters for each of the updated baseline parameter groups lies within a specified tolerance. To account for the possibility of multiple baseline parameter groups in the structural model, step 3 is required for selection of the candidate baseline parameter group for subdivision. In addition, step 4 searches for the candidate parameter group for further subdivision by comparing the values of the grouping index $\tilde{J}$ associated with the parameter groupings that correspond to subdividing each of the possible parameter subgroups. After the candidate parameter group is subdivided, the parameter grouping is updated and the group parameters are estimated. Notice that the group level for each updated parameter group is also modified to maintain the hierarchical order of the parameter grouping. Moreover, in case where the updated baseline parameter grouping consists of multiple parameter groups, the values of parameters for the updated baseline parameter groups that are not subjected to subdivision must be fixed at the nominal baseline values during the parameter group-updating process in step 4. Upon completion of step 4 (i.e., when the deepest leveled groups contain only the isolated elements), the algorithm proceeds to step 5 to update the baseline parameter grouping with the isolated elements. In particular, the baseline parameter grouping is modified by incorporating additional groups of the isolated elements to the original baseline parameter groups. Subsequently, the localization process is repeated until the termination criterion in step 2 is satisfied.

1. *a*. Set the initial baseline grouping $\Omega^{(0)}$ based on the given baseline grouping Ω^*.
   b. Initialize number of baseline parameter groups $N_g^{(0)}$.
   c. Initialize group level of each parameter group.
   d. Estimate parameters $\mathbf{x}^{(0)}$ by measurement selection process and GPE algorithm.

2. If the grouping termination criterion is satisfied, **EXIT**.
   $\mathbf{x}^{(0)}$ and $\Omega^{(0)}$ are the required solutions.

3. *a*. Set $k = 1$.
   b. Set $\tilde{J}_{\min} = 10^3$ (a large number).
   c. Determine the candidate baseline parameter group for subdivision.
      do $i = 1,..., N_g^{(0)}$
      - set $\Omega_i^{(k)}$ by subdividing the ith baseline group
      - estimate parameters $\mathbf{x}_i^{(k)}$ by measurement selection and GPE algorithm
      - compute $\tilde{J}(\mathbf{x}_i^{(k)})$
      - if $\tilde{J}(\mathbf{x}_i^{(k)}) < \tilde{J}_{\min}$ then $\tilde{J}_{\min} = \tilde{J}(\mathbf{x}_i^{(k)})$ and $i_{\min} = i$

   d. Set $\Omega^{(k)}$ and $\mathbf{x}^{(k)}$ by subdividing the baseline group $i_{\min}$.
   e. Update number of parameter groups $N_g^{(k)}$.
   f. Update group level for the subdivided parameter groups.

4. *a*. Set $k = k + 1$.
   b. Set $\tilde{J}_{\min} = 10^3$ (a large number).
   c. Determine the deepest level of grouping.
   d. If the deepest leveled group contains a single element, go to 5.
   e. Otherwise, determine the candidate parameter group for subdivision.
      do $j = 1, 2$
      - set $\Omega_j^{(k)}$ by subdividing the jth possible subgroup
      - estimate parameters $\mathbf{x}_j^{(k)}$ by measurement selection and GPE algorithm
      - compute $\tilde{J}(\mathbf{x}_j^{(k)})$
      - if $\tilde{J}(\mathbf{x}_j^{(k)}) < \tilde{J}_{\min}$ then $\tilde{J}_{\min} = \tilde{J}(\mathbf{x}_j^{(k)})$ and $j_{\min} = j$

   f. Set $\Omega^{(k)}$ and $\mathbf{x}^{(k)}$ by subdividing the subgroup $j_{\min}$.
   g. Update $N_g^{(k)}$.
   h. Update group level for the subdivided parameter groups.
   i. Repeat 4.

5. *a*. Set the updated baseline grouping $\Omega^{(0)}$ based on the original baseline grouping Ω^* and the newly isolated elements.
   b. Update $N_g^{(0)}$.
   c. Update group level for the updated parameter groups.
   d. Estimate parameters $\mathbf{x}^{(0)}$ by measurement selection process and GPE algorithm.
   e. Go to 2.

Figure 3.5 Parameter group-updating algorithm.

In general, the number of unknown parameters in the finite element model increases continuously along the parameter group-updating process. Hence, it is essential that the index of identifiability β, as defined in equation (2.13), be examined at each subdivision step to ensure that the parameter estimation problem (2.4) is possible. In case where $\beta < 1$ before the termination criterion is satisfied, the localization process will be terminated prematurely. In this case, the isolated elements associated with the most recently updated baseline grouping can be regarded as the set of potential damage locations that can be identified based upon the available measurement information.

3.2.5 Damage Localization: An Illustrative Example

In this section, a simple example is presented to illustrate the damage localization process. The example structure is modeled with 16 rectangular elements as shown schematically in Figure 3.6. We assume that each of the elements in the structural model can be characterized with a single stiffness parameter. Further, we assume that damage is associated with a reduction of the stiffness parameter at the element level and we denote the location of damage in the structure by the shaded area. Since the main objective of the present example is to illustrate the parameter group-updating process, hence the measurement selection process can be disregarded.

Figure 3.6 shows the damage localization process by determining the candidate parameter group for subdivision at each level of grouping. The initial baseline parameter grouping is shown in step 1 as the starting point of the parameter group-updating scheme. The group level starts from $\mathcal{L} = 0$ as denoted inside the box representing a parameter group. The statistics of the parameter estimates for the initial baseline parameter group of the current structure must be examined with respect to the values obtained from the baseline structure using the same parameter grouping and measurement locations. Based on the termination criterion of equation (3.1), the localization process is terminated if the deviation of the mean of the system parameters for the current and the baseline structure lies within a specified tolerance. In step 2, the initial baseline group is divided in half to produce two subgroups, which are indicated by group level $\mathcal{L} = 1$. Subsequently, two different parameter groupings are investigated in step 3 by subdividing the parameter groups with the deepest level of grouping ($\mathcal{L} = 1$) from step 2. These groupings are

compared based upon the value of the grouping index $\tilde{J}$ as defined by equation (3.2). The best parameter grouping is determined as the one with a smaller value of $\tilde{J}$. The subdivided parameter groups in the selected parameter grouping are then assigned with a new group level $\mathcal{L} = 2$. The process is repeated until no alternative grouping is available as illustrated in step 5 where each of the deepest leveled groups ($\mathcal{L} = 4$) contain only a single element. Notice that the group level for the singly isolated elements is fixed at $\mathcal{L} = \oplus$ in step 6, which indicates that these parameter

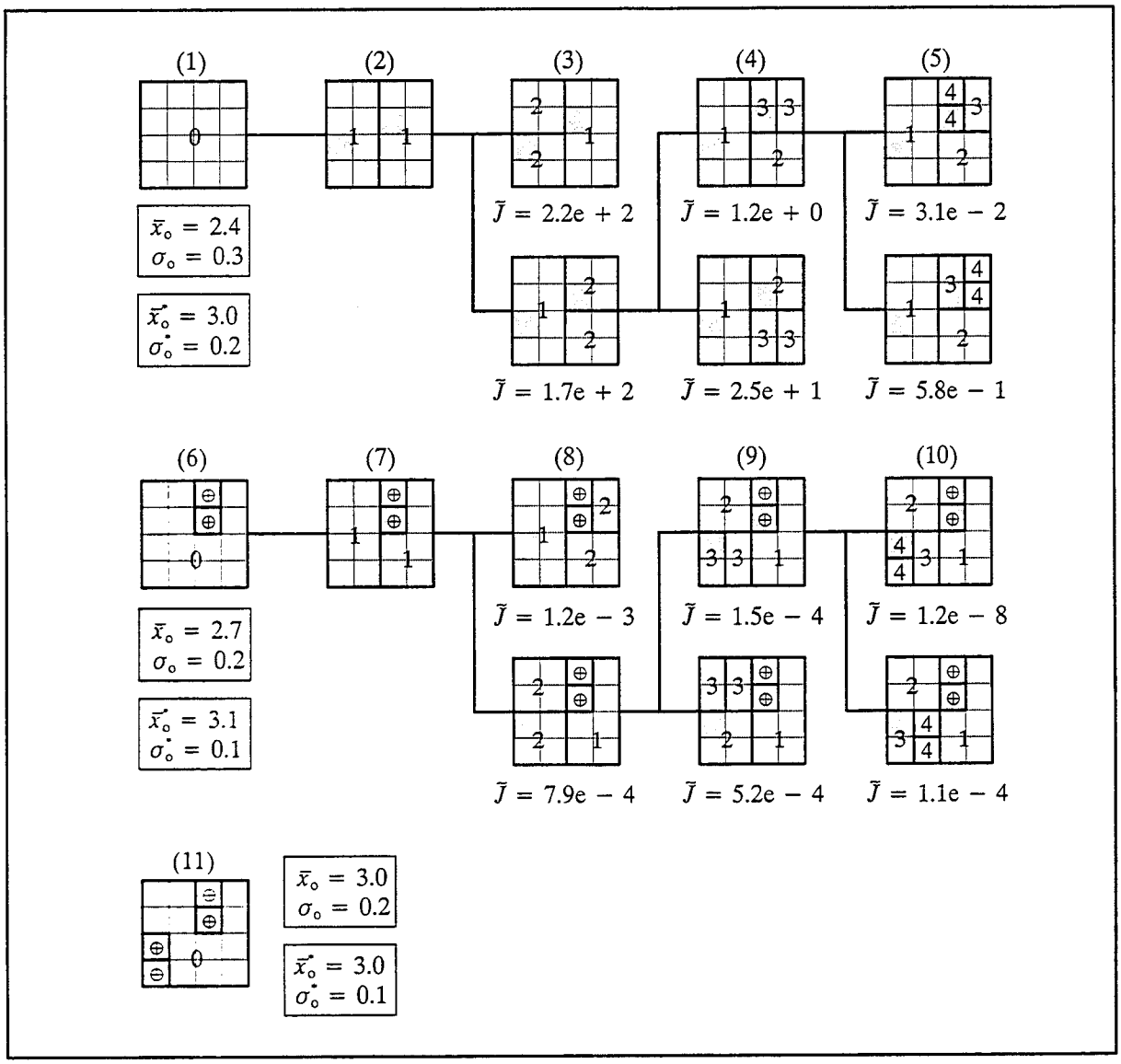

Figure 3.6 Schematic illustration of the parameter group-updating process for damage localization of a rectangular structure.

groups are not subjected to any further subdivision. In step 6, the baseline parameter grouping is updated based on the initial baseline group of step 1 and the newly created parameter groups for the isolated elements. The group level for the updated baseline group is modified as $\mathcal{L} = 0$ as shown in the illustration. The algorithm proceeds from step 6 to step 10 by subdividing the candidate subgroups in the direction that the value of the grouping index decreases the most. During the subdivision process, the group level of the newly subdivided groups is updated by increasing the value of the previous group level by 1. In step 11, the deepest level of grouping from step 10 is fixed at $\mathcal{L} = \oplus$, and the baseline grouping is updated with the isolated elements. Since the difference in the value of the mean of parameter estimates for the updated baseline parameter group of the damaged and the associated baseline structure falls within a bound set by the values of the corresponding standard deviations, thus, the localization process stops and the isolated elements in step 11 are the potential damage locations.

3.3 Assessment of Damage

The next step of the global damage detection and assessment algorithm is the evaluation of damage in the isolated elements obtained from the parameter group-updating scheme. Each of the isolated elements from the localization process are regarded as potential damage locations in the structure that require further investigation. To determine which elements are actually damaged and to what extent, the parameter estimates associated with each of these elements must be examined. In general, when the measured data are noise-free, an element can be viewed as damaged if its estimated parameter is different from the baseline value. This simple assessment is complicated by the presence of measurement noise. The noise in the measurements can cause the estimated parameter for an element to be different from the baseline value even if there is no damage at all. It therefore seems reasonable to incorporate the sensitivity of the estimated parameter to noise in evaluating the severity of damage.

A simple measure of the sensitivity of the system parameters to noise is the statistical distribution of the parameter estimates. Papadopoulas and Garcia (1998) used a comparison between the probability density functions of the healthy and estimated damage stiffnesses at the element level to identify damage. A set of graphical and statistical probability damage quotients were employed

to determine the confidence level on the existence of damage. The method provides no information on the severity of damage in the structural members. Yeo et al. (2000) determined the damage status of a member in the current structure using a hypothesis test. A critical value of the estimated parameter, which is determined based upon the statistical distribution of the baseline parameter estimates, is used as a basis for rejection of the hypothesis that a structural member is not damaged. Both of the proposed approaches approximate the distribution of the estimated system parameters with a normal probability density function. However, the normal approximation is not a valid representation of the statistical distribution of the system parameters in a general case.

Let us assume that the statistical distribution of the parameter estimates of element m is known for both the baseline and the current structures. Further, let us denote a random variable X_m as the parameter estimate for element m in the current structure with certain parameter grouping and locations of measurements and a random variable X_m^* as the parameter estimate for the same element which corresponds to a parameter estimation problem of the associated baseline structure using the same parameter grouping and locations of measurements. Damage in element m of the current structure can be assessed by comparing the statistical distributions of the element parameters in the baseline and the current structure as shown in Figure 3.7 where the random variables X_m and X_m^* are assumed to be continuous. In the illustration, f_{X_m} and F_{X_m} denote the probability density function and the cumulative distribution function of the random variable X_m, and f_{X_m} denote the probability density function of the random variable X_m^*. Element m is regarded as damaged in the event that $X_m < X_m^*$. This event can be described in terms of probability $P(X_m < X_m^*)$ to account for the uncertainty of the parameter estimates. The probability $P(X_m < X_m^*)$ represents a realistic measure of the state of the structural system. Let us denote x_m and $\hat{x}_m^*$ as a current estimate and the a priori known baseline parameter value for element m, respectively. We define the level of damage as

$$\theta_m \equiv \frac{\hat{x}_m^* - x_m}{\hat{x}_m^*} \tag{3.7}$$

With the above definition, the state of element m in the current structure can be described by the event that the true level of damage lies beyond the prescribed level of damage (i.e.,

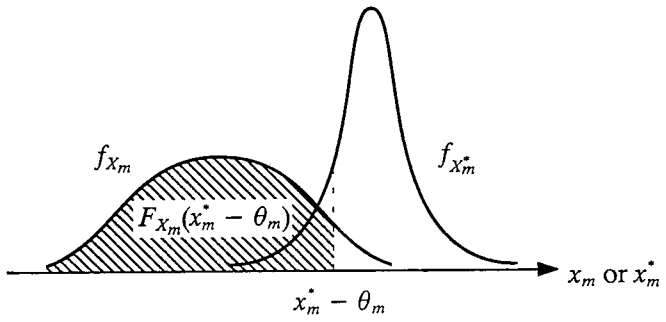

Figure 3.7 Assessment of damage based on statistical distribution of parameters.

$X_m < X_m^* - \theta_m$). Let us assume, for the moment, that X_m and X_m^* are discrete random variables. With a specified level of damage θ_m, the required probability can be formulated as follows:

$$P(X_m < X_m^* - \theta_m) = \sum_{\text{all } x_m^*} P(X_m < X_m^* - \theta_m | X_m^* = x_m^*) P(X_m^* = x_m^*) \tag{3.8}$$

It is reasonable to assume that the parameter estimates in the current and the baseline structure, X_m and X_m^*, are statistically independent; that is,

$$P(X_m < X_m^* - \theta_m | X_m^* = x_m^*) = P(X_m < x_m^* - \theta_m) \tag{3.9}$$

For continuous X_m and X_m^*, equation (3.8) becomes

$$P(X_m < X_m^* - \theta_m) = \int_0^\infty F_{X_m}(x_m^* - \theta_m) f_{X_m^*}(x_m^*) dx_m^* \tag{3.10}$$

The quantity $F_{X_m}(x_m^* - \theta_m)$ on the right hand side of the above equation is illustrated by the shaded area under the curve f_{X_m} in Figure 3.7 in the range $(-\infty, x_m^* - \theta_m]$.

To obtain the statistical distribution of a system parameter, the measured data perturbation scheme of Shin and Hjelmstad (1994) can be used to generate a Monte Carlo sample of the system parameters. As described in Chapter 2, a series of parameter estimation is performed in the data perturbation method using the perturbed data sets, which are generated from a given set of measured eigenvector. Each artificial set of perturbed eigenvector is created by adding a uniformly

distributed random noise vector to the measured eigenvector. Note that the measured data perturbation scheme is applied to obtain the sensitivity information for the cluster of solutions around the noise-free global minimum of the parameter estimation objective function. Hence, the mean of the global minima $\bar{\mathbf{x}}^{**}$, previously identified using the GPE algorithm, can be used as a fixed starting point in the parameter estimation algorithm for each perturbed data set.

3.4 Summary

Global damage detection of structural systems using measured modal response is a complicated problem. For complex structures where the measured data are typically sparse, the limited quantity of data must be utilized to detect damage locations. The algorithm outlined in this chapter approaches the problem with a parameter group-updating strategy. We have focused on the question of uniqueness of solutions to the parameter estimation problem with sparse and noisy data. A unified approach, based upon the method of random starting points and the optimum sensitivity analysis described in Chapter 2, has been adopted to assess the multiplicity of solutions and the sensitivity of parameter estimates to noise. Selection of noisy subsets of measurement locations that reduce errors in the parameter estimates has been considered in the algorithm. The use of the best solution cluster, indicated by the lowest parameter estimation objective function, as a basis for group subdivision in the damage localization process has been described. A new parameter grouping index for determining which parameter group should be subdivided at each level of the parameter group-updating process has been proposed. The sensitivity of the system parameters to noise in the measurements is explicitly taken into account in developing the termination criterion of the algorithm. The algorithm assesses the severity of damage in an element by comparing the statistical distributions of the element parameter for the damaged and the associated baseline structures under the same test conditions. To represent a realistic measure of the state of the structural system, a probability value for the event that the true level of damage in an element is larger than the prescribed level of damage is calculated for each suspected level of damage.

CHAPTER 4

SIMULATION STUDY – A BRIDGE TRUSS

4.1 Introduction

A global damage detection method was presented in the previous chapter based on a parameter estimation method using a finite element model and the measured modal response of a structure. The algorithm detects the location and size of damage based on the changes in the element constitutive parameters from the baseline values. The location of damage is determined by using a parameter group-updating scheme to find the optimal parameter grouping in which the damaged elements are grouped separately from undamaged elements. Upon completion of the parameter group-updating process, damage in each of the isolated elements is assessed based on the statistical distribution of the element parameters for the current and the associated baseline structure to account for the sensitivity of parameter estimates to measurement errors.

Measured free-vibration response of a structure required in global damage detection is usually obtained from a modal test. In the testing process, the test structure is subject to excitations from which the structural responses are measured. Generally, the measured response of the test structure tends to be polluted with measurement noise. In the presence of noisy measurements, the damage detection algorithm will give results different from those with noise-free data. The noise in the measurements can cause the algorithm to identify the damaged elements as undamaged or undamaged elements as damaged, or the algorithm may fail to localize damage at all. Practical applications of a global damage detection algorithm requires that the effect of measurement noise on the algorithm be taken into account.

In this chapter, the effect of measurement errors on the behavior of the proposed damage detection and assessment algorithm is examined using a numerical study of a bridge truss. The simulation study is selected over the real case study because the intent of the present chapter is not to illustrate the use of algorithm in practice, but rather to study its behavior in the face of noisy information. Simulation is a method of experimentation that allows such a study to be carried out

in a controlled environment. In simulation studies, the issue of modeling error is avoided by generating the measured data with the model that is used as the basis of the damage detection scheme. Thus, the assumed mathematical model can be taken as a valid representation of the real structure. In the present study, the measured data are generated by adding proportional random errors with known statistical properties to the analytical response of the finite element model of the structure. Different levels of noise in the measurements are investigated by varying the amplitude of the imposed proportional errors.

In accord with the assumptions of the algorithm, the baseline parameter values must be known at the outset of the damage detection process. These values may be determined by a prior application of the parameter estimation algorithm with measured data from the undamaged structure. The purpose of the baseline parameters is threefold. First, the random starting points used in identification of the multiple solutions to the parameter estimation problem associated with each step of damage localization are calculated based upon the values of the baseline parameters. Second, the baseline parameters provide the basis for termination of the parameter group-updating algorithm. Finally, the statistical distribution of the baseline parameters is used in an assessment of damage. In addition to the baseline information, field test conditions of the current structure (e.g., number and locations of model degrees of freedom with measurement information and amplitude of noise in the measurements) are essential to the current damage detection algorithm. The initial set of measured locations is used in selection of the near-optimal subset of measurements for the parameter estimation problem at each damage localization step. In addition, the amplitude of measurement noise is used as input to the measured data perturbation scheme (Shin and Hjelmstad 1994) to examine the sensitivity of parameter estimates to noise.

4.2 Description of the Example Structure

The structure we investigate herein is a two-span continuous truss structure with the geometry and topology shown in Figure 4.1. The finite element model of the truss structure consists of 35 elements with 28 degrees of freedom. The baseline properties of the truss members are characterized by four parameter groups that comprise the initial baseline parameter grouping. The sectional area and the mass of the truss members associated with each of the initial baseline groups

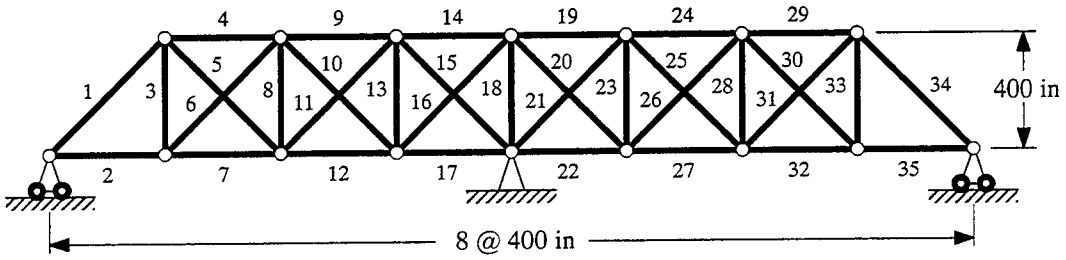

Figure 4.1 Geometry and topology of bridge truss.

are listed in Table 4.1. Note that in addition to the self-weight of the structural members shown in the table, we assume that the dead load of the structure is uniformly distributed along all 35 members with a mass density equal to 0.017 kips$-$ sec^2 /ft/ft. Moreover, all members are assumed to have Young's modulus of 4.176×10^6 kips/ft^2.

In the current algorithm, the number of structural vibration modes with measurement information and the locations of measurements must be specified as input for the parameter estimation problem at each step of the parameter group-updating process. We assume that the natural frequencies and mode shapes of the first six modes of the structure are available as our measurement information. In addition, the mode shapes are assumed to be measured at a certain subset of degrees of freedom of the structural model as shown in Figure 4.2. The structural responses obtained from a free-vibration eigenvalue analysis of the baseline structure at the sampling locations are shown in Table 4.2. In the table, the ith mode shape $\boldsymbol{\phi}_i$ is scaled such that $\boldsymbol{\phi}_i^T \mathbf{M} \boldsymbol{\phi}_i = 1$.

Table 4.1 Baseline properties of bridge truss.

Group	Member	Area (in^2)	Mass (kips$-$ sec^2 /ft/ft)
1	Top	40.0	0.00425
2	Bottom	48.0	0.00510
3	Vertical	30.0	0.00340
4	Diagonal	32.0	0.00318

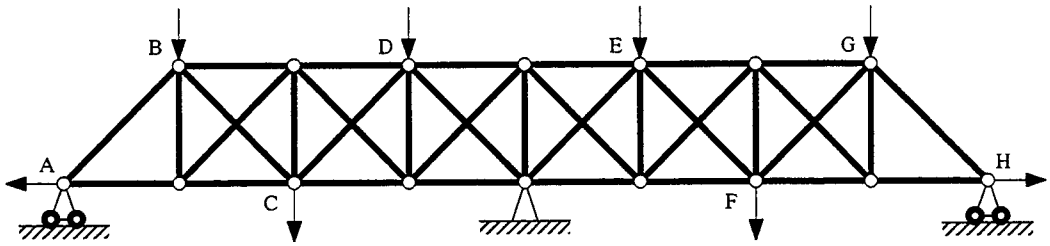

Figure 4.2 Initial set of measured degrees of freedom for bridge truss.

4.3 Damage Detection and Assessment

Four damage scenarios are investigated in the current example to study the behavior of the proposed damage detection and assessment algorithm. For each damage case, damage is simulated with the reduction in the sectional area of the truss member. Table 4.3 summarizes different cases of damage considered in this study. Note that the modal displacements of the damaged structure sampled at the model degrees of freedom shown in Figure 4.2 are used as the initial set of measurements during the damage localization process for each of the damage cases in the table. In addition, based on the parameter group-updating scheme, since the initial baseline grouping consists of multiple parameter groups, the group parameters for the initial and updated baseline

Table 4.2 Noise-free data for baseline structure.

	1st Mode	2nd Mode	3rd Mode	4th Mode	5th Mode	6th Mode
Natural Frequency (Hz)	4.79	6.09	8.75	10.45	14.37	15.64
Mode Shape						
Point A	-0.48518	-0.25268	0.65308	0.94340	0.16854	0.27592
Point B	-0.58165	-0.67426	-0.37846	-0.05442	0.86871	0.94557
Point C	-0.77195	-0.86837	-0.46069	-0.14472	0.05697	-0.10140
Point D	-0.55223	-0.57483	-0.10827	0.08419	-0.84991	-0.94273
Point E	0.55223	-0.57483	0.10827	0.08419	-0.84991	0.94273
Point F	0.77195	-0.86837	0.46069	-0.14472	0.05697	0.10140
Point G	0.58165	-0.67426	0.37846	-0.05442	0.86871	-0.94557
Point H	-0.48518	0.25268	0.65308	-0.94340	-0.16854	0.27592

Table 4.3 Different damage scenarios for bridge truss.

Case	Damaged Members	Noise Level	Remarks
I	$A_{12} = 12.0\ in^2$	5%	- Single damaged member
		10 %	- Different levels of noise
		20 %	
II	$A_{12} = 38.4\ in^2$	5%	- Single damaged member
		10 %	- Light damage
		20 %	- Different levels of noise
III	$A_{12} = 12.0\ in^2$	5%	- Two damaged members
	$A_{14} = 10.0\ in^2$	10 %	- Different levels of noise
		20 %	
IV	$A_5 = 8.0\ in^2$	5%	- Three damaged members
	$A_{12} = 12.0\ in^2$	10 %	- Different levels of noise
	$A_{14} = 10.0\ in^2$	20 %	

groups that are not subjected to subdivision must be fixed at the nominal baseline values during the search for the damaged element within the subdivided baseline group.

The random starting point method adopted in the current algorithm requires that a sufficient number of population of random starting points be created in order to assess the multiplicity of solutions to the parameter estimation problem with confidence. For the present study we found that a sample of 100 starting points were adequate for finding all of the possible solutions to the parameter estimation problem at any step of the damage detection algorithm. The corresponding feasible domain of the parameter estimates is limited by the upper bounds of five times the a priori known baseline parameter values $\hat{\mathbf{x}}^*$ and the lower bounds at zero.

In simulation studies, measurement errors can be added to the simulated response of the structure either as proportional errors or absolute errors. Proportional errors generate the largest error at the maximum value of the measurements while absolute errors are added to the simulated measurements regardless of their magnitudes. The actual error in the field falls somewhat between these two types of errors. Nonetheless, we select the proportional error to represent noise in the measurements in the current study. In particular, we simulate noisy measurements from the

noise-free data in accord with equation (2.23) in Chapter 2. The measurement errors in equation (2.23) are randomly distributed with a uniform probability density function, which represents a banded type of error with equal probability of occurrence throughout a predefined limit. For the current study three different levels of noise, i.e., $\varepsilon = 5\%$, 10%, and 20% are investigated. Note that the noise-free data are obtained from a free-vibration eigenvalue analysis of the parameterized finite element model of the structure that corresponds with each damage scenario. Further, since natural frequencies of the structure can be measured accurately in a modal test, we assume that these measured values are noise-free and that only the measured modal displacements are polluted with measurement noise.

4.3.1 Damage Case I

The current simulation is for the case where the sectional area of member 12 is reduced by 75% from 48.0 in.^{2} to 12.0 in.^{2} To generate the measured data we perform an analysis of the finite-element model with the reduced area in member 12. The computed responses are then polluted with proportional random noise using three different amplitudes; $\varepsilon = 5\%$, 10%, and 20%, respectively, in accord with equation (2.23). For each of the noise levels considered, we generate three different measurement data sets from the simulated noise-free response. Note that in the current simulation study, the specific parameter grouping and set of measurement locations determined by the proposed algorithm are applied to the current and the associated baseline structures to obtain the statistical information required for an assessment of damage for the individual noisy data sets. Consequently, the results of the algorithm for each of the noisy data sets can be viewed as statistically independent; that is, no statistical information on the performance of the algorithm can be obtained from using a larger sample of the simulated noisy data sets. Although the possibility that the algorithm will perform poorly with a specified level of measurement noise may be arrived by generating a larger population of simulated measurement data, the cost of the required computations is usually prohibitive for large and complex structures. In the present study, three simulated noisy data sets are sufficient to illustrate the performance of the proposed algorithm in the presence of the measurement noise.

The results of the damage localization process are shown in Figures 4.3, 4.4, and 4.5 for different simulated measurement data sets with 5%, 10%, and 20% noise, respectively. For each of the noisy data sets the near-optimal sets of measurement locations that correspond with the final parameter grouping are illustrated. In the illustration, the lightened lines indicate the isolated structural members from the damage localization process. These isolated members represent potential damage locations in the structure that require further assessment. To assess damage in a structural member, we calculate the probability of the event that the value of the estimated parameter for that member is smaller than the value of the corresponding parameter estimate for the same member in the associated baseline structure to a certain extent. By associating the probability value, $P(X_m < X_m^* - \theta_m)$, with each prescribed level of damage θ_m, we can plot the probability distribution for the range of $0-100\%$ of the level of damage for all members in the structure as shown in the illustration.

The plot of the probability distribution for a structural member can be divided into three parts starting from no damage to 100% damage. The constant unit probability value at low levels of damage indicates that the actual value of the member parameter is actually smaller than the parameter values associated with the damage at these levels. Likewise, the zero probability value at high levels of damage imply that there is no chance for the actual severity of damage to fall within these regions. Generally, the actual level of damage lies in the transition region between the unit probability and zero probability zones that appears as a slope in the probability distribution. Note that the sensitivity of a member parameter to the measurement noise can be drawn from the probability distribution. A sharp drop in the probability values within the transition region indicates a low sensitivity of the member parameter to noise. A member parameter that is more sensitive to noise shows a more gradual decrease in the probability values within the transition zone. Hence, it might be difficult to identify a precise level of the actual damage from the probability distribution when the level of noise in the measurements is high. However, one can always describe the suspected level of damage in terms of probability to ensure the level of confidence in the results.

It can be seen from Figure 4.3 that damage in member 12 is successfully located and quantified for all three data sets with 5% noise. From the plot of the probability distribution, the severity

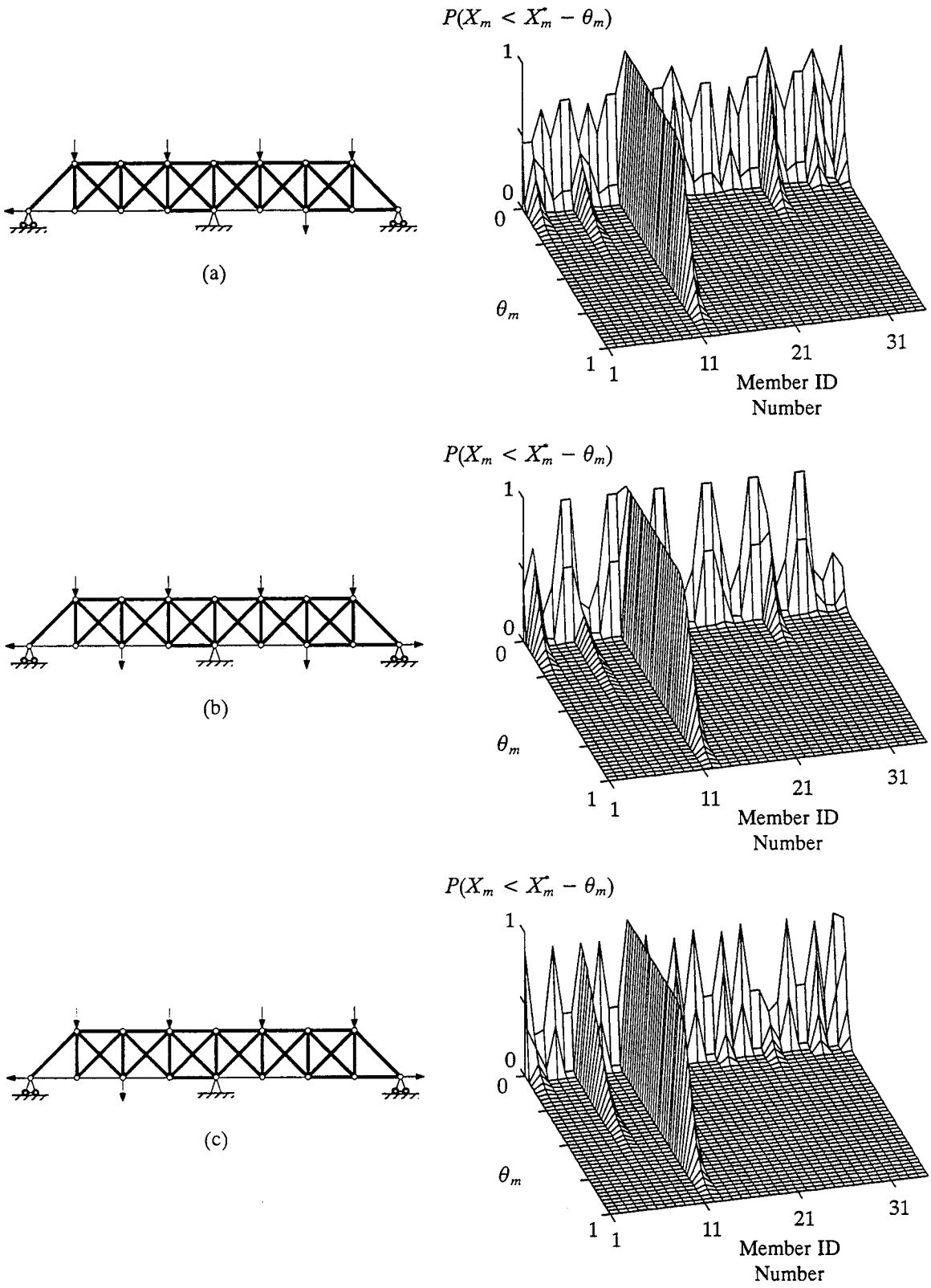

Figure 4.3 Probability distribution in Damage Case I with respect to different levels of damage for three noisy data sets (a), (b), and (c) with 5% noise.

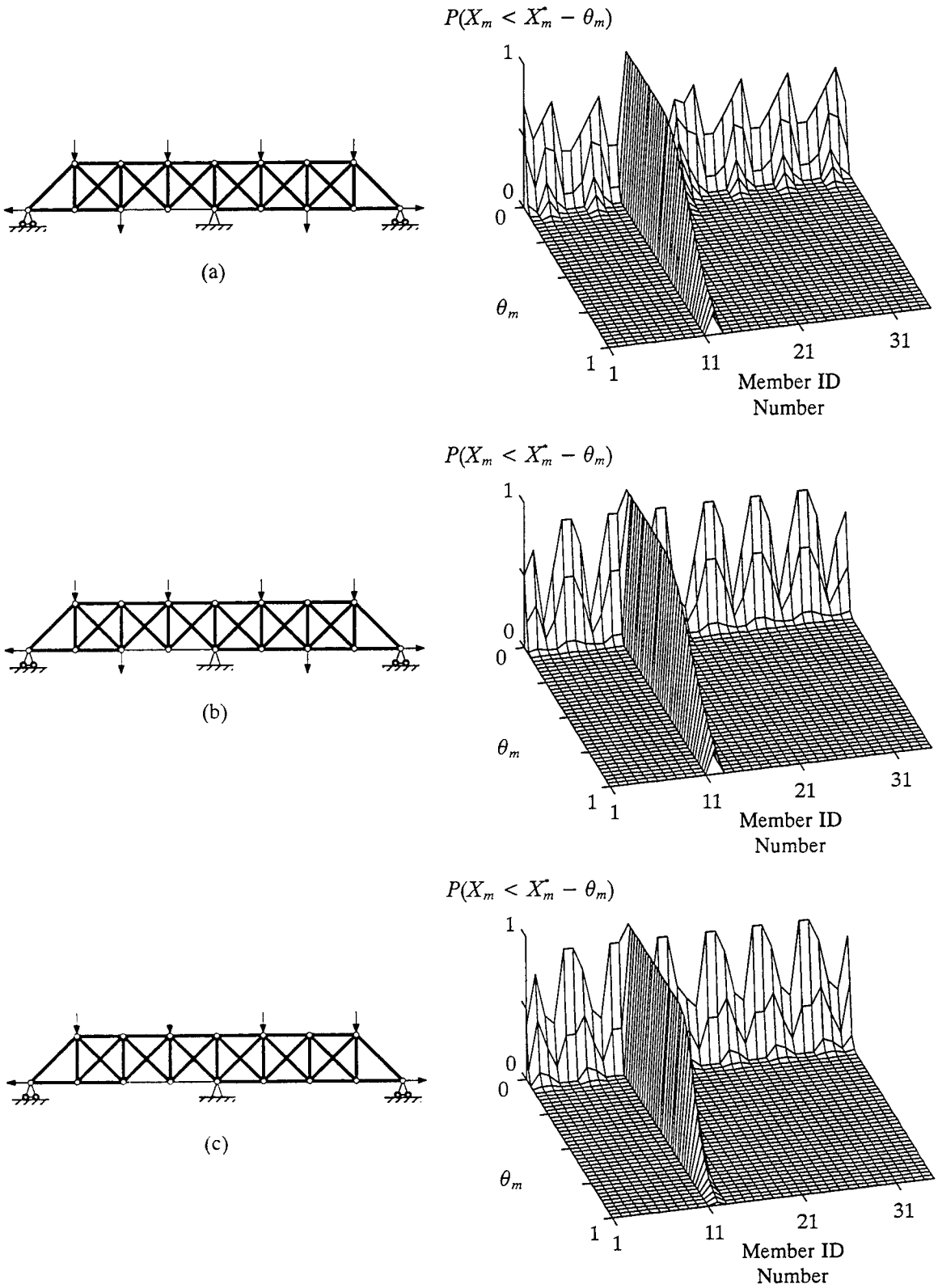

Figure 4.4 Probability distribution in Damage Case I with respect to different levels of damage for three noisy data sets (a), (b), and (c) with 10% noise.

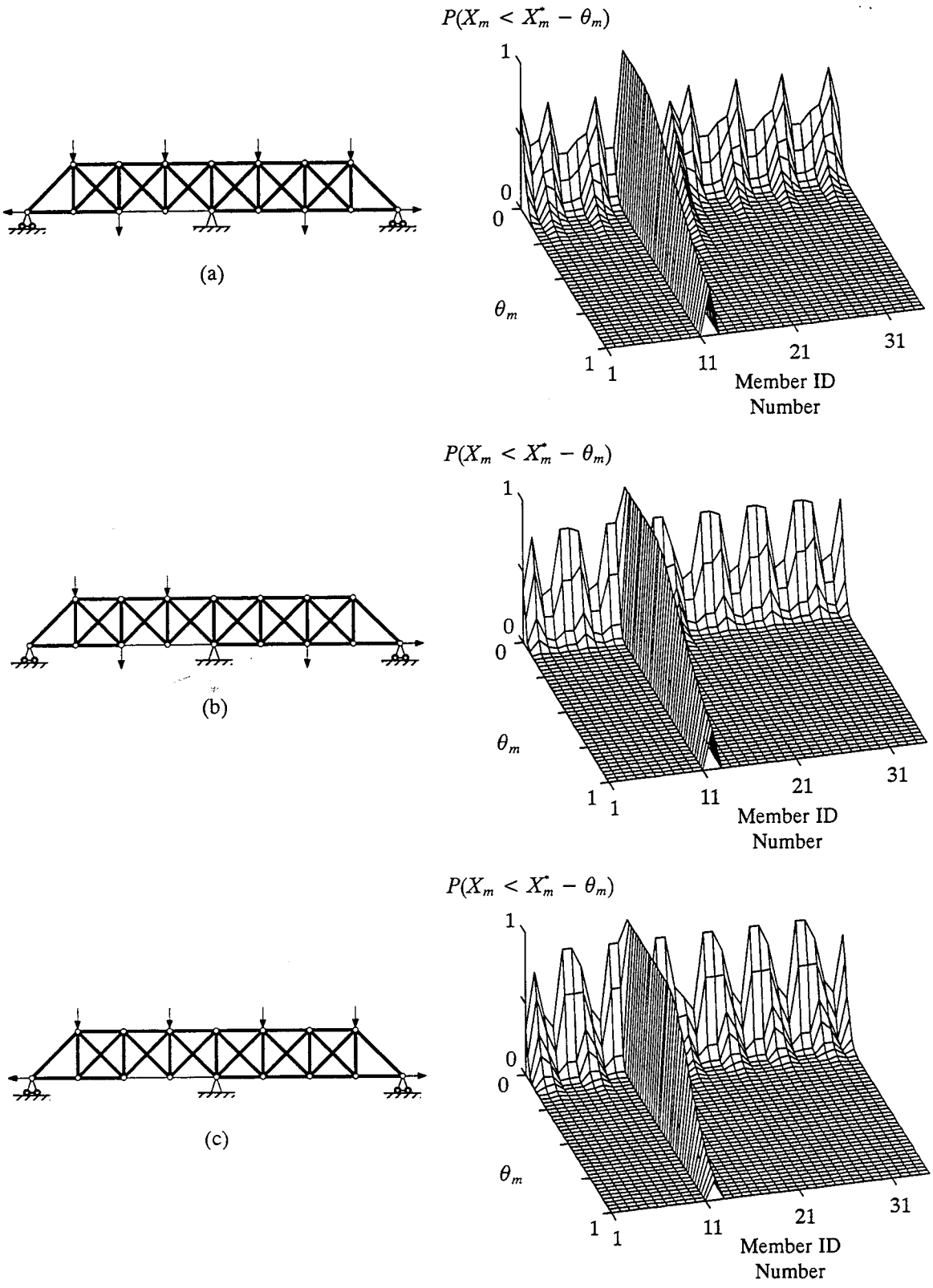

Figure 4.5 Probability distribution in Damage Case I with respect to different levels of damage for three noisy data sets (a), (b), and (c) with 20% noise.

of damage in member 12 is suspected to fall in the range of 60–90%. The level of confidence in identifying a suspected level of damage as the actual damage severity is indicated by the value of $P(X_m < X_m - \theta_m)$. For example, the probability value of 0.85 for 65% damage in member 12 indicates that it is 85% likely that the actual value of the member parameter is smaller than the value of the estimated parameter for member 12 with 65% damage. For the current data sets, members 2, 7, 22 and 27 are also identified as potential damage locations from the localization process. However, based on the probability distribution for the structural members, it is concluded that all these isolated members are not likely to be damaged except for member 7 using data set (c), which indicates a slight chance of the member being lightly damaged. Nonetheless, the probability of damage in member 7 is small compared with that of member 12.

For all measurement cases with 10% and 20% noise, as shown in Figures 4.4 and 4.5, member 12 is also identified as damaged. In addition, it is observed that as the level of noise in the measurements increases, the decrease in the probability values for a structural member in the transition region becomes more gradual. Hence, it is more difficult to identify the actual level of damage in an isolated member. Nevertheless, it is seen from the results of the current simulation that all undamaged members show significantly lower probability of being damaged compared with the actual damaged member.

The set of measurement locations used to obtain sensitivities of the parameter estimates for the current and the baseline structures in an assessment of damage depends upon the final parameter grouping, which is identified from the damage localization process. Generally, different parameter groupings and corresponding sets of measured locations may be obtained from using different noisy data sets. Hence, each noisy data set requires one independent run of the proposed damage localization algorithm, and an individual comparison must be made between the current and the baseline structure to assess the severity of damage for each noisy data set.

4.3.2 Damage Case II

In this damage scenario, the sectional area of element 12 is reduced by 20% from 48.0 in.^{2} to 38.4 in.^{2}, which can be regarded as lightly damaged compared to the previous case. Three different levels of measurement noise are investigated for the current damage case as summarized

in Table 4.3. For each of the noise levels investigated, we generate three different noisy data sets in accord with equation (2.23).

The damage detection and assessment results are illustrated in Figure 4.6 for the three measurement cases with 5% noise. For all measurement cases member 12 can be correctly identified as damaged. The estimated severity of damage falls in the range of 5–30%. For measurement case (a), member 32 shows a tendency of being slightly damaged. However, there is no constant unit-probability zone in the distribution of $P(X_m < X_m^* - \theta_m)$ for this member. Without the existence of this unit-probability zone for the assessed member, one cannot be absolutely positive that damage exists in that member. Hence, it is concluded that the deviation of the parameter estimate for member 32 is merely due to the measurement noise.

The results of the damage detection and assessment algorithm using different simulated data sets with 10% and 20% noise are illustrated in Figures 4.7 and 4.8, respectively. For all measurement cases with 10% noise, the algorithm fails to identify damage in member 12 even though the member has been identified as potential damage location from the damage localization process. Furthermore, the damage localization algorithm was unable to isolate any elements at all with 20% noisy measurements. Hence, it is evident from the current example that the ability of the proposed algorithm to detect damage in a structural system is limited by the severity of the damage in the structural components and the magnitude of noise in the measurements.

4.3.3 Damage Case III

As the third example, let us consider the case where two structural members are damaged, i.e., members 12 and 14. Each of the assumed damage locations are selected from different baseline parameter groups in order to test the capability of the damage detection and assessment algorithm in detecting multiple damage with spatially isolated locations. Damage is simulated with 75% reduction in the sectional area of both members 12 and 14. Three levels of measurement noise are considered: ε = 5%, 10%, and 20%. We simulate three noisy measured data sets for each level of noise.

The results for the simulated noisy data sets with three levels of noise are shown in Figures 4.9–4.11. In these illustrations, the near-optimal set of measurement locations obtained from

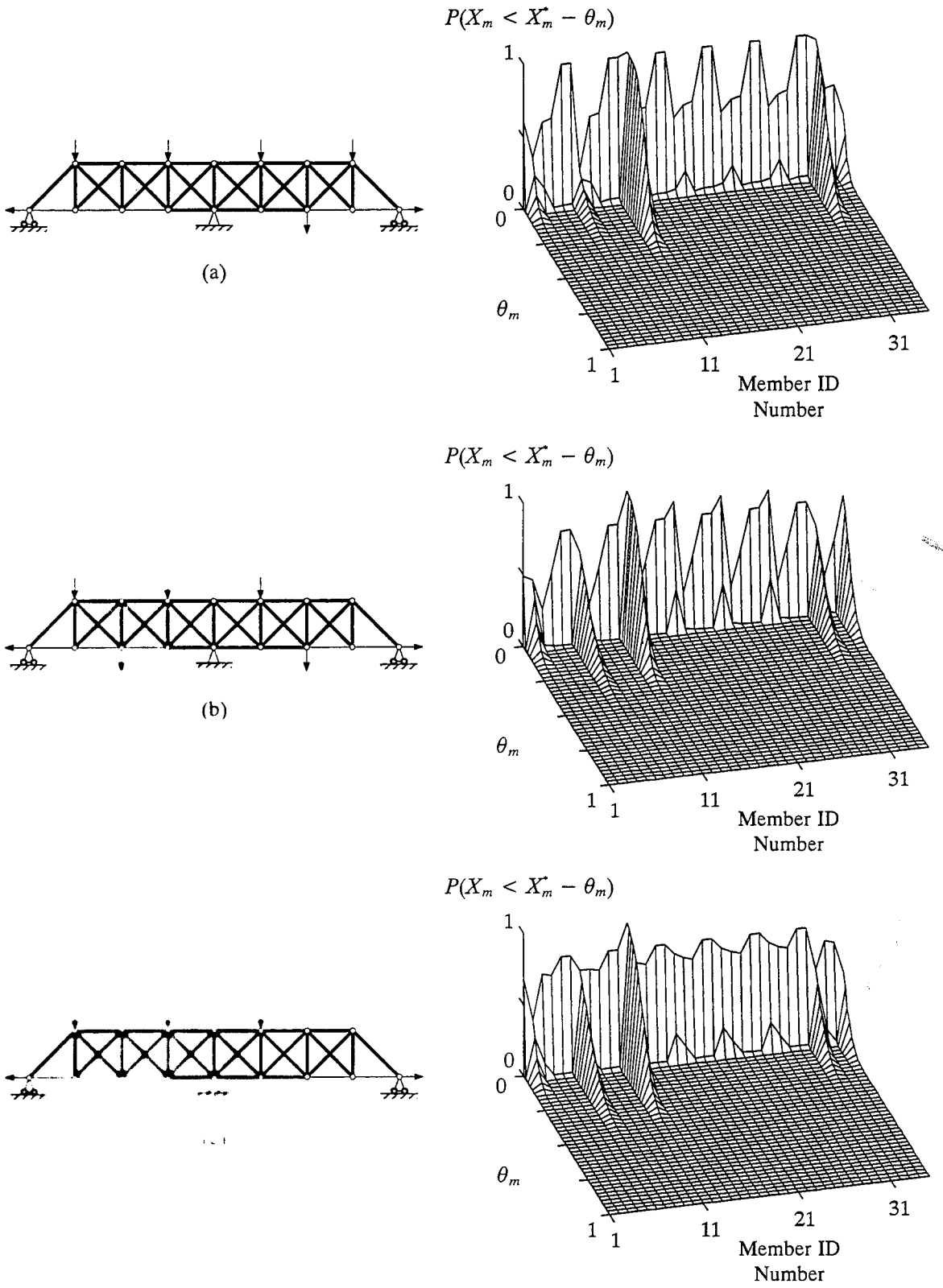

Figure 4.6 Probability distribution in Damage Case II with respect to different levels of damage for three noisy data sets (a), (b), and (c) with 5% noise.

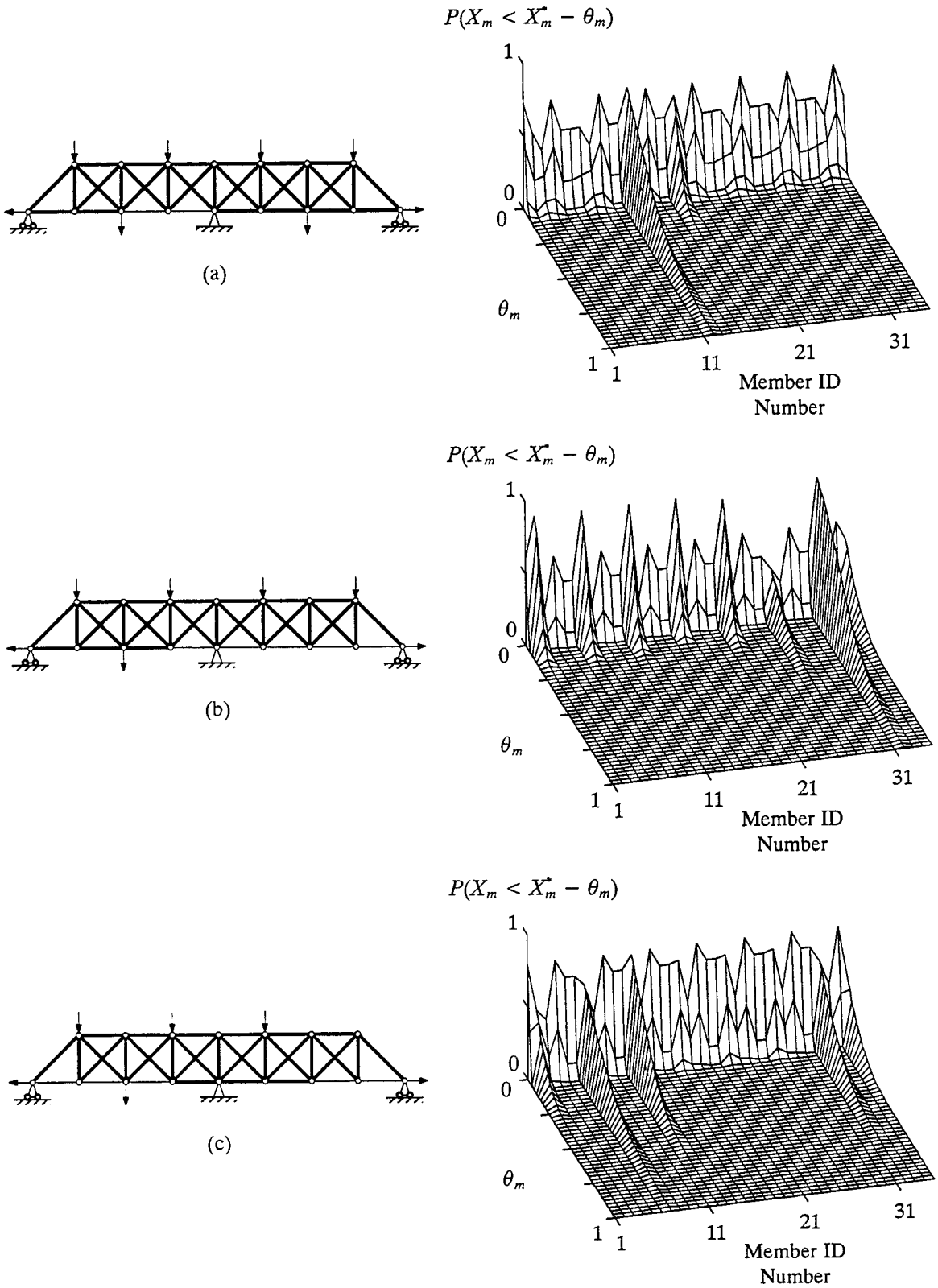

Figure 4.7 Probability distribution in Damage Case II with respect to different levels of damage for three noisy data sets (a), (b), and (c) with 10% noise.

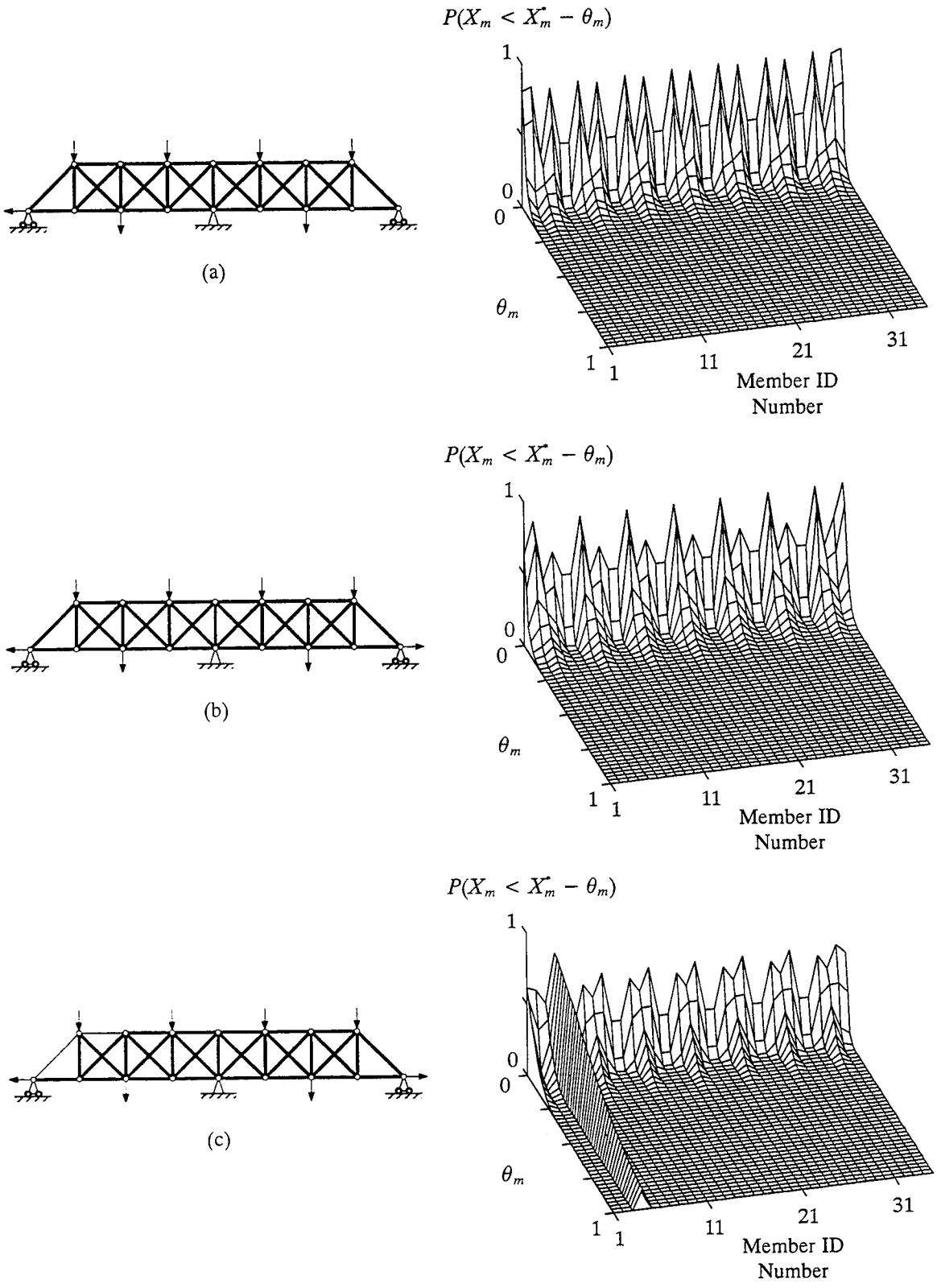

Figure 4.8 Probability distribution in Damage Case II with respect to different levels of damage for three noisy data sets (a), (b), and (c) with 20% noise.

the measurement selection process are shown for each measurement case. The lightened truss members represent the potential damage locations obtained from using the parameter group-updating algorithm. The parameter estimates for these members are subject to evaluation based upon the distribution of $P(X_m < X_m^* - \theta_m)$. In all the measurement cases with 5% noise the algorithm perform well as evident from the correct identification of the actual damage locations. The algorithm was able to isolate members 12 and 14. In addition, the suspected level of damage lies in the vicinities of the actual damage level. However, it is seen that some of the isolated members from the localization process, other than the actual damaged members, also show the probability of being damaged. After a detail examination of the values of $P(X_m < X_m^* - \theta_m)$ for the isolated members, it is concluded that there is little chance of damage in these members.

The results of the algorithm using the simulated noisy data sets with 10% noise illustrates that the actual damage can be accurately located and quantified for all three measurement cases. In addition, based on the distribution of $P(X_m < X_m^* - \theta_m)$ for the structural members, all undamaged elements are correctly identified as undamaged. It is clear that when the existence of the constant unit-probability zone is taken into account, the possibility of mistakenly identifying the false damage locations as damaged is eliminated. Similar results are shown for the 20% noisy measurement cases. In these cases, the probability distribution for the isolated members shows higher sensitivities of the parameter estimates to the measurement noise.

4.3.4 Damage Case IV

This damage case consists of three damaged members. Member 5 is regarded as an additional damaged member from the previous case. The sectional area of member 5 is reduced by 75% from 32.0 in. to 8.0 in. Members 12 and 14 are assumed to have the same level of damage as in Case III. Three different noisy measurements are examined for each of the three levels of noise: $\varepsilon = 5\%$, 10% and 20%.

Figures 4.12 – 4.14 show the probability distribution, $P(X_m < X_m^* - \theta_m)$, for each level of damage θ_m in the structural members using different sets of simulated noisy measurements. It is seen that all damaged members can be detected for all measurement cases with 5% noise. Some undamaged members show the possibility of being slightly damaged. However, since there is no

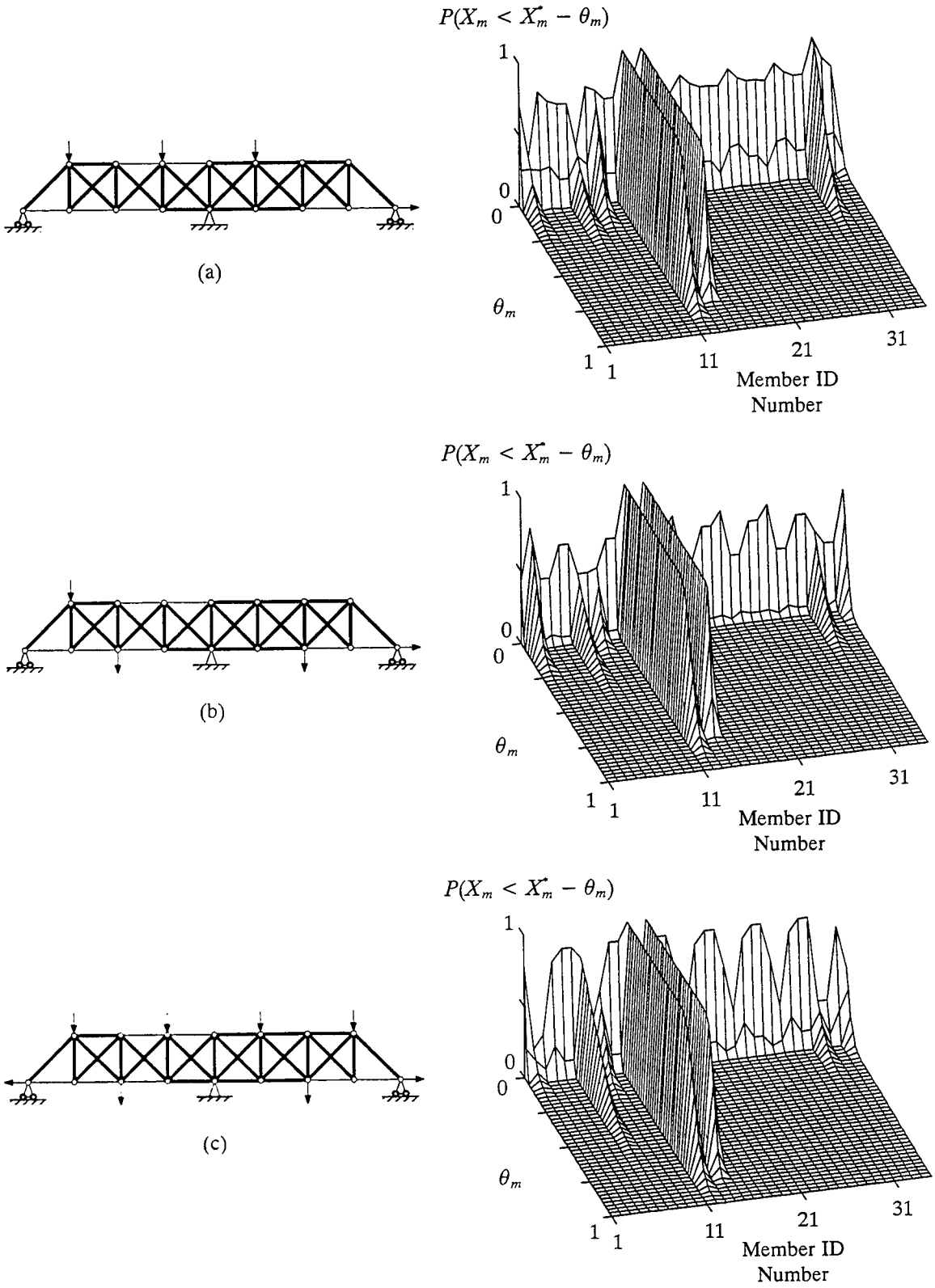

Figure 4.9 Probability distribution in Damage Case III with respect to different levels of damage for three noisy data sets (a), (b), and (c) with 5% noise.

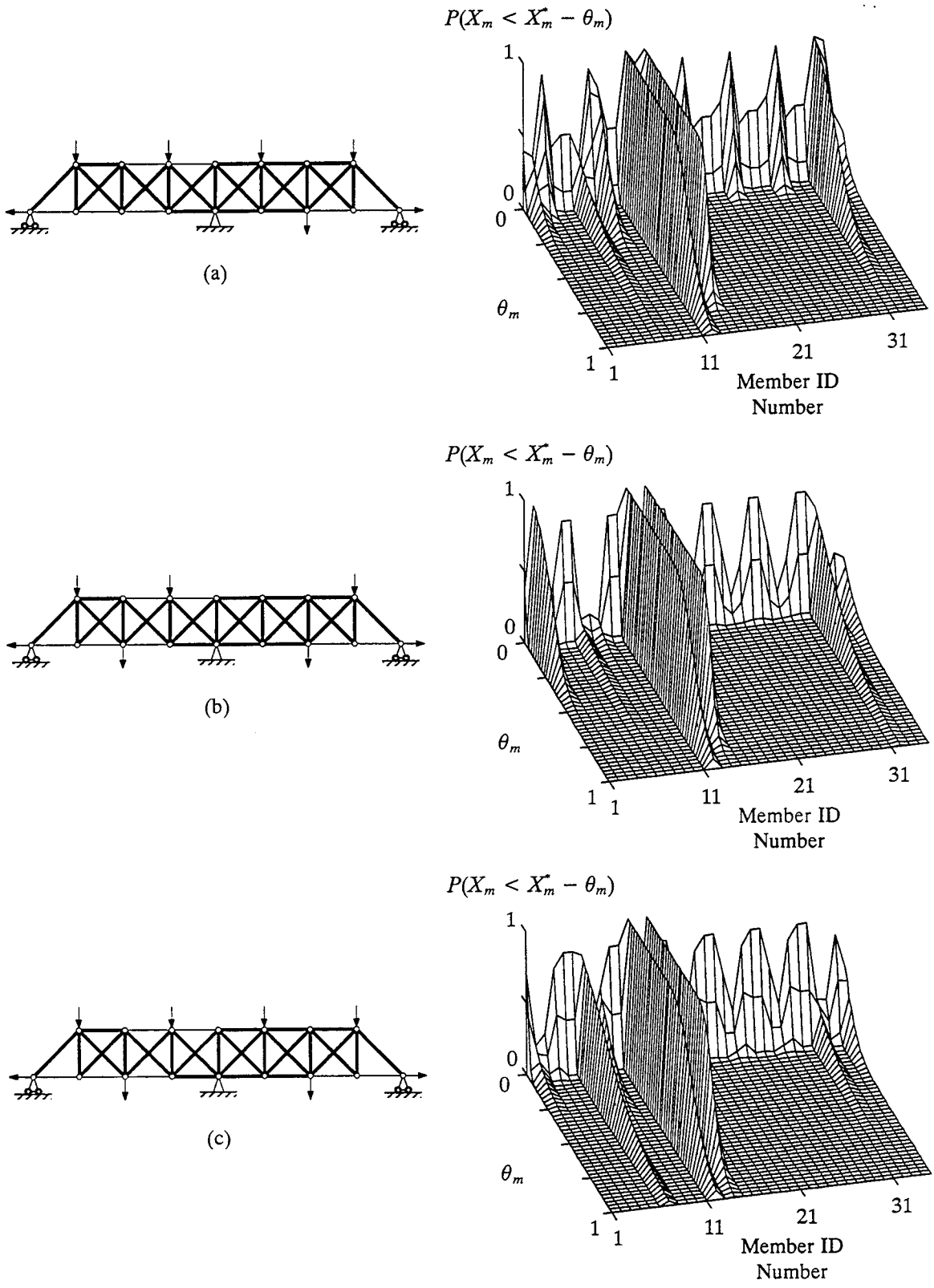

Figure 4.10 Probability distribution in Damage Case III with respect to different levels of damage for three noisy data sets (a), (b), and (c) with 10% noise.

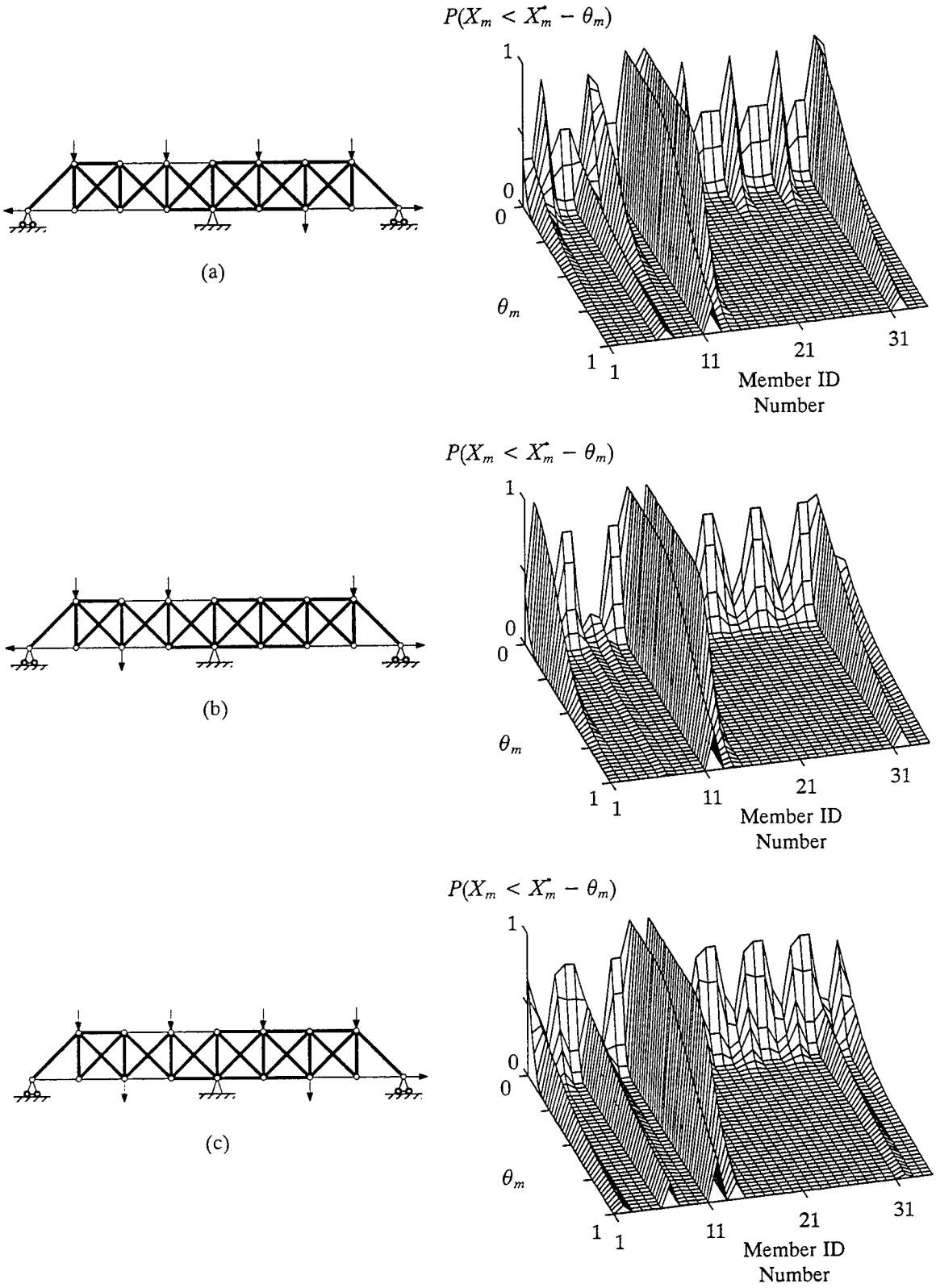

Figure 4.11 Probability distribution in Damage Case III with respect to different levels of damage for three noisy data sets (a), (b), and (c) with 20% noise.

constant unit-probability zone in the probability distribution for these members, they are identified as undamaged. From the results of the damage detection algorithm using different measured data sets with 10% and 20% random noise, it is observed that the parameter group-updating algorithm fails to isolate member 5 as a potential damage location. For 10% noisy measurements, the algorithm incorrectly identifies member 2 as an additional damaged members from the actual ones. The same sort of results are shown for the 20% noisy measurements. It is suspected that failure of the algorithm to isolate member 5 leads to an inaccurate assessment of damage in other members.

It is evident from the present example that the performance of the proposed damage detection and assessment algorithm decreases as the level of noise in the measurements increases. The current algorithm detects and assesses damage in a structure based upon changes in the structural response as a result of damage. When the measured response of the structure is significantly polluted with noise, these changes are difficult, if not impossible, to detect. In other words, the essential information for detection of damage in the structure are swamped out by noise in the measurements. In addition, damage in an insensitive structural member, such as a diagonal member of a truss, is generally more difficult to detect compared with the sensitive members. However, as evident from the above example, any insensitive but damaged member can be detected by the developed algorithm when the amplitude of noise is small enough.

4.4 Summary

The damage detection and assessment procedure developed in the previous chapter has been tested with a certain set of simulation case studies for a two-span continuous truss structure. Through simulation studies, the procedure of assessing damage in the presence of the measurement noise was illustrated. Evaluation of the statistical distribution of the parameter estimates at the potential damage locations has proved reliable as a method for assessing whether damage is detectable above the noise in the measurements. From the simulation results, it is concluded that the proposed algorithm can detect and assess damage effectively using sparse and noisy data. Although there are always cases where actually damaged elements are detected as undamaged

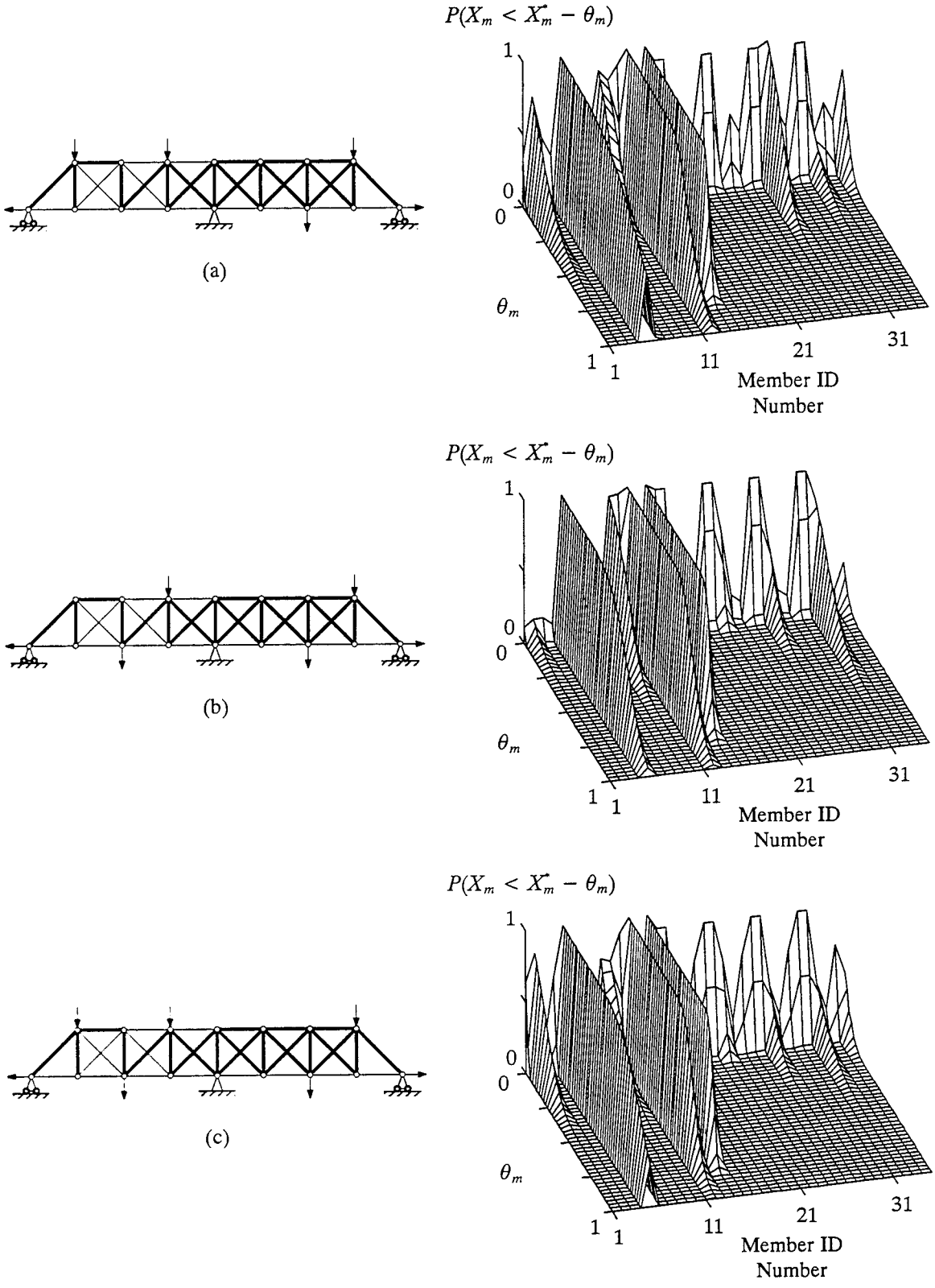

Figure 4.12 Probability distribution in Damage Case IV with respect to different levels of damage for three noisy data sets (a), (b), and (c) with 5% noise.

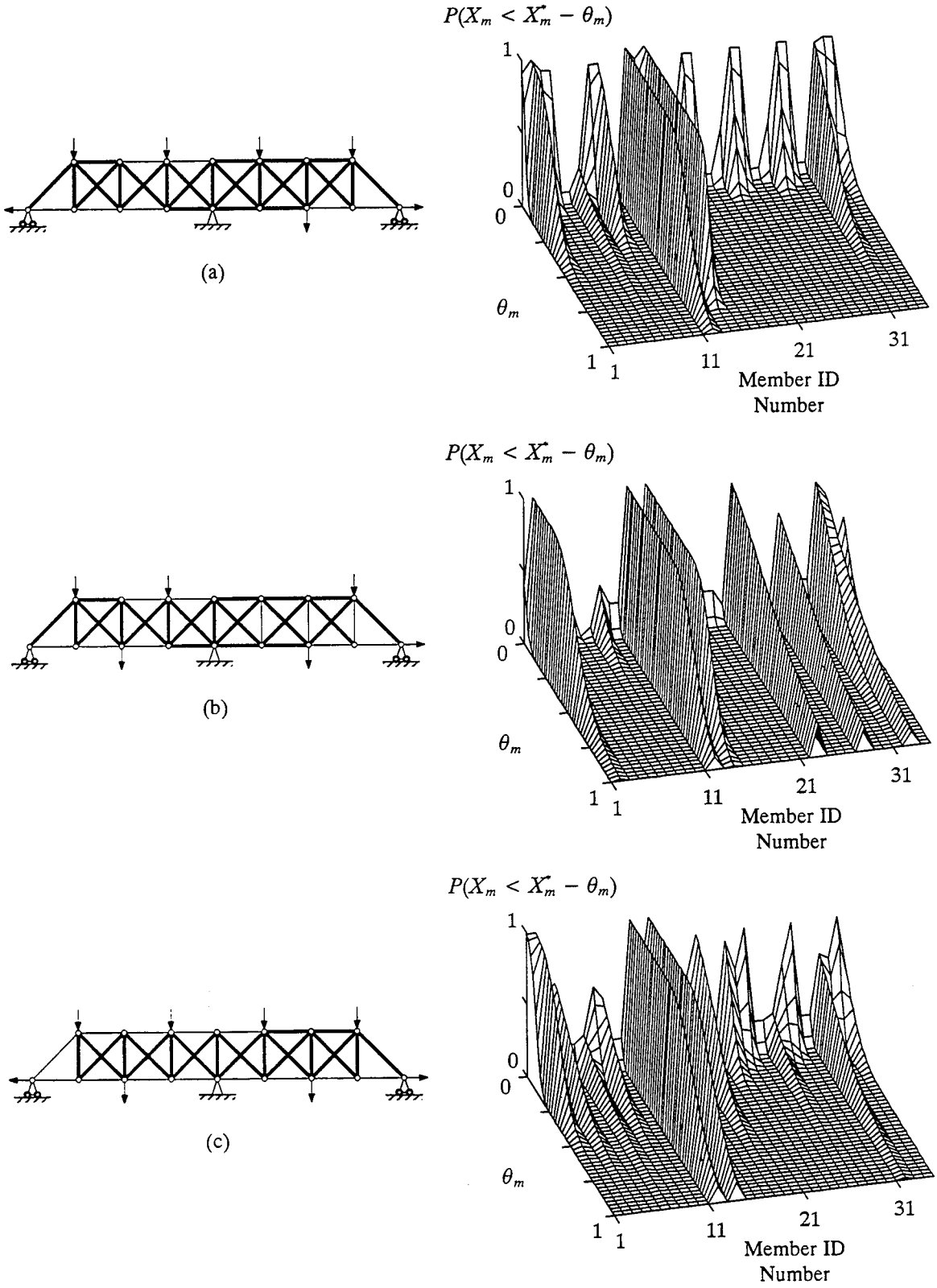

Figure 4.13 Probability distribution in Damage Case IV with respect to different levels of damage for three noisy data sets (a), (b), and (c) with 10% noise.

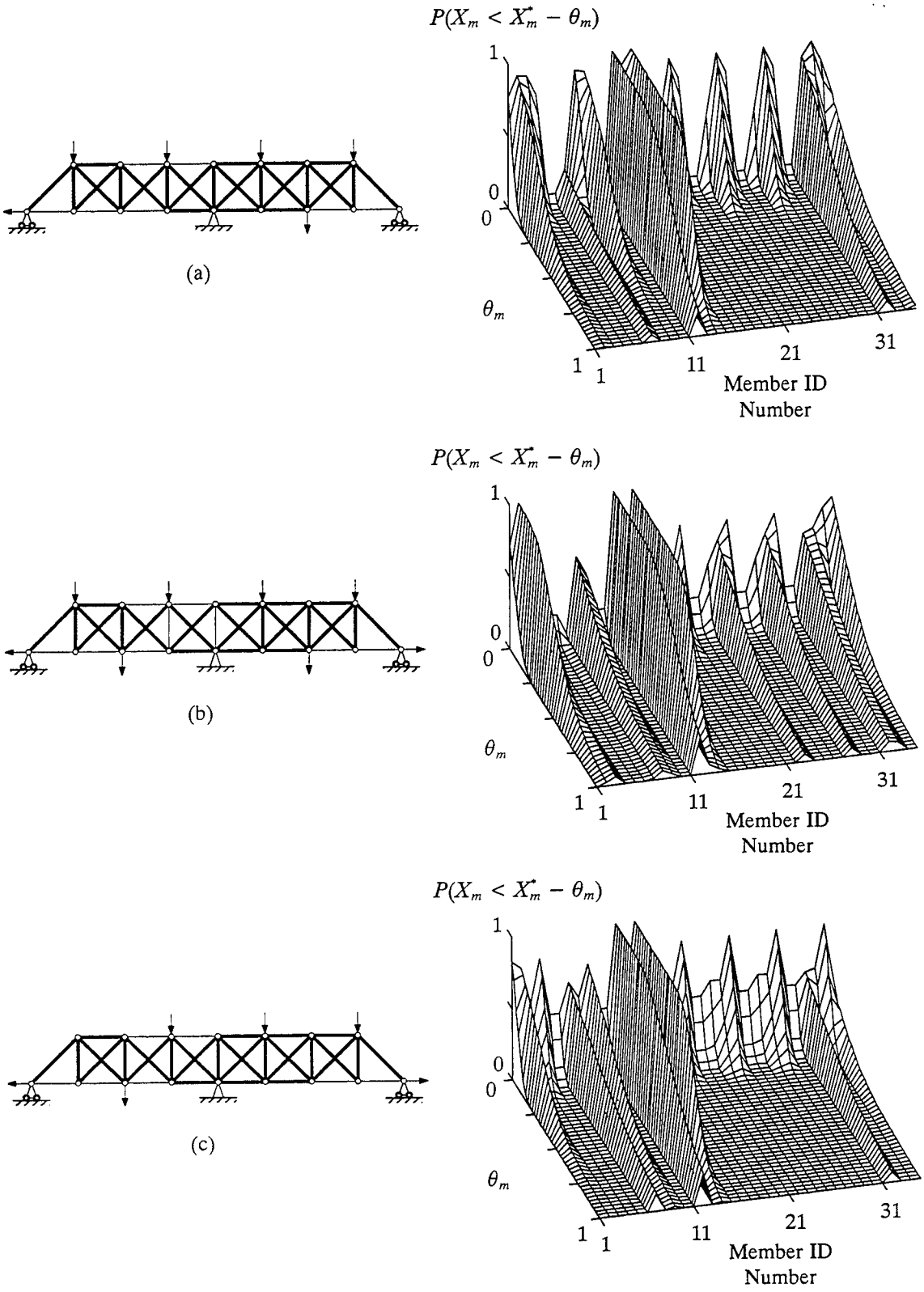

Figure 4.14 Probability distribution in Damage Case IV with respect to different levels of damage for three noisy data sets (a), (b), and (c) with 20% noise.

or actually undamaged elements are detected as damaged, the results has been shown to improve dramatically when the level of noise in the measurements decreases.

One of the advantages of the present algorithm is that the algorithm takes into account explicitly the multiplicity of solution to the parameter estimation problem associated with each step of the damage localization process. In general, parameter estimation problems can have multiple solutions when the measured data are spatially sparse. Without considering the possibility of solution multiplicity, the algorithm may lead to erroneous damage locations or the algorithm may fail to converge at all. Furthermore, the systematic statistical evaluation of damage in the current algorithm allows an assessment of damage in a more reliable manner by incorporating the sensitivity of the member parameter due to the current measurement conditions. With the present method, damage in all members of a structure can be evaluated regardless of their sensitivities, even though damage in an insensitive member might be difficult to detect if the noise level is high. In addition, the algorithm can evaluate the sensitivity of each member parameter simultaneously with the parameter group-updating process. Hence, the sensitivities of the member parameters need not be determined before attempting to detect damage in the structure.

CHAPTER 5

SIMULATION STUDY – A TOWER TRUSS

5.1 Introduction

It has been shown in the previous chapter that the proposed damage detection and assessment algorithm can be used to evaluate damage in a two-span bridge truss effectively even when the measured data are spatially sparse and are noise-polluted to a certain level. In this chapter, the algorithm is tested with an additional structure: a tower truss. In the current example, the structure is modeled with simple truss elements whose responses are measured in a three-dimensional coordinate space. It is expected that the modes of behavior of the tower truss and, hence, the outcome of the corresponding parameter estimation problem will be significantly different from those of the bridge truss in the previous example. The main objective here is to study the performance of the present algorithm in detecting damage in a different type of structures using sparse and noisy measurements.

Numerical simulation studies are employed herein to examine the capabilities of the algorithm in detecting and assessing damage in the tower truss. Damage is simulated with a reduction in the sectional area of the truss members. The modal response of the tower truss is computed from a free-vibration eigenvalue analysis of the finite element model of the structure with reduced sectional areas in certain truss members in accord with each damage scenario. Different levels of noise in the measurements are investigated by adding different amplitudes of proportional random errors to the calculated structural responses.

5.2 Description of the Example Structure

Let us consider a tower structure with pinned base as illustrated in Figure 5.1. The structure is modeled as a three-dimensional truss with 76 elements and 72 degrees of freedom. The initial baseline parameter grouping for the finite-element model of the structure consists of nine parameter groups. The sectional area and the mass of the structural members in each baseline parameter

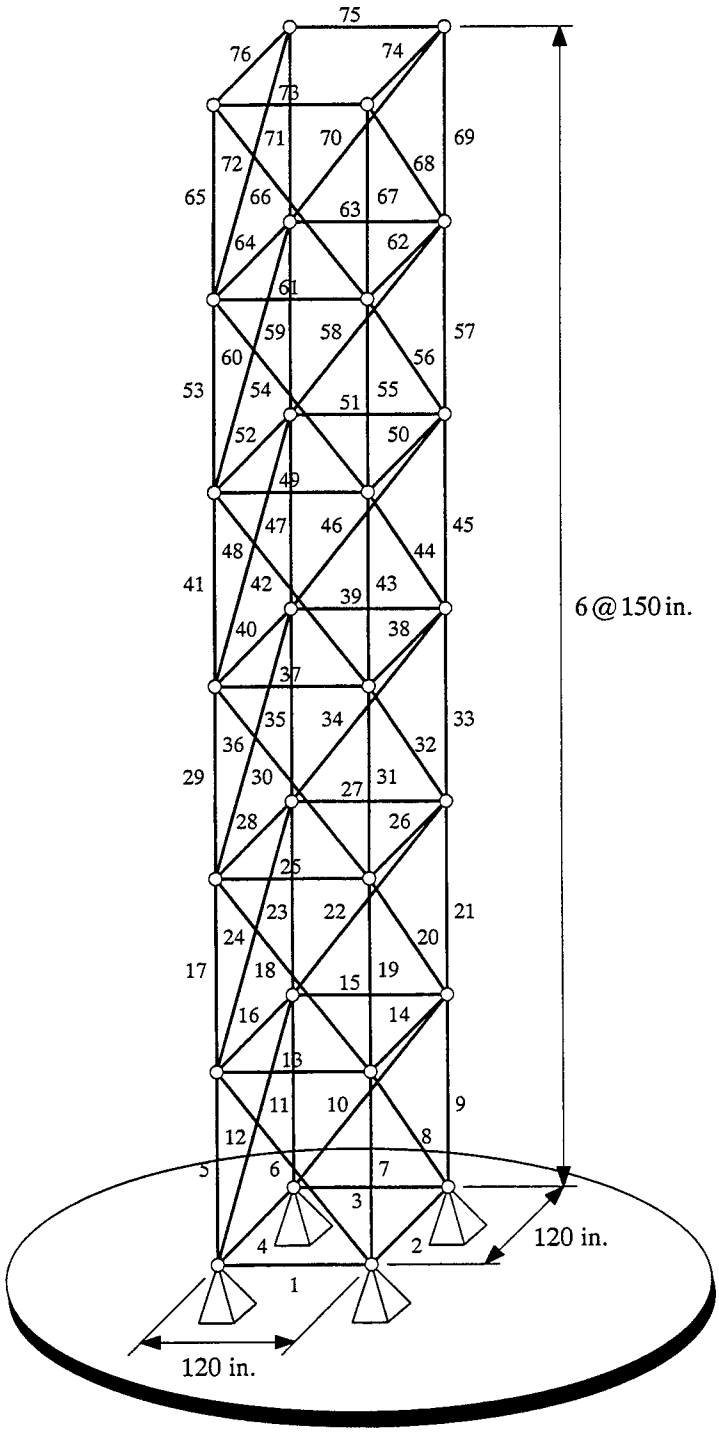

Figure 5.1 Geometry and topology of tower truss.

group are summarized in Table 5.1. Note that the mass of the truss members is assumed to be known in advance and does not change as a result of damage. In addition, the initial baseline parameter grouping in Table 5.1 is employed to enhance computational efficiency of the parameter group-updating scheme in localizing multiple damage locations in the truss structure. By assigning a small number of structural members to each baseline parameter group, the number of parameter grouping steps required in localization of potential damage locations within each of the baseline parameter groups is reduced, and hence the algorithm is able to isolate multiple damage more efficiently. In the current study we assume that all the truss members have Young's modulus of 4.176×10^6 kips/ft^2.

As mentioned in the previous chapter, the initial subset of model degrees of freedom of the structure must be specified for selection of the near-optimal set of measurement locations in the damage detection process. We shall assume that the modal displacements of the structure are measured at the degrees of freedom of the finite-element model as shown in Figure 5.2. In addition, we assume that the natural frequencies and mode shapes at the sampling locations for the first ten modes of the structure are given as our measurement information. The modal response of the structure obtained from a free-vibration eigenvalue analysis of the baseline finite-element model is illustrated schematically in Figure 5.3. In the illustration, ω_i denotes the natural frequency of the ith vibration mode of the structure.

Table 5.1 Baseline properties for tower truss.

Group	Member	Area (in.^{2})	Mass (kips$-$ sec^2 /ft/ft)
1	5, 7, 9, 11, 17, 19, 21, 23	40.0	0.004032
2	29, 31, 33, 35, 41, 43, 45, 47	40.0	0.004032
3	53, 55, 57, 59, 65, 67, 69, 71	40.0	0.004032
4	1-4, 13-16, 25-28	20.0	0.002016
5	37-40, 49-52	20.0	0.002016
6	61-64, 73-76	20.0	0.002016
7	6, 8, 10, 12, 18, 20, 22, 24	22.0	0.002218
8	30, 32, 34, 36, 42, 44, 46, 48	22.0	0.002218
9	54, 56, 58, 60, 66, 68, 70, 72	22.0	0.002218

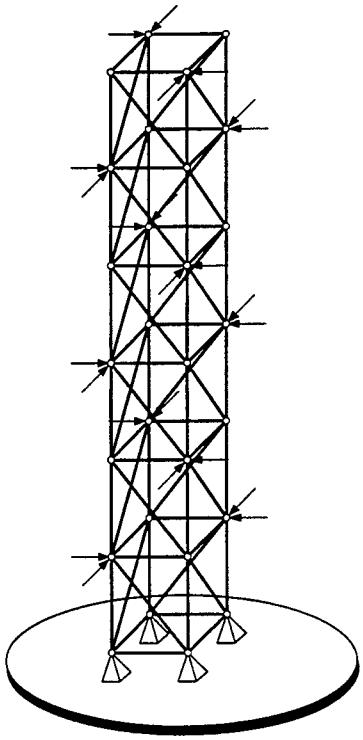

Figure 5.2 Initial set of measured degrees of freedom for tower truss.

5.3 Damage Detection and Assessment

To investigate the behavior of the global damage detection and assessment algorithm, we perform two simulation case studies: a single damage and multiple damage. The detail of these case studies are summarized in Table 5.2. In accord with the assumption of the algorithm, damage is simulated with a reduction in the sectional area of the truss members. It should be noted that all of the degrees of freedom associated with the nodes of members 1–4 in the finite-element model of the structure can be disregarded from the stiffness assembly because of the pin supports. Consequently, the modal response of the structure is independent of the stiffness contribution from members 1–4 hence, the stiffness parameters of these members need not be estimated and can be fixed at the nominal baseline values.

In the current simulation studies, we use 100 random starting points to assess the multiplicity of solution to the parameter estimation problem at each step of the parameter group-updating algorithm. The mean and covariance of the parameter estimates associated with each of the indi-

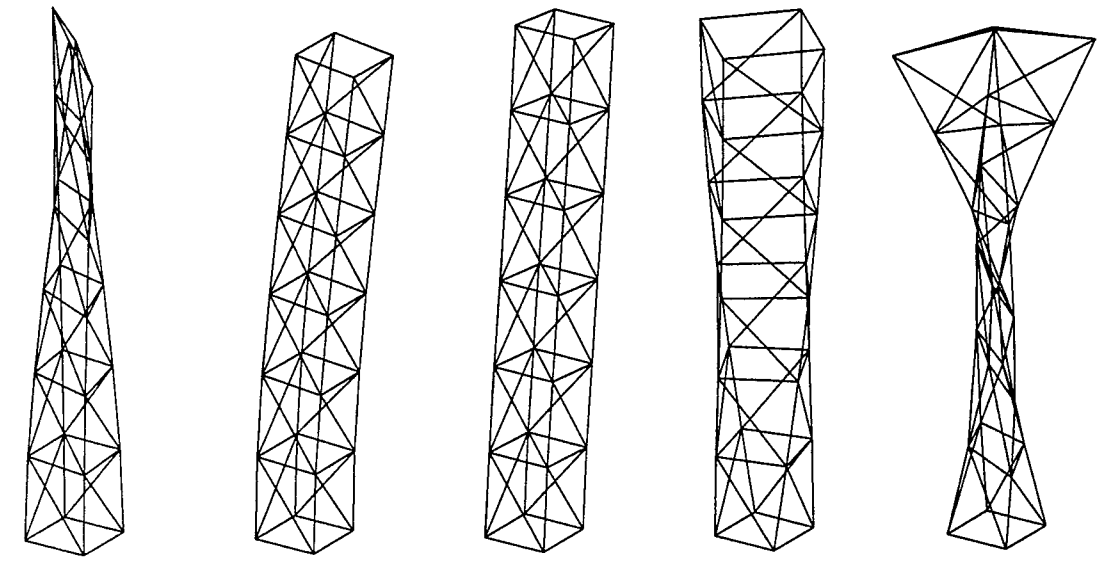

Mode 1 $\omega_1 = 4.10$ Hz | Mode 2 $\omega_2 = 4.87$ Hz | Mode 3 $\omega_3 = 4.87$ Hz | Mode 4 $\omega_4 = 10.00$ Hz | Mode 5 $\omega_5 = 19.70$ Hz

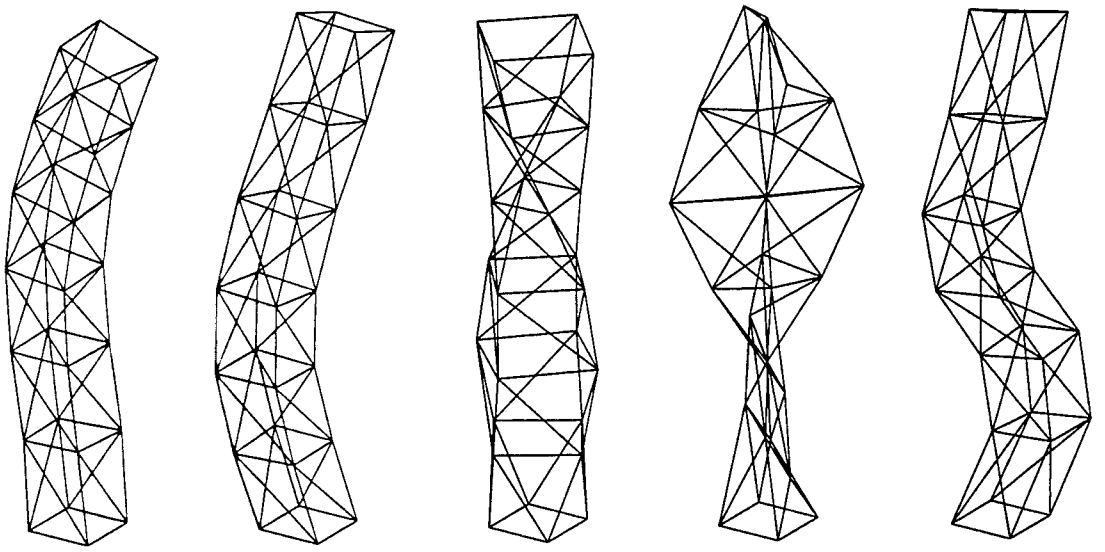

Mode 6 $\omega_6 = 20.67$ Hz | Mode 7 $\omega_7 = 20.67$ Hz | Mode 8 $\omega_8 = 30.15$ Hz | Mode 9 $\omega_9 = 42.57$ Hz | Mode 10 $\omega_{10} = 43.93$ Hz

Figure 5.3 Natural frequencies and mode shapes for the first ten modes of baseline tower truss.

Table 5.2 Different damage scenarios for tower truss.

Case	Damaged Members	Noise Level	Remarks
I	A_{45} = 16.0 in.^{2}	1%	- Single damaged member
		5%	- Different levels of noise
		10%	
II	A_{42} = 4.4 in.^{2}	1%	- Two damaged members
	A_{57} = 20.0 in.^{2}	5%	- Lower levels of noise

vidual solutions are computed using the optimum sensitivity method of equations (2.20) and (2.21) by specifying the amplitude of random perturbation with respect to the level of noise in the simulated data. The noisy measurements are simulated by adding a uniform white noise with a specified range of noise amplitudes to the noise-free analytical responses of the structure obtained from a free-vibration eigenvalue analysis of the finite-element model for each damage case.

5.3.1 Damage Case I

The current simulation is for the case where the sectional area of member 45 is reduced by 60% from 40.0 in.^{2} to 16.0 in.^{2} The measured natural frequencies are assumed to be noise-free and the measured modal displacements are polluted with three levels of noise; ε = 1%, 5%, and 10%, respectively. Four noisy measured data sets are simulated from the noise-free data in accord with equation (2.23) for each level of noise.

The results of the damage detection algorithm are shown in Figure 5.4 for the four noisy data sets with 1% noise. The identified near-optimal set of measurement locations is shown in the illustration for each of the data sets investigated. Note that the lightened lines in the illustration represent the isolated structural members obtained from the damage localization process. From the results of the simulation study, it is seen that damage in member 45 is successfully located and quantified for all the simulated 1% noisy data sets. The suspected level of damage in member 45 falls in the range of 50−65%. Although member 61 shows the probability of being slightly

damaged using data set (b), there is no clear existence of the constant unit-probability zone in the distribution of $P(X_m < X_m^* - \theta_m)$ for the member. Hence, it is concluded that there is little chance of damage in this member.

The results of the algorithm when the level of noise in the measurements is increased to 5% are shown in Figure 5.5. For all measurement data sets, the algorithm was able to localize member 45 and identify it as damaged. Even though the sensitivity of the member parameters to noise increases with the noise level, all undamaged members are still correctly identified as undamaged. For 10% noise, the results are shown in Figure 5.6 for the four noisy measurements examined. It can be seen that the simulation results using measurements with 10% noise exhibit higher variation in the parameter estimates compared with the cases with lower levels of noise as evident from a more gradual decrease in the probability distribution. In addition, using data set (b), member 66 is identified as an additional damaged member.

5.3.2 Damage Case II

In this damage case the sectional area of member 42 is reduced from 22.0 in.^{2} to 4.4 in.^{2} and the sectional area of member 57 is reduced from 40.0 in.^{2} to 20.0 in.^{2} Only two levels of measurement noise, i.e., $\varepsilon = 1\%$ and 5% are investigated in the present case study.

The results from using the proposed damage detection and assessment algorithm are shown in Figures 5.7 and 5.8 for different noisy data sets with 1% and 5% noise levels, respectively. For all simulated noisy data sets with 1% noise, both members 42 and 57 are identified as damaged with correct estimates of the severity of damage. All undamaged elements are correctly identified as undamaged. Simulation studies of the damage detection and assessment algorithm using different measured data sets with 5% noise show similar results as for the cases with 1% noise. The algorithm is shown to be successful in detecting damage at both actual damage locations.

There are some groups of undamaged members that show the probability of being slightly damaged although the individual members in these groups are not isolated from the damage localization process. The damage localization algorithm fails to identify the location of these potentially damaged members because the parameter estimates for these member groups are insensitive to parameter group subdivision. In this case, the variation in the distribution of

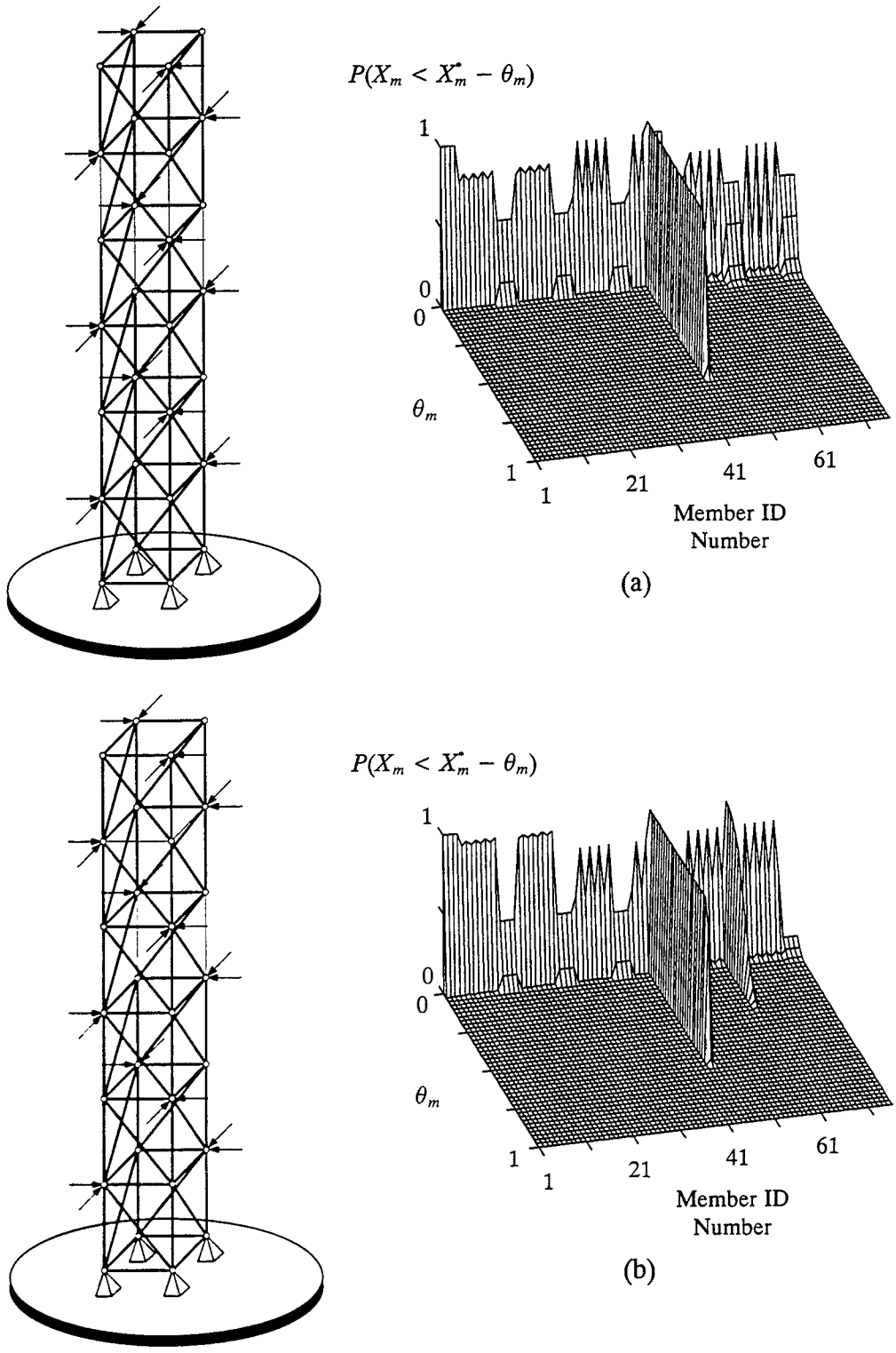

Figure 5.4 Probability distribution in Damage Case I with respect to different levels of damage for noisy data sets (a) and (b) with 1% noise.

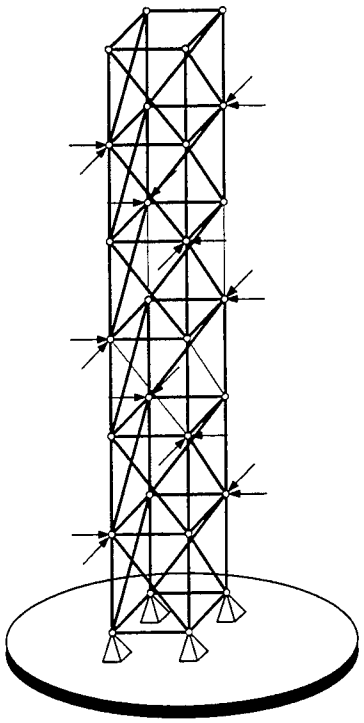

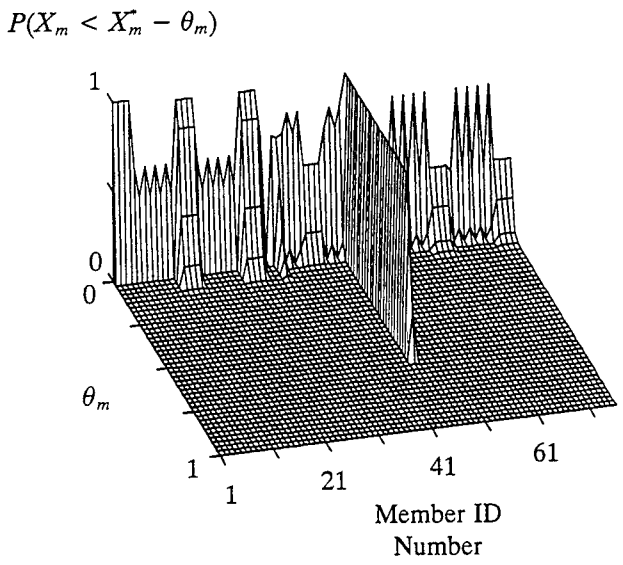

(c)

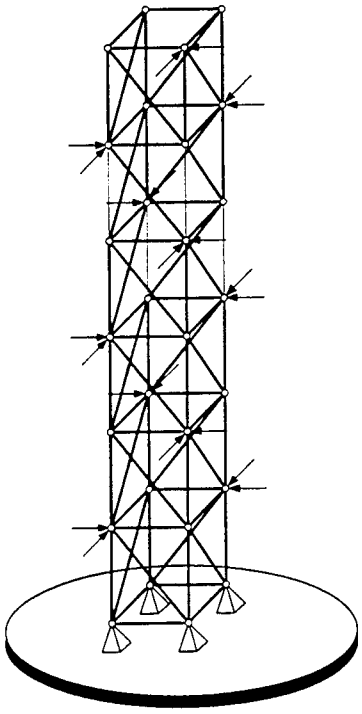

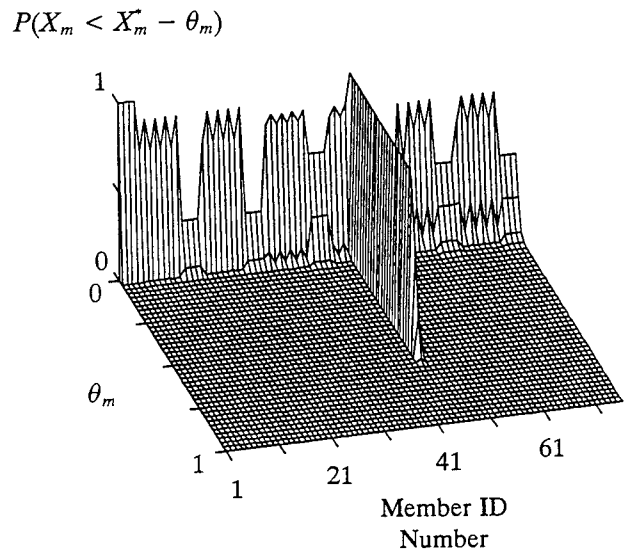

(d)

Figure 5.4 (cont.) Probability distribution in Damage Case I with respect to different levels of damage for noisy data sets (c) and (d) with 1% noise.

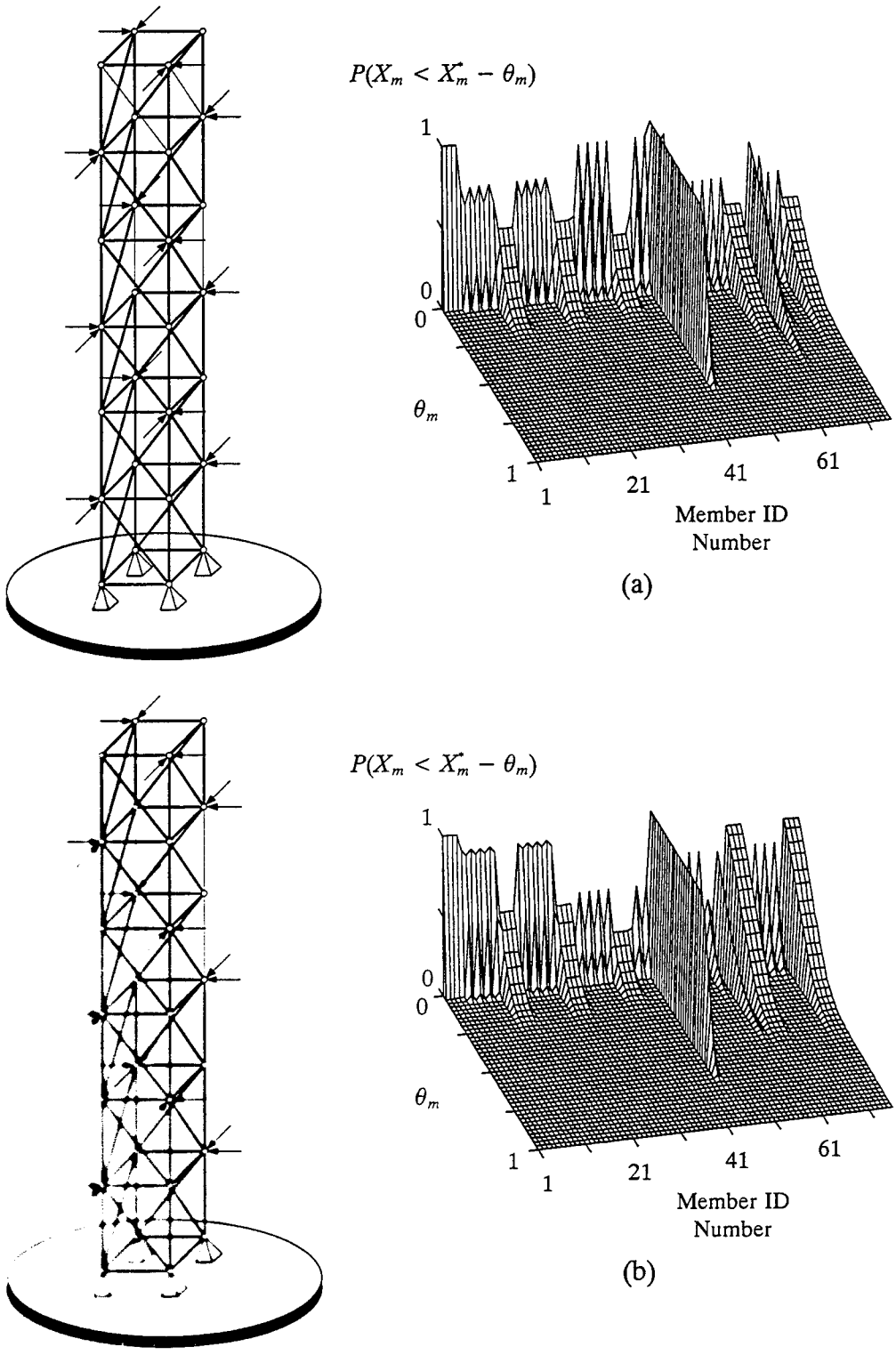

Figure 5.5 Probability distribution in Damage Case I with respect to different levels of damage for noisy data sets (a) and (b) with 5% noise.

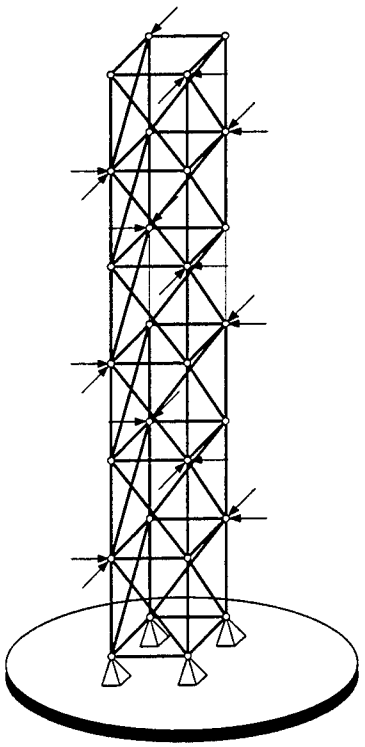

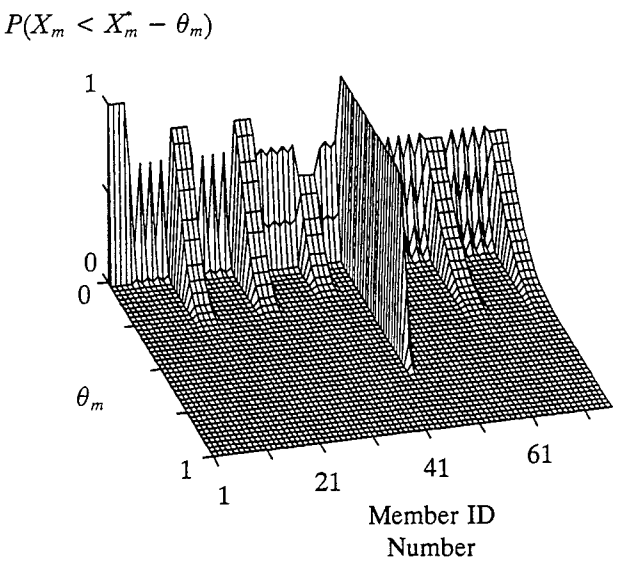

(c)

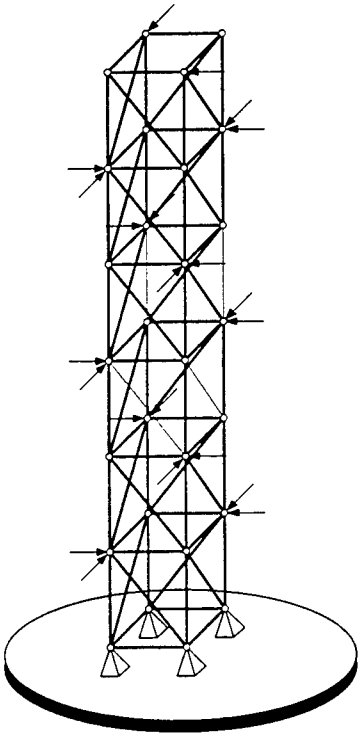

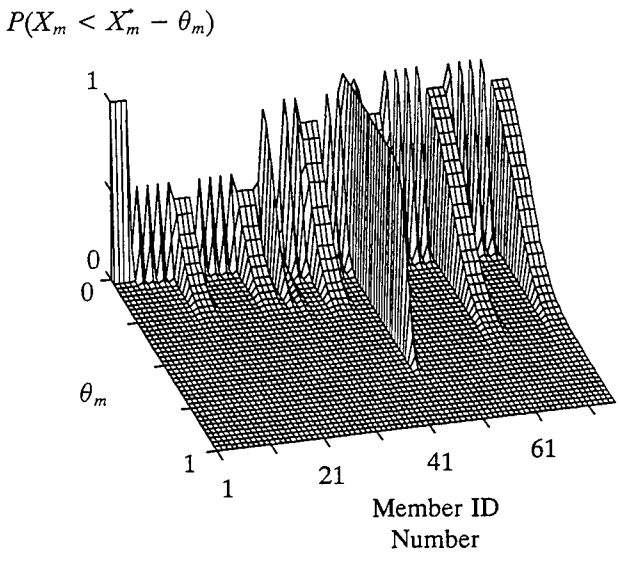

(d)

Figure 5.5 (cont.) Probability distribution in Damage Case I with respect to different levels of damage for noisy data sets (c) and (d) with 5% noise.

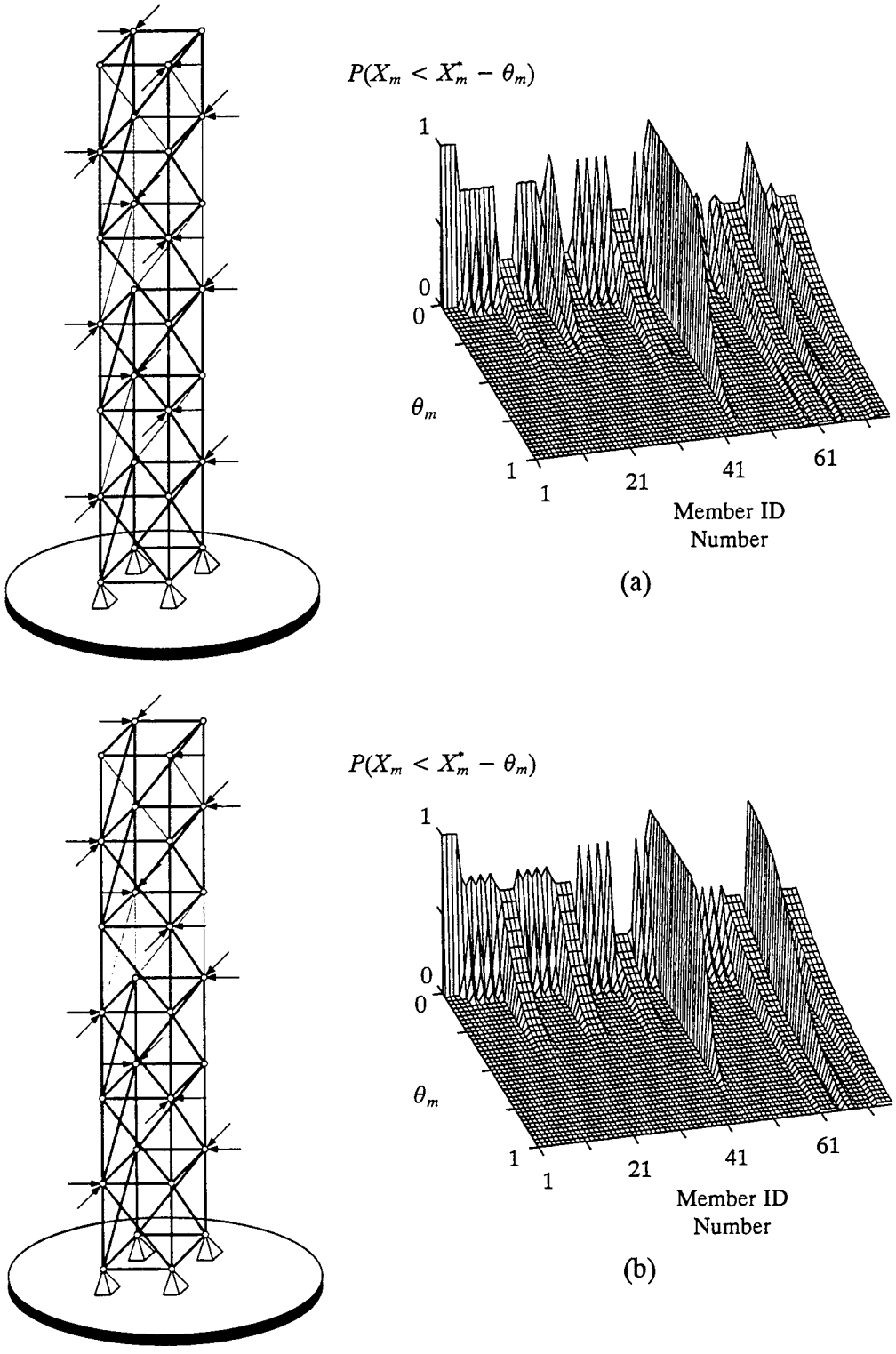

Figure 5.6 Probability distribution in Damage Case I with respect to different levels of damage for noisy data sets (a) and (b) with 10% noise.

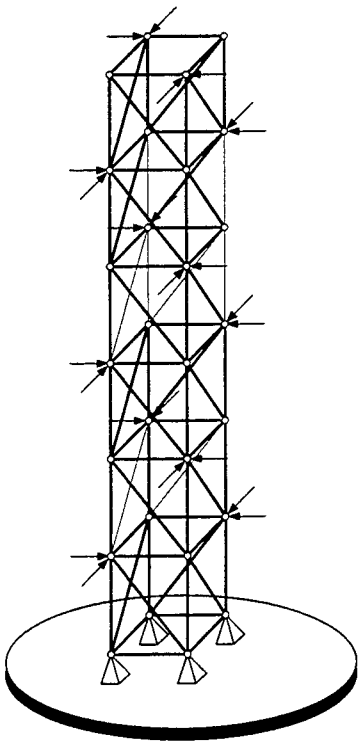

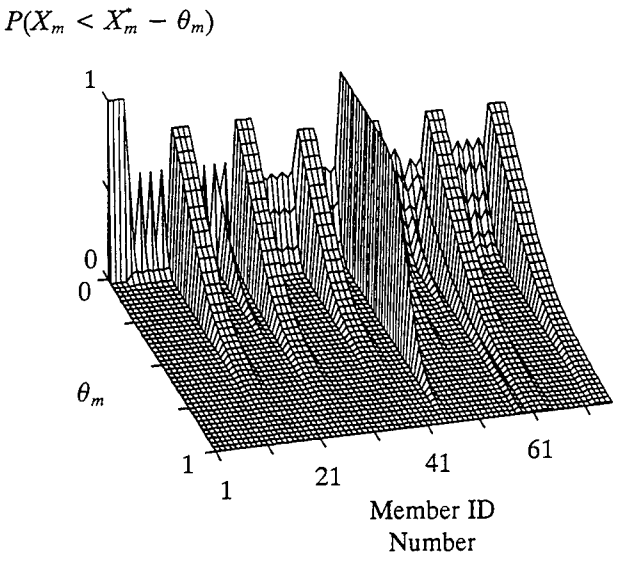

(c)

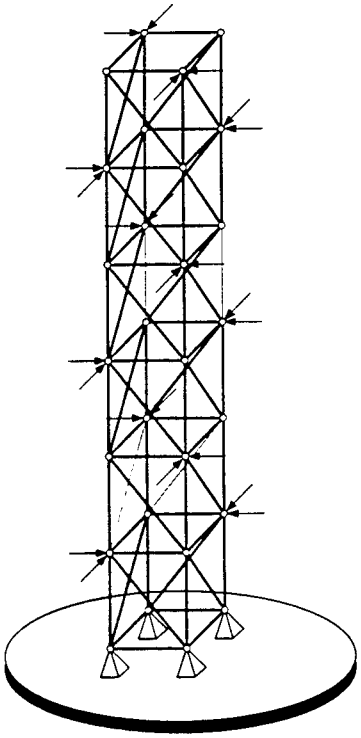

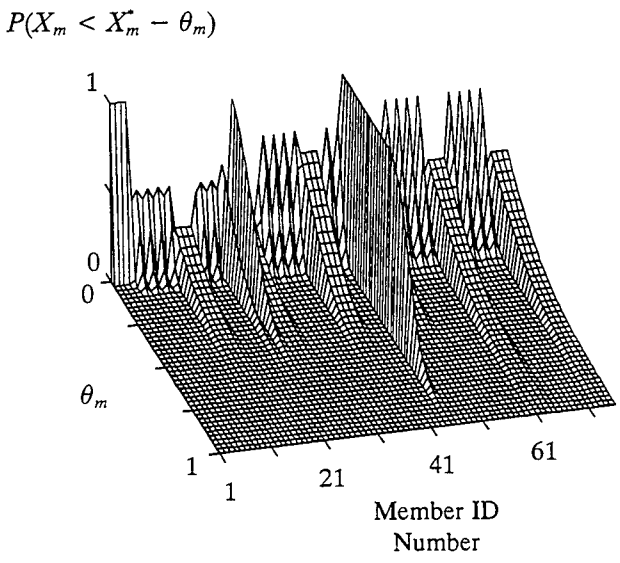

(d)

Figure 5.6 (cont.) Probability distribution in Damage Case I with respect to different levels of damage for noisy data sets (c) and (d) with 10% noise.

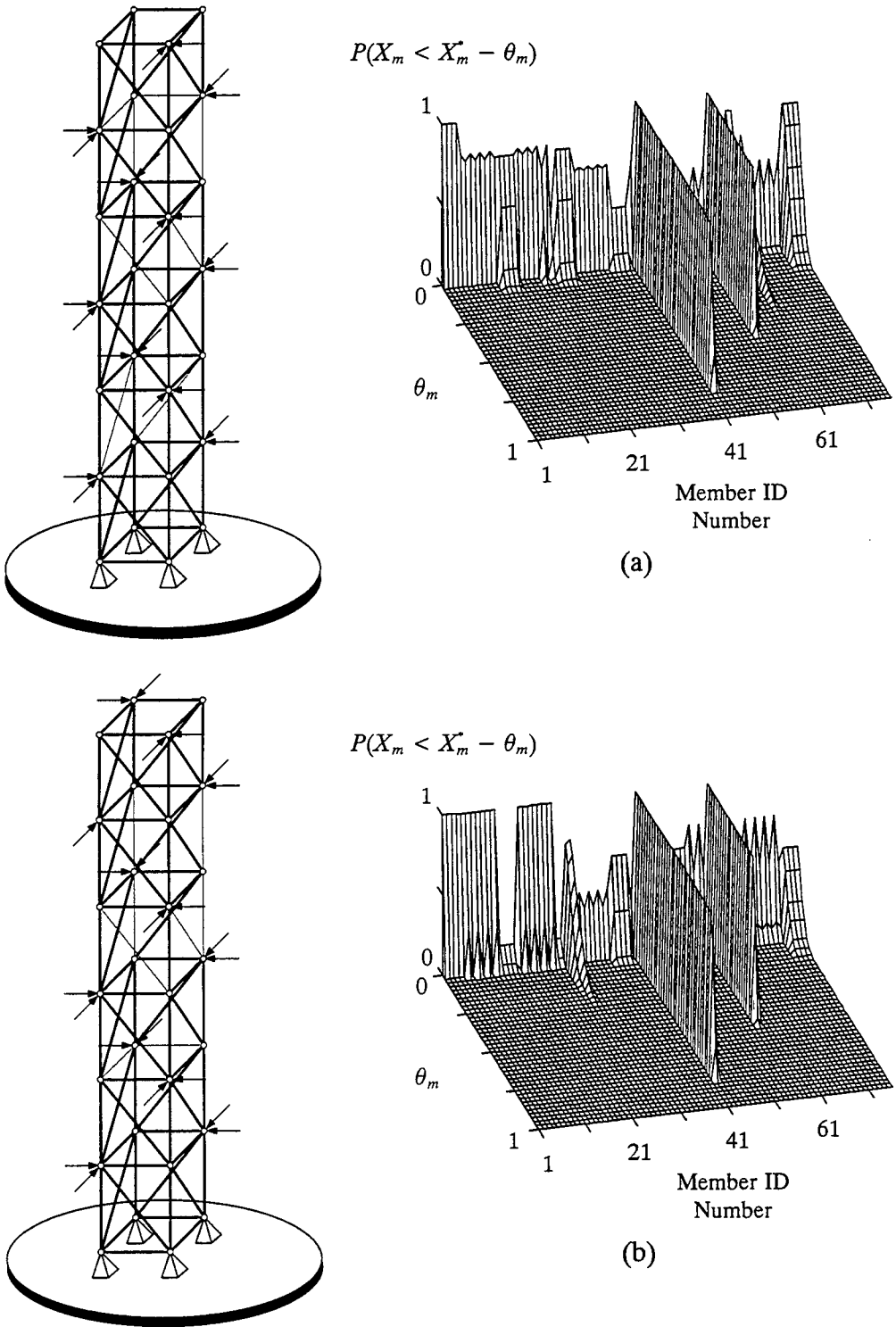

Figure 5.7 Probability distribution in Damage Case II with respect to different levels of damage for noisy data sets (a) and (b) with 1% noise.

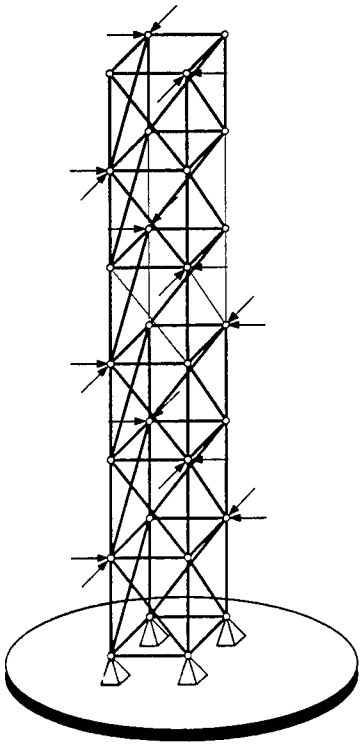

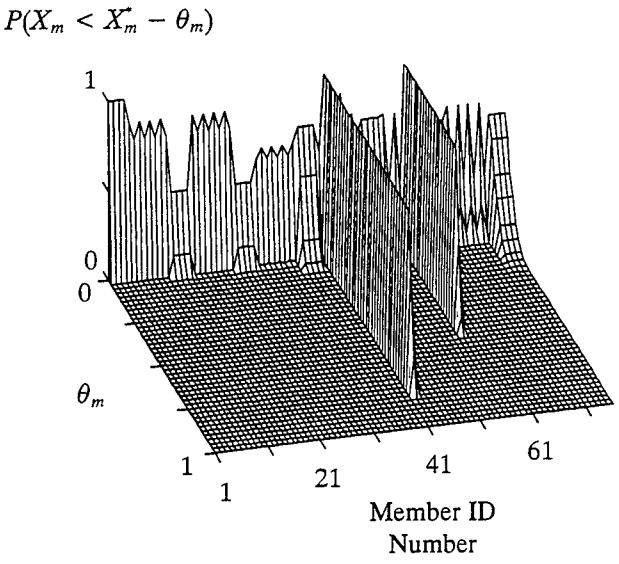

(c)

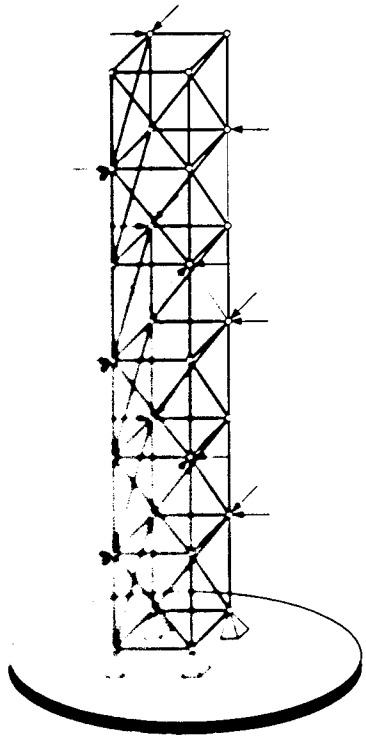

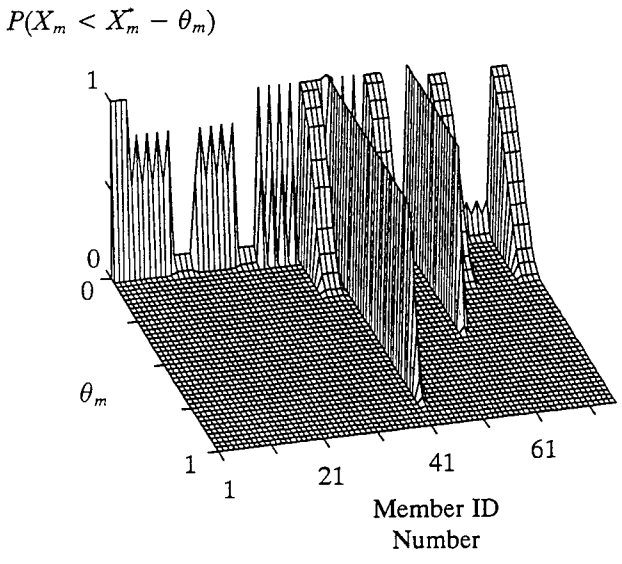

(d)

Figure 5.7 (cont.) Probability distribution in Damage Case II with respect to different levels of damage for noisy data sets (c) and (d) with 1% noise.

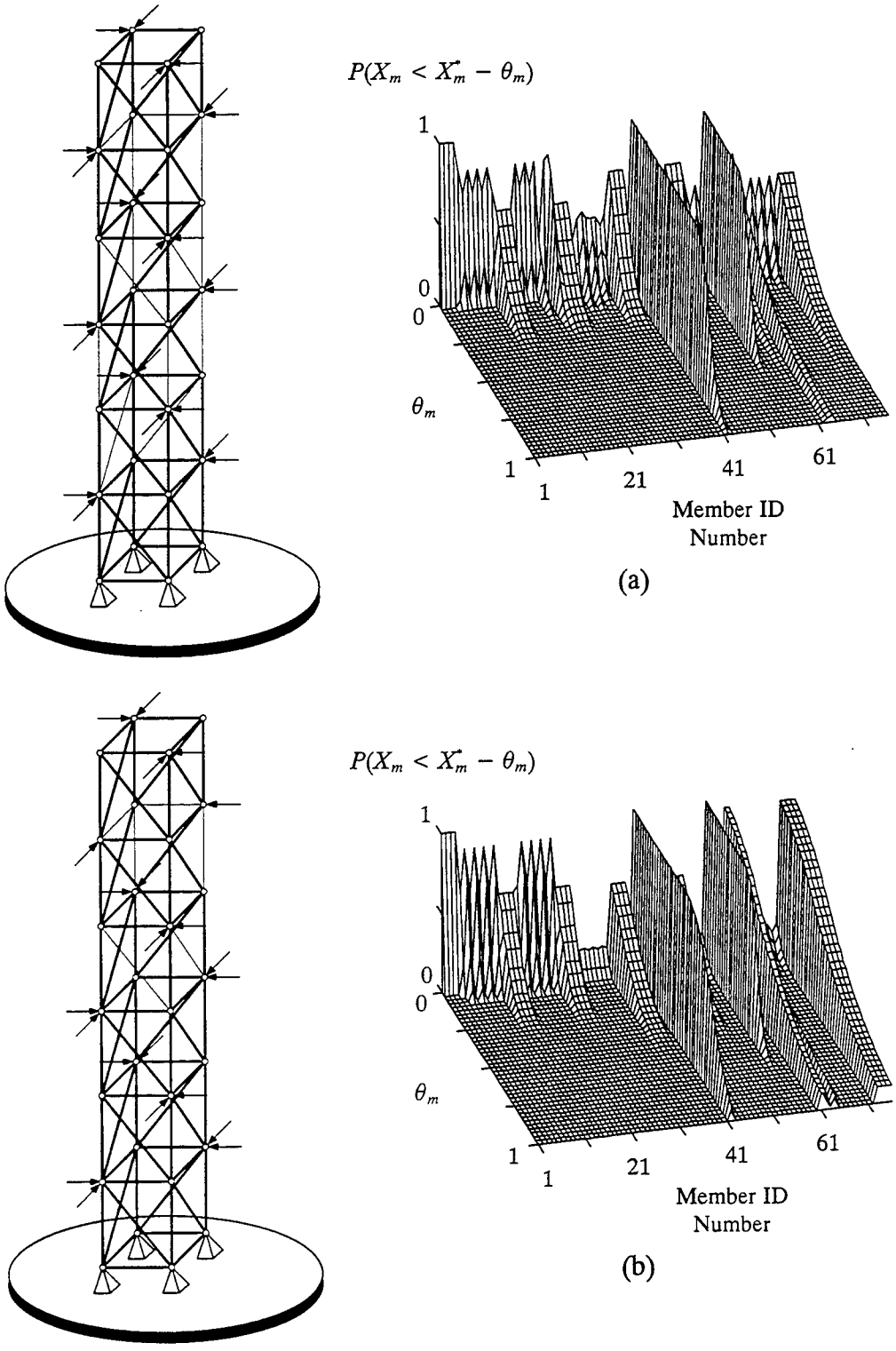

Figure 5.8 Probability distribution in Damage Case II with respect to different levels of damage for noisy data sets (a) and (b) with 5% noise.

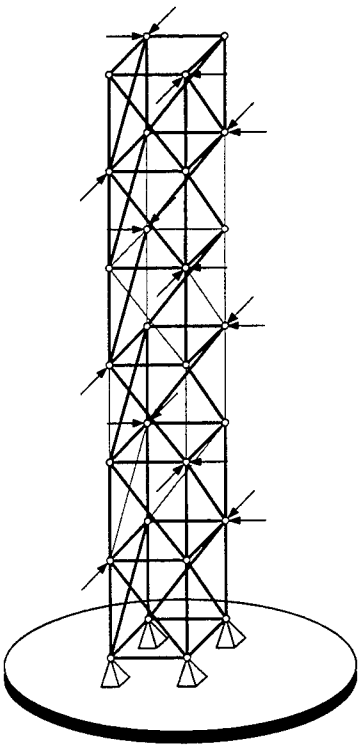

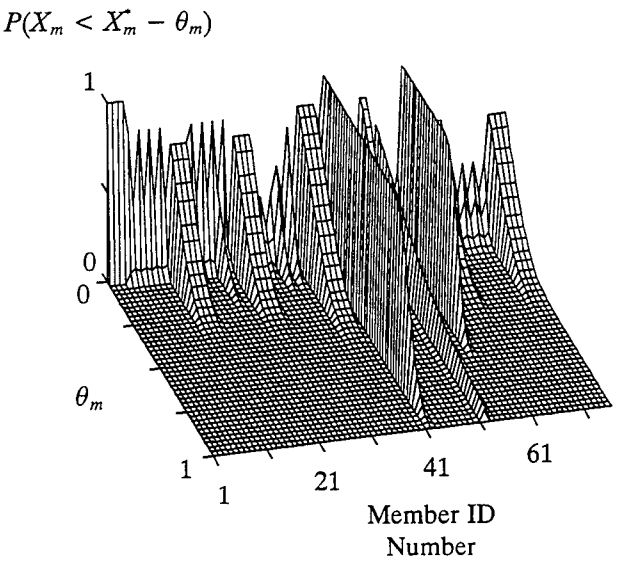

(c)

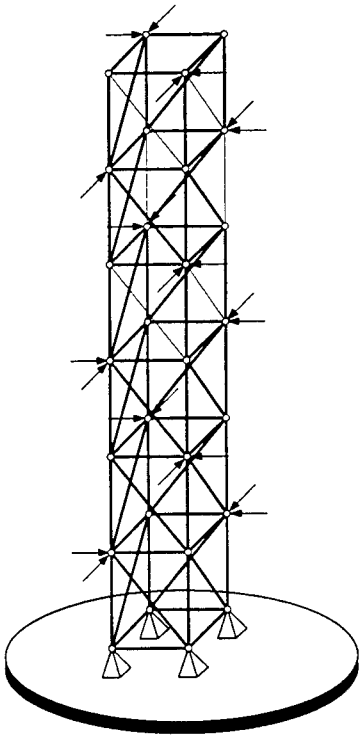

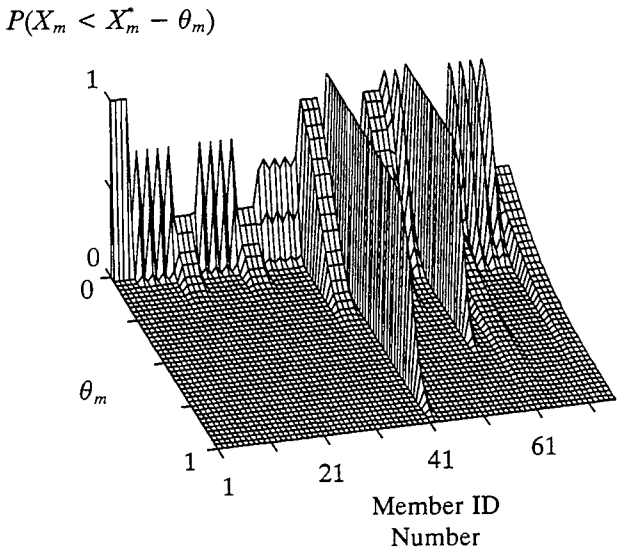

(d)

Figure 5.8 (cont.) Probability distribution in Damage Case II with respect to different levels of damage for noisy data sets (c) and (d) with 5% noise.

$P(X_m < X_m^* - \theta_m)$ is mainly due to the effect of noise in the measurements, not from the actual damage in these members.

It should be noted that the computation time used in detection of damage in the three-dimensional tower truss is significantly larger than the planar bridge truss in Chapter 4. This computational burden is due to the fact that the size of the analytical matrices required in the parameter estimation algorithm grows larger as the number of elements and degrees of freedom required to model the structural system increases. In addition, when the number of model degrees of freedom increases, a larger number of degrees of freedom with measurement information is usually required as the initial set of measured locations, and hence, the number of different sets of measured locations that must be examined during the measurement selection process is increased. Since each member of the population of starting points in the random starting point method requires one execution of the parameter estimation algorithm for each of the sets of measurement locations being investigated, the computation time required by the current algorithm to detect and assess damage can be large for complexed structural models with many measured degrees of freedom.

5.4 Summary

The damage detection and assessment procedure of Chapter 3 has been tested with an additional structure which is represented with a more complex finite-element model. The structure is a three-dimensional tower truss that requires a larger number of unknown parameters to characterize the behavior of the structural response compared with the previous example. With a certain set of simulation case studies, we have illustrated the use of the proposed algorithm to detect possible damage sites in the tower truss and to assess the severity of damage at these potential damage locations. We have shown that the proposed algorithm can detect and assess damage effectively even when the measured data are noise-polluted and when the locations of damage are sparsely isolated throughout the spatial domain of the structure.

In the parameter group-updating scheme, the intial baseline parameter grouping can be modified to facilitate multiple damage detection. As illustrated in the simulation study of a tower truss, computational efficiency of the damage localization algorithm can be improved by assigning a

small number of structural members to the individual baseline parameter groups. With the intuitive assignment of the baseline parameter grouping, the number of parameter group-updating steps required for the isolation of potentially damaged members within each of the baseline parameter groups can be reduced. Consequently, the algorithm can identify the locations of damage within the structure more efficiently.

CHAPTER 6

CONCLUSIONS

Global damage detection of structural systems using measured modal response is a complicated problem. Various difficulties can arise in the practical application of global damage detection in which field measurements of the structural responses are obtained through testing. The focuses of the present research are on the sparseness of the measured data and the presence of the measurement noise. We have presented an approach to the problem of global damage detection of a structure based upon the measured modal information that are spatially sparse and noise-polluted. We have assumed that a structure can be characterized with a parameterized finite element model with known topology and geometry. We have adopted the technique of parameter grouping to reduce the number of unknown parameters in the structural model. In addition, damage was regarded as a reduction in the element stiffness parameter. Hence, the nonlinearity effect of the structural damage was not taken into account.

The key element of the present damage detection algorithm is the estimation of the system parameters from the measured modal response. For large and complex structures, sparseness of measured data is often unavoidable since only a limit number of degrees of freedom of the structure can be measured. We have implemented an output error estimator as the tool for parameter estimation in the face of data sparseness. The question of uniqueness of solutions to the parameter estimation problem was addressed. In particular, we have adopted the random starting point scheme to assess the multiplicity of the parameter estimation solutions.

The success of the output error estimator also depends on the behavior of the algorithm in the presence of the measurement errors. With a selected subset of measurement locations, one can limit error in the parameter estimation results. We have presented a general framework of an error sensitivity analysis to obtain a near-optimal subset of measured degrees of freedom that can improve the outcome of parameter estimation. The method of random starting points was employed to locate the noise-free multiple solutions to the parameter estimation problem. Consequently,

the optimum sensitivity method was used to extract the sensitivity information for the individual solutions and the global minimum of the parameter estimation objective function was identified. In addition, we have illustrated through a simple example that the proposed method can be used to select the noisy subsets of measurement locations that will produce small errors in the parameter estimates. The algorithm performed well in the illustrated example for a wide range of noise.

For structural systems where the measured data are spatially sparse, the limited quantity of data must be utilized to detect damage. The algorithm outlined in this dissertation approached the problem with a parameter group-updating strategy. A unified approach, based upon the random starting point scheme and the optimum sensitivity analysis, has been proposed to assess solution multiplicity and sensitivity of parameter estimates to noise. The use of the best solution cluster, indicated by the lowest objective function for the mean of the solutions inside the cluster, as a basis for group subdivision in the damage localization process has been described. In addition, we have proposed a new index for determining which parameter group should be subdivided within the parameter group-updating process. The sensitivity of the system parameters to noise was explicitly taken into account in developing the termination criterion of the algorithm. The algorithm assessed damage of an element by comparing the statistical distribution of the element parameter for the damaged and the associated baseline structures under the same test conditions. One advantage of the proposed algorithm is that the statistical information for the baseline structure can be obtained simultaneously with the parameter group-updating process.

We have demonstrated the use of the damage detection and assessment algorithm on two example structures: a two-span continuous bridge truss and a three-dimensional tower truss. Numerical simulation studies were employed to examine the capabilities of the algorithm in detecting and assessing damage. Noisy measurements were simulated by adding different amplitudes of proportional random errors to the noise-free analytical modal response of the structures. It has been shown that the algorithm was able to detect and assess damage in the structural systems successfully even when the measured data are spatially sparse and noise-polluted. Although there are always cases where actually damaged elements are detected as undamaged or actually undamaged elements are detected as damaged, the results has been shown to improve dramatically when the level of noise in the measurements decreases.

One of the advantages of the parameter group-updating scheme is that the intial baseline grouping can be modified to facilitate the detection of multiple damage locations in a structure. As illustrated in the simulation study of a tower truss, the computational burden of the algorithm can be greatly reduced by further subdividing the original baseline parameter groups into a set of groups with smaller size. With the reassigned baseline grouping, the number of parameter grouping steps required to localize potential damaged elements within each of the baseline groups is reduced and hence the algorithm is able to isolate the locations of damage more efficiently. Furthermore, the algorithm takes into account explicitly the multiplicity of solution to the parameter estimation problem, which is associated with each step of the damage localization process. In general, parameter estimation problems can have multiple solutions when the measured data are spatially sparse. Ignoring the possibility of solution multiplicity can lead to erroneous damage locations or the algorithm can fail to converge at all.

Another advantage of the present algorithm is the systematic statistical evaluation of system parameters for damage. The statistical framework allows an assessment of damage in a more reliable manner by incorporating the sensitivity of each element parameter due to the current measurement conditions. With the present method, damage in all the structural members can be evaluated regardless of their sensitivities, even though damage in an insensitive member might be difficult to detect if the noise level is high. Moreover, the proposed algorithm can evaluate the sensitivity of each element parameter simultaneously with the process of parameter group-updating. Hence, the sensitivities of the members need not be determined before attempting to detect damage in the structure.

From simulation studies, it has been found that the computation time used by the proposed algorithm in detecting damage can increase enormously as the structural model becomes more complex. In general, this computational burden depends on the number of degrees of freedom and number of elements in the finite element model of the structure. Furthermore, in the current algorithm each random starting point requires one execution of parameter estimation for each of the patterns of measurements being investigated. Hence, the computation time is directly proportional to the specified number of random starting points and the number of measurement locations in the initial set of measurements for the measurement selection process at each step of the

parameter group-updating algorithm. Possible alternatives should be investigated to improve the computation efficiency of the algorithm. One possible approach to reduce the computational burden of the current algorithm is to improve the solution algorithm for the parameter estimation problem.

In the current research, numerical simulations were performed on the cases where each structural element is modeled with a single stiffness parameter. In general, some structural models may have element stiffness matrices that depend upon different modes of deformation. These different modes of behavior can give rise to multiple element constitutive parameters that may have different levels of sensitivity to the measurement noise. Further investigations need to be carried out to examine the behavior of the proposed damage detection and assessment algorithm in the cases where a structural member is modeled with multiple stiffness parameters.

Damage in a structure generally presents itself in the form of geometric defects (e.g. crack) of a structural member. It therefore seems intuitively clear that the present approach in which we modeled damage as a reduction in the constitutive parameters cannot do better than an approach that geometrically models defects. However, identification of the geometric defects in a solid body requires that nonlinearity of the defects be taken into account and hence is more difficult, if not impossible, than identification of the constitutive parameters. The merit of the present approach lies in its generality. One needs not know in advance the general information of a defect before attempting to assess it. In addition, the method can be applied to a variety of defects without requiring a reformulation and is well-suited to the problem of damage detection in large and complex structures.

APPENDIX

A NUMERICAL EXAMPLE USING THE DATA PERTURBATION SCHEME

A.1 Introduction

In this section we investigate the use of the data perturbation scheme on noisy measurements to simulate the sensitivity of the noise-free multiple solutions of the output error estimator to the measurement noise. A two-parameter model is selected as an illustrative example since the sensitivity of each solution can be characterized on a two-dimensional plot. The aim of this study is to verify the use of the random perturbation on a given measured data set to obtain the statistical properties of the parameter estimates associated with each of the identified multiple solutions as previously discussed in Chapter 2.

A.2 A Two-Parameter Model

Let us consider a six-story shear building with fixed base as illustrated in Figure A.1. The structural model has six degrees of freedom, the horizontal translations at the story levels, from which some of them are measured. The structure is parameterized with two parameters, $\mathbf{x} = \{x_1, x_2\}^T$. The stiffness of the ith story, which belongs to parameter group k, is given by $k_k = x_k k_0$. The nominal properties of the structure is chosen such that $k_0/m_0 = 1.2\ /\text{sec}^2$. The actual values of paramaters are given as $\hat{\mathbf{x}} = \{2.0, 1.0\}^T$.

The results from a free-vibration eigenvalue analysis of the nominal model of the structure are shown in Table A.1 where the ith mode shape $\boldsymbol{\phi}_i$ is scaled such that $\boldsymbol{\phi}_i^T \mathbf{M} \boldsymbol{\phi}_i = 1$. In the present example, the natural frequencies and mode shapes of all six modes of the structure are considered to be available as our noise-free database. The set of noisy data shown in the table are generated by adding uniform random variates to the noise-free data in accord with equation (2.22) using two levels of noise amplitudes: $\varepsilon = 10\%$ and 20%, respectively. Throughout the study we will assume that the natural frequencies can be measured with negligible error compared with the mode shapes and are considered to be noise-free.

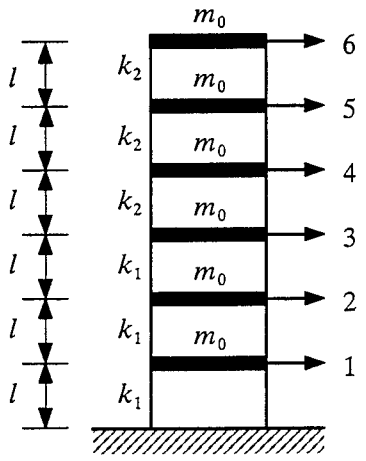

Figure A.1 The six-degree-of-freedom shear building.

A.3 Organization of the Study

To investigate the behavior of the data perturbation scheme on noisy measurements, three different patterns of measurements as illustrated in Figure A.2 are used as input to the parameter estimation problem. For each pattern of measurements, the noise-free and the individual simulated noisy data sets (Case I–Case VI) are investigated separately. The six simulated noisy data sets are used to represent a sample of the noise-polluted data from field measurements.

For each of the seven available data sets, two distinct types of simulations were performed. The first type concerns identification of the multiplicity of solutions for each pattern of measurements. In these simulations, the random starting point scheme is used to find various solutions for each of the data sets considered. In particular, we use 100 random starting points for each data set to generate a sample of solutions. Thus, each case requires 100 executions of the parameter estimation scheme. The second type of simulation concerns evaluation of the sensitivity of the identified multiple solutions to a series of random perturbations. We perturbed each simulated noisy data sets for each pattern of measurements in accord with equation (2.14) using four different amplitudes of random perturbation, $\alpha = 0.05$, 0.10, 0.20, and 0.40, respectively. For the noise-free data sets, only two perturbation amplitudes, $\alpha = 0.10$ and 0.20, were used to study the sensitivity of the noise-free solutions to the measurement noise. In the current simulations,

Table A.1 Noise-free and simulated noisy measurements.

Mode		Noise-free	10% Noise			20% Noise		
			Case I	Case II	Case III	Case IV	Case V	Case VI
1	Natural Frequency (Hz)	0.33612	0.33612	0.33612	0.33612	0.33612	0.33612	0.33612
	Mode Shape							
	Level 1	0.03263	0.02947	0.03459	0.03270	0.02630	0.03499	0.03285
	Level 2	0.06373	0.06298	0.05918	0.06561	0.06224	0.06313	0.06868
	Level 3	0.09183	0.08524	0.09755	0.08272	0.07865	0.08305	0.07928
	Level 4	0.13937	0.13403	0.14398	0.13369	0.12868	0.16721	0.16349
	Level 5	0.17380	0.18781	0.15990	0.16125	0.20182	0.14085	0.16832
	Level 6	0.19186	0.18380	0.18961	0.18006	0.17575	0.21421	0.21790
2	Natural Frequency (Hz)	0.88279	0.88279	0.88279	0.88279	0.88279	0.88279	0.88279
	Mode Shape							
	Level 1	-0.09481	-0.09003	-0.09923	-0.08608	-0.08525	-0.10016	-0.11137
	Level 2	-0.15884	-0.17411	-0.15718	-0.17283	-0.18938	-0.12727	-0.13791
	Level 3	-0.17129	-0.16528	-0.18802	-0.18737	-0.15927	-0.15727	-0.13781
	Level 4	-0.08495	-0.08956	-0.09008	-0.07807	-0.09418	-0.07532	-0.06974
	Level 5	0.05656	0.05162	0.06054	0.05927	0.04667	0.05650	0.06401
	Level 6	0.16133	0.16557	0.14869	0.16719	0.16980	0.18965	0.18703
3	Natural Frequency (Hz)	1.41151	1.41151	1.41151	1.41151	1.41151	1.41151	1.41151
	Mode Shape							
	Level 1	-0.10439	-0.09627	-0.10186	-0.09813	-0.08815	-0.11015	-0.12407
	Level 2	-0.12212	-0.11700	-0.11211	-0.11899	-0.11187	-0.12685	-0.12122
	Level 3	-0.03847	-0.03743	-0.03877	-0.03885	-0.03638	-0.03502	-0.03858
	Level 4	0.19270	0.21032	0.19100	0.19314	0.22793	0.19000	0.18225
	Level 5	0.10393	0.10238	0.10983	0.10204	0.10082	0.08945	0.12079
	Level 6	-0.15740	-0.15256	-0.15201	-0.16625	-0.14773	-0.12959	-0.13790
4	Natural Frequency (Hz)	1.90783	1.90783	1.90783	1.90783	1.90783	1.90783	1.90783
	Mode Shape							
	Level 1	0.12439	0.13348	0.11345	0.12459	0.14257	0.13697	0.12561
	Level 2	0.06013	0.05568	0.05593	0.05784	0.05123	0.06758	0.06831
	Level 3	-0.09533	-0.09183	-0.10072	-0.10473	-0.08834	-0.08157	-0.09383
	Level 4	-0.11710	-0.12426	-0.12332	-0.11051	-0.13141	-0.13312	-0.12098
	Level 5	0.21631	0.22073	0.21231	0.23240	0.22515	0.21289	0.22079
	Level 6	-0.10639	-0.11342	-0.09963	-0.11574	-0.12045	-0.12285	-0.11134
5	Natural Frequency (Hz)	2.16294	2.16294	2.16294	2.16294	2.16294	2.16294	2.16294
	Mode Shape							
	Level 1	-0.18499	-0.16716	-0.18815	-0.19645	-0.14932	-0.15604	-0.20692
	Level 2	-0.00938	-0.00894	-0.00953	-0.01001	-0.00849	-0.00973	-0.00796
	Level 3	0.18452	0.17571	0.18371	0.19944	0.16690	0.16309	0.14932
	Level 4	-0.14704	-0.16011	-0.15107	-0.13941	-0.17318	-0.16413	-0.11765
	Level 5	0.09464	0.09643	0.09301	0.08669	0.09822	0.07637	0.08939
	Level 6	-0.03265	-0.03149	-0.03526	-0.03412	-0.03033	-0.03661	-0.02775
6	Natural Frequency (Hz)	2.82794	2.82794	2.82794	2.82794	2.82794	2.82794	2.82794
	Mode Shape							
	Level 1	-0.17133	-0.18844	-0.15476	-0.18768	-0.20556	-0.18374	-0.16942
	Level 2	0.22824	0.21966	0.21480	0.20714	0.21109	0.19195	0.18947
	Level 3	-0.13273	-0.12588	-0.13067	-0.12218	-0.11904	-0.13792	-0.10692
	Level 4	0.02988	0.02969	0.02778	0.02922	0.02949	0.02732	0.03243
	Level 5	-0.00666	-0.00682	-0.00646	-0.00686	-0.00699	-0.00626	-0.00688
	Level 6	0.00118	0.00122	0.00114	0.00127	0.00126	0.00119	0.00102

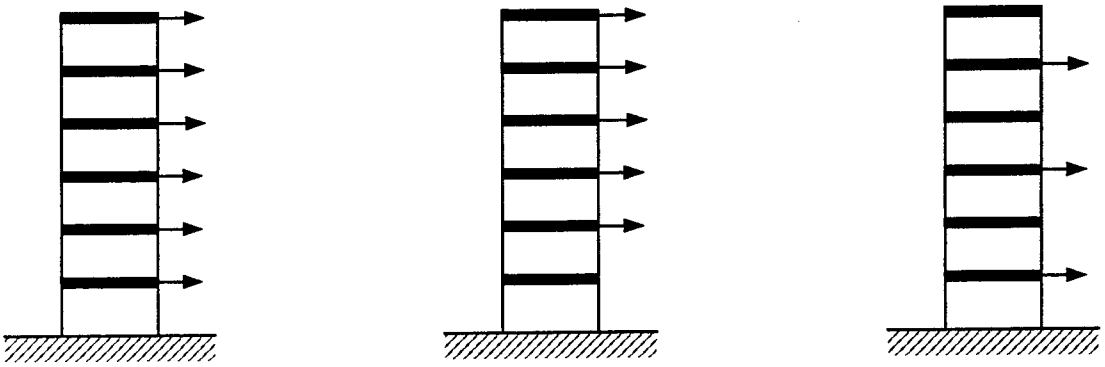

Figure A.2 Different patterns of measurements for the parameter estimation problem.

we generate 50 perturbed measurements for each amplitude of perturbation and start the estimation from 100 random starting points. Hence, each case requires 5000 executions of the parameter estimation algorithm.

A.4 Simulation Results

The results from investigating the three different sets of measurement locations with all six modes are shown in descending orders of the number of measured degrees of freedom of the structural model, starting with the case with full measurements (Case A). Note that the minimum number of measured degrees of freedom is three (Case C) in the current investigation.

The case of complete measurements is illustrated in Figure A.3 for all noisy data sets with four levels of perturbation. The results from the noise-free data set are also shown in the illustration for the two levels of perturbation considered. Figure A.3 illustrates the two-dimensional parameter space $x_1 - x_2$. The circle in each figure is the solution associated with the smallest value of objective function for the unperturbed measurements. In addition, estimates from the individual trials of random perturbation are plotted as small triangles.

It should be noted that the solution to the parameter estimation problem for the complete measurement case is unique for all unperturbed data sets. The 100 random starting points converged to the same solution in the absence of the random perturbation. The uniqueness of solution holds

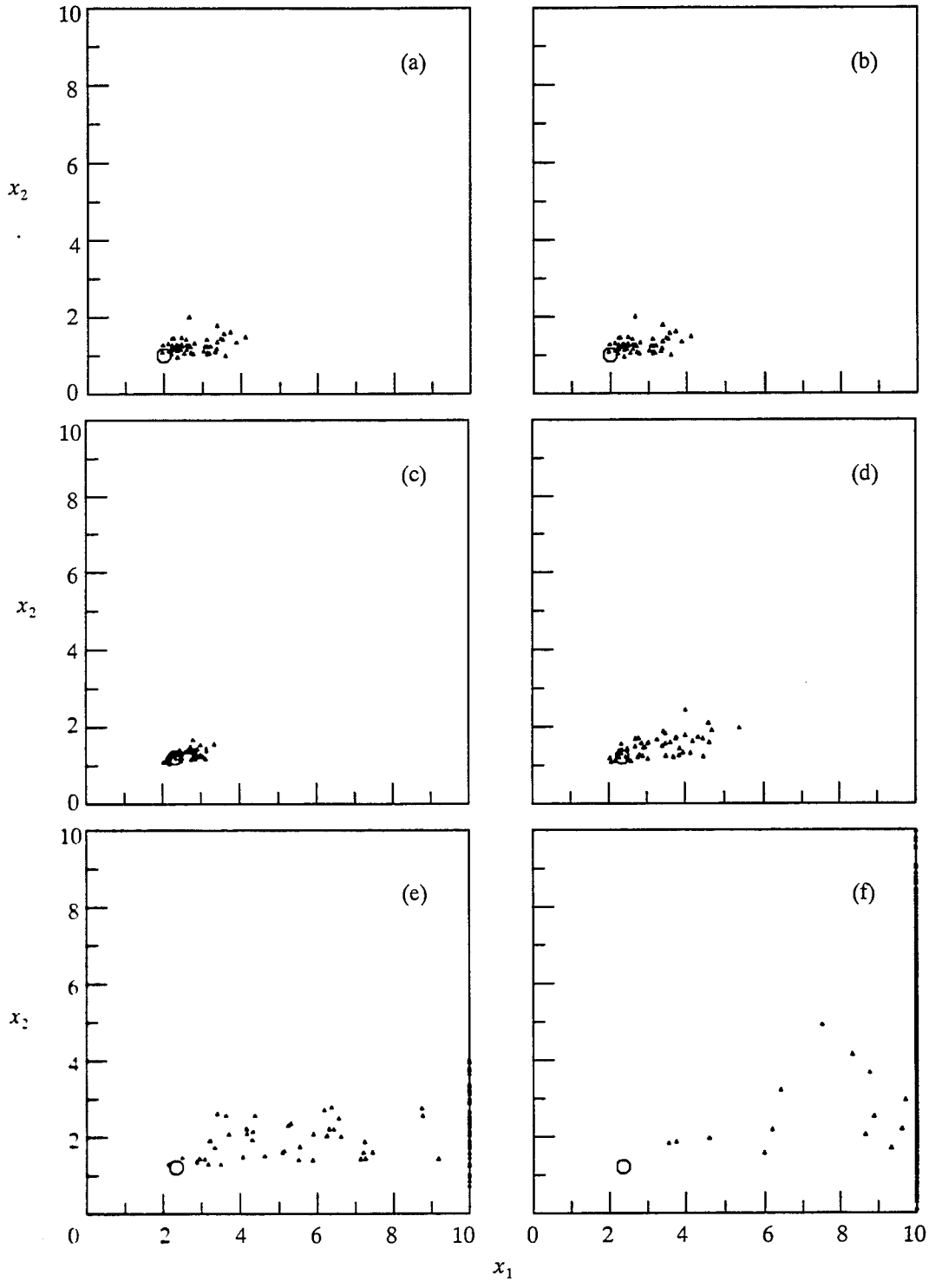

Figure A.3 Noisy solutions for complete measurements (Case A) using different noisy data sets: (a) Noise-free + ($\alpha = 0.10$); (b) Noise-free + ($\alpha = 0.20$); (c) Case I + ($\alpha = 0.05$); (d) Case I + ($\alpha = 0.10$); (e) Case I + ($\alpha = 0.20$); (f) Case I + ($\alpha = 0.40$).

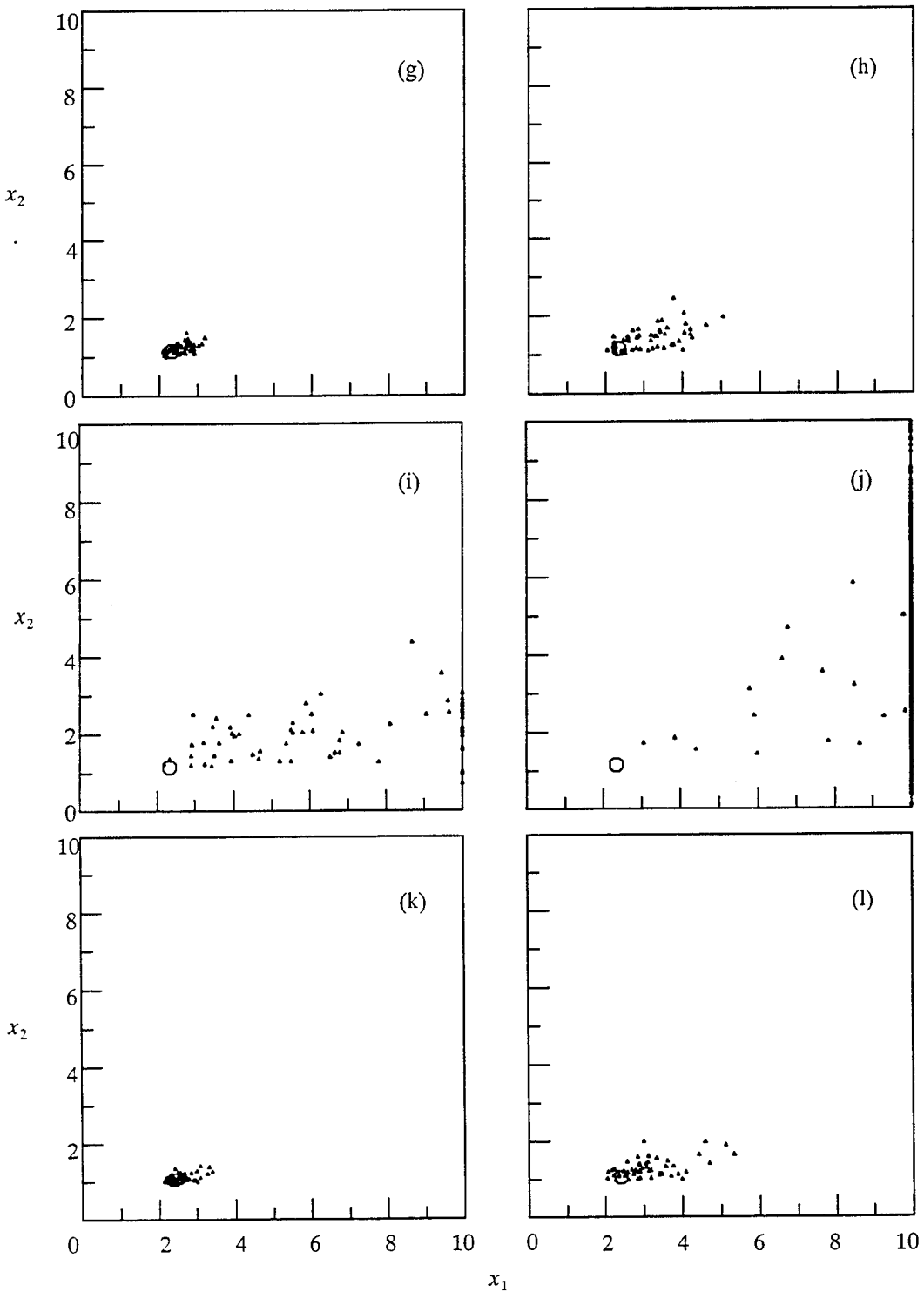

Figure A.3 (cont.) Noisy solutions for complete measurements (Case A) using different noisy data sets: (g) Case II + ($\alpha = 0.05$); (h) Case II + ($\alpha = 0.10$); (i) Case II + ($\alpha = 0.20$); (j) Case II + ($\alpha = 0.40$); (k) Case III + ($\alpha = 0.05$); (l) Case III + ($\alpha = 0.10$).

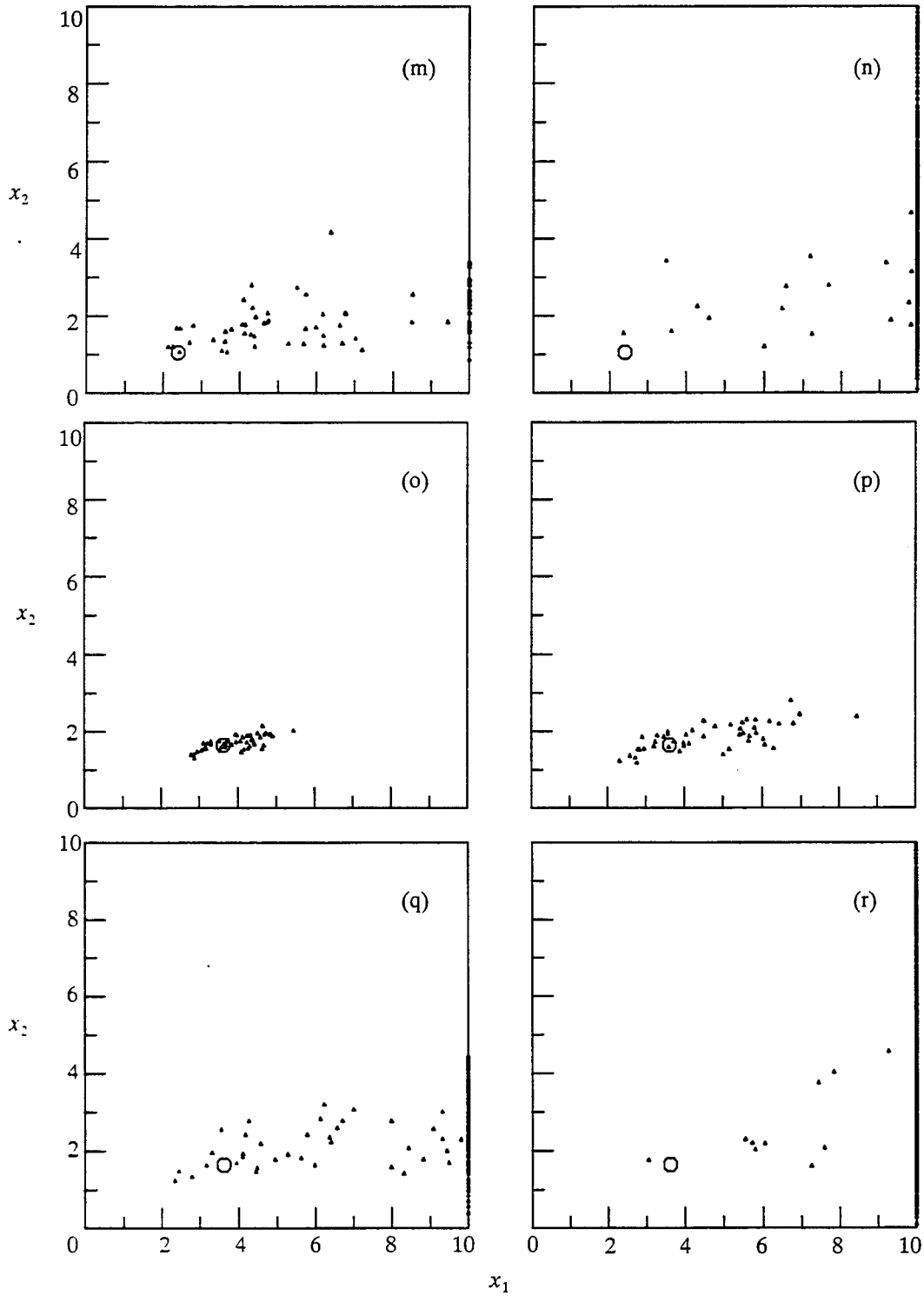

Figure A.3 (cont.) Noisy solutions for complete measurements (Case A) using different noisy data sets: (m) Case III + ($\alpha = 0.20$); (n) Case III + ($\alpha = 0.40$); (o) Case IV + ($\alpha = 0.05$); (p) Case IV + ($\alpha = 0.10$); (q) Case IV + ($\alpha = 0.20$); (r) Case IV + ($\alpha = 0.40$).

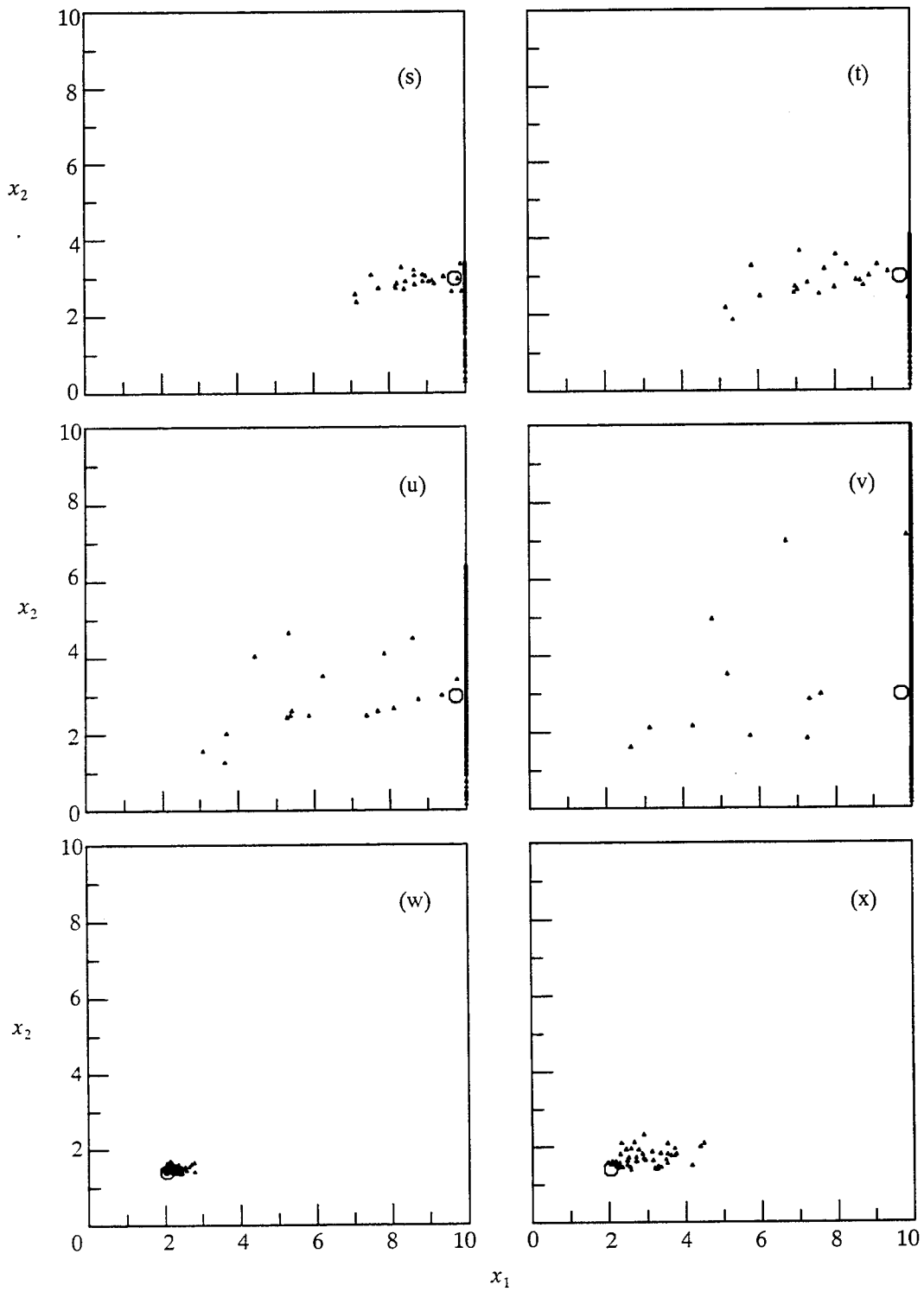

Figure A.3 (cont.) Noisy solutions for complete measurements (Case A) using different noisy data sets: (s) Case V + ($\alpha = 0.05$); (t) Case V + ($\alpha = 0.10$); (u) Case V + ($\alpha = 0.20$); (v) Case V + ($\alpha = 0.40$); (w) Case VI + ($\alpha = 0.05$); (x) Case VI + ($\alpha = 0.10$).

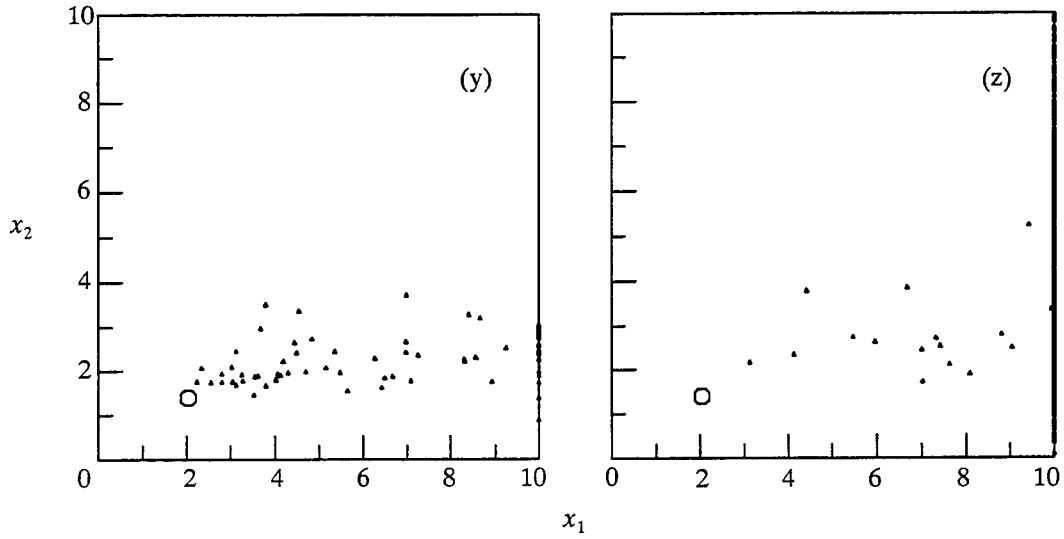

Figure A.3 (cont.) Noisy solutions for complete measurements (Case A) using different noisy data sets: (y) Case VI + ($\alpha = 0.20$); (z) Case VI + ($\alpha = 0.40$).

true even when each data set is subjected to a random perturbation. The scatter of the estimates comes from the difference in the magnitude of the random vector for different trials of perturbation. In other words, all the 100 random starting points converged to the same solution for a particular trial of perturbation. However, this statement is not true for the cases where the solutions hit the upper bound because these solutions get stuck at the bound before converging to the true basins of attraction. This situation is shown in most noisy data sets with high level of perturbation, e.g. $\alpha > 0.20$. For noise-free measurements, the unperturbed solution is located at exactly the same location as the true solution. The unperturbed solution for each noisy data set is in the vicinities of the true solution, except for Case V where the solution shows the greatest bias. One can observe that the distribution of the perturbed solutions in the two-dimensional parameter space for each noisy data set is similar to the noise-free case if the unperturbed solution is close to the correct solution. In particular, the simulation results show remarkable similarities between each of the 10% noisy data sets (Case I–Case III) and the noise-free data set using the same level of perturbation ($\alpha = 0.10$). Also, the scatter of the perturbed solutions for the noise-free data set with $\alpha = 0.20$ is almost the same as the 20% noisy data sets (Case IV–Case VI) with $\alpha = 0.20$.

However, in case V most perturbed solutions get stuck at the upper bound and thus the true scatter of solutions is not clear from the plot.

Let us turn our attention to the five-measurement case (Case B). The simulation results for this case are shown in Figure A.4. In the illustration, the open squares represent the identified multiple solutions of the parameter estimation problem from 100 random starting points and each circle denotes the best solution associated with the smallest value of objective function. While the number of unperturbed solutions has increased over the complete measurement case, the scatter in the estimates has been reduced to some degree. This aspect of the parameter estimation problem has been studied in detail by Hjelmstad (1996). As shown in Figure A.4, the same sort of results have been observed again as in the case with complete measurements. All unperturbed solutions for the 10% noisy data sets lie close to the unperturbed solutions for the noise-free data. Also, the scatter of the three 10% noisy data sets (Case I–Case III) with $\alpha = 0.10$ resembles the noise-free case with the same level of perturbation. Moreover, the results of the 20% noisy data sets (Case IV–Case VI) with $\alpha = 0.20$ are close to the noise-free data set with $\alpha = 0.20$. The solutions show a bit larger scatter using the amplitude of perturbation $\alpha = 0.20$ compared with $\alpha = 0.10$. For all data sets, the scatter of solutions using $\alpha = 0.40$ is considerably large compared with the lower levels of perturbation. It is therefore suggested that an upper limit on the level of perturbation should be specified to get any meaningful results.

The results of the case with three measurements (Case C) are illustrated in Figure A.5. The scatter of the parameter estimates has is dramatically reduced while the number of multiple solutions is considerably larger compared with Case A and Case B. There is a clear connection between the scatter of solutions for the noisy data sets and the noise-free data that are subjected to the same level of perturbation. Also, the scatter of the parameter estimates for each of the six noisy data sets with high level of perturbation ($\alpha > 0.20$) is quite large compared with the noise-free data with lower levels of perturbation.

To summarize the effect of the data perturbation scheme, let us assume that the scatter of the solutions to the parameter estimation problem for the noise-free data with $\alpha = 0.10$ and $\alpha = 0.20$ replicates the sensitivity of the noise-free solutions to the measurement noise with

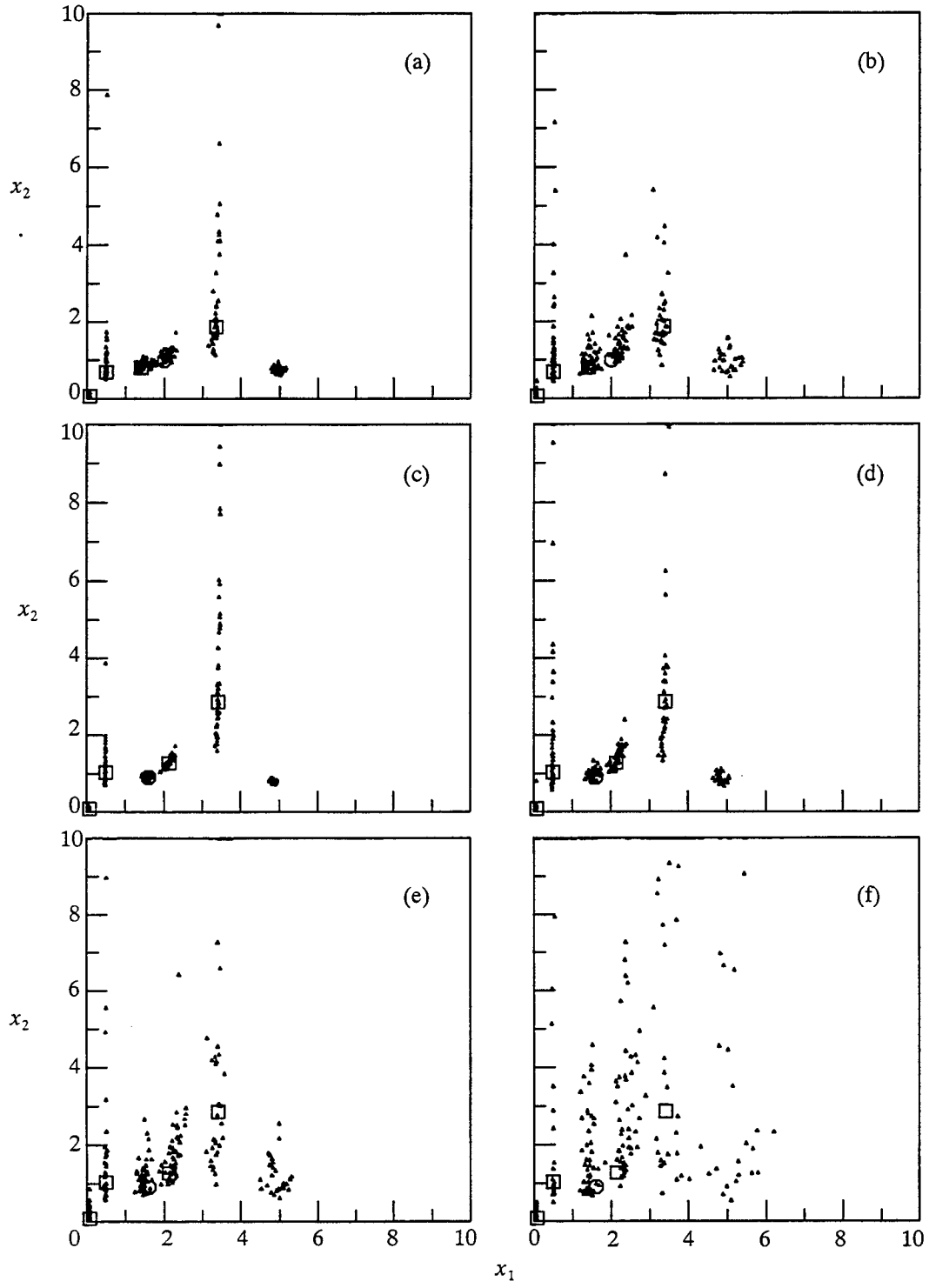

Figure A.4 Noisy solutions for the five-measurement case (Case B) using different noisy data sets: (a) Noise-free + ($\alpha = 0.10$); (b) Noise-free + ($\alpha = 0.20$); (c) Case I + ($\alpha = 0.05$); (d) Case I + ($\alpha = 0.10$); (e) Case I + ($\alpha = 0.20$); (f) Case I + ($\alpha = 0.40$).

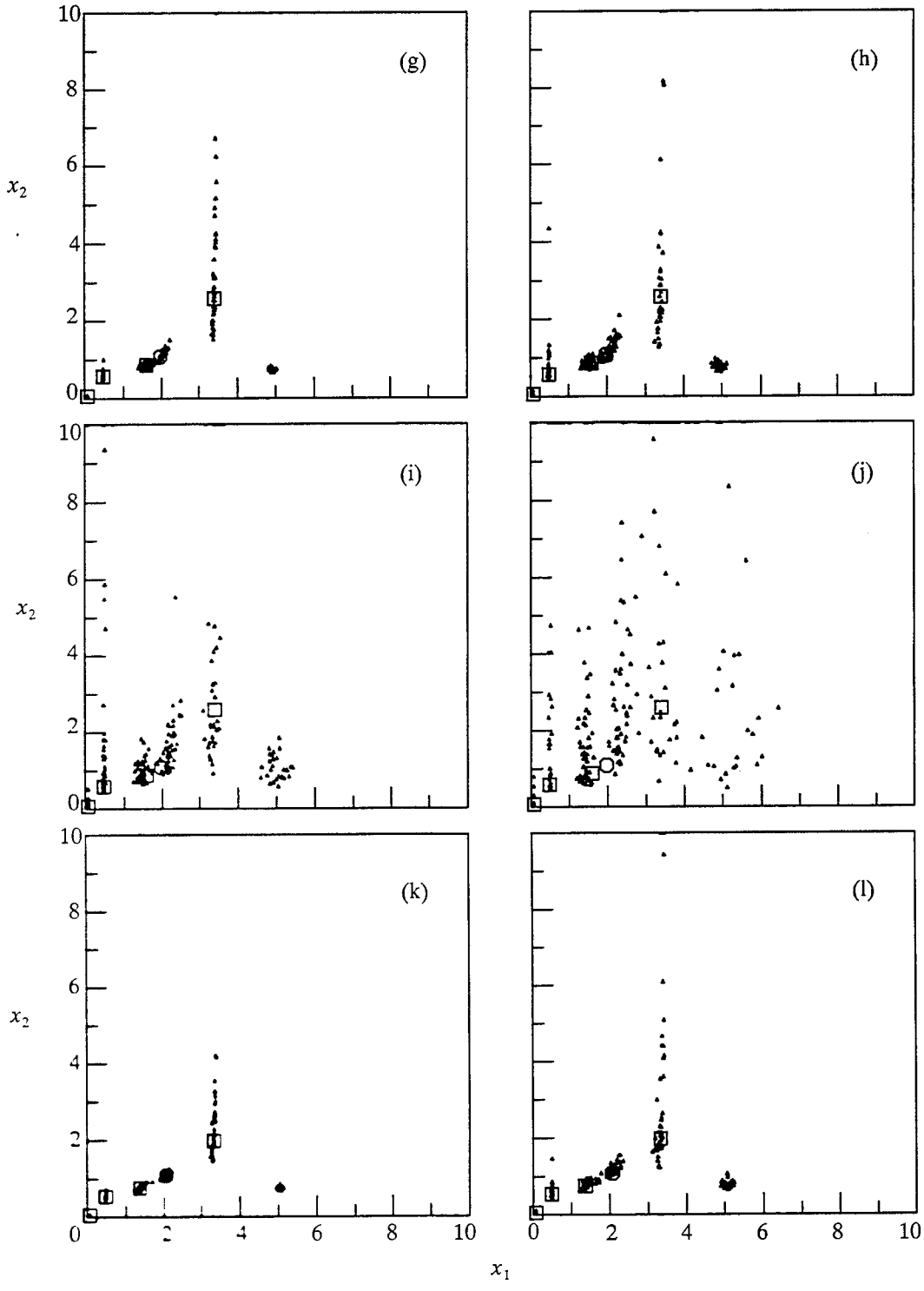

Figure A.4 (cont.) Noisy solutions for the five-measurement case (Case B) using different noisy data sets: (g) Case II + ($\alpha = 0.05$); (h) Case II + ($\alpha = 0.10$); (i) Case II + ($\alpha = 0.20$); (j) Case II + ($\alpha = 0.40$); (k) Case III + ($\alpha = 0.05$); (l) Case III + ($\alpha = 0.10$).

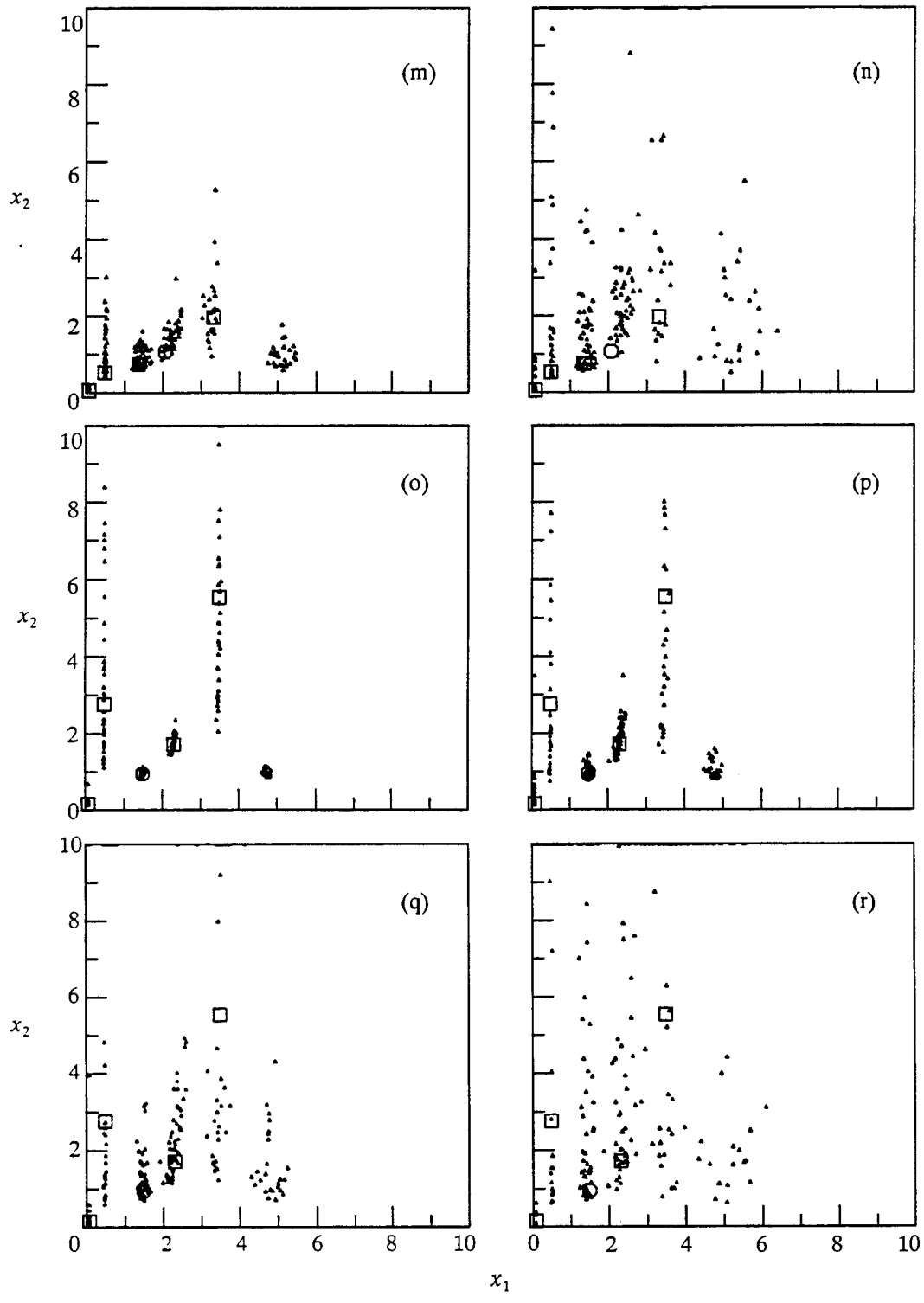

Figure A.4 (cont.) Noisy solutions for the five-measurement case (Case B) using different noisy data sets: (m) Case III + ($\alpha = 0.20$); (n) Case III + ($\alpha = 0.40$); (o) Case IV + ($\alpha = 0.05$); (p) Case IV + ($\alpha = 0.10$); (q) Case IV + ($\alpha = 0.20$); (r) Case IV + ($\alpha = 0.40$).

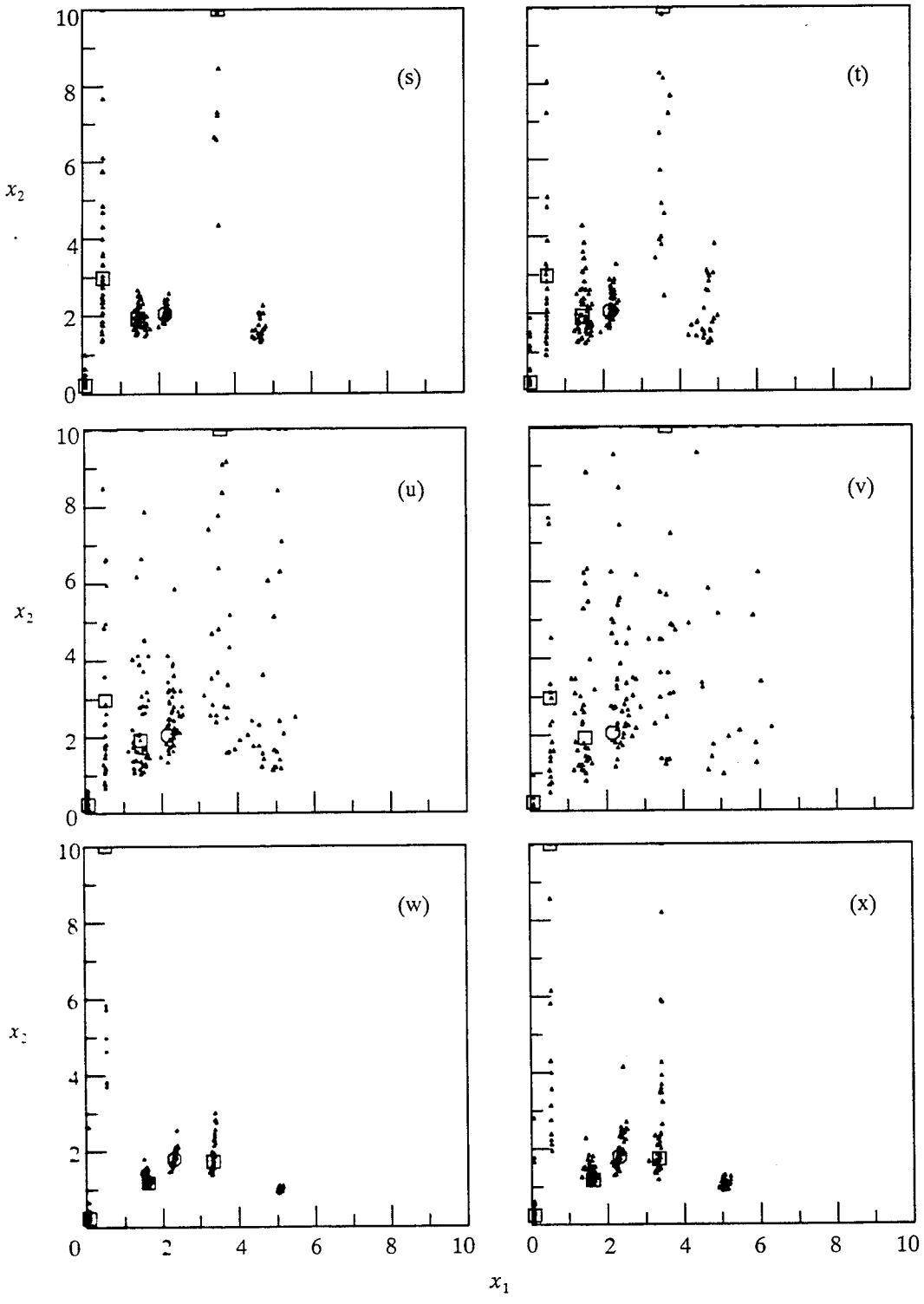

Figure A.4 (cont.) Noisy solutions for the five-measurement case (Case B) using different noisy data sets: (s) Case V + ($\alpha = 0.05$); (t) Case V + ($\alpha = 0.10$); (u) Case V + ($\alpha = 0.20$); (v) Case V + ($\alpha = 0.40$); (w) Case VI + ($\alpha = 0.05$); (x) Case VI + ($\alpha = 0.10$).

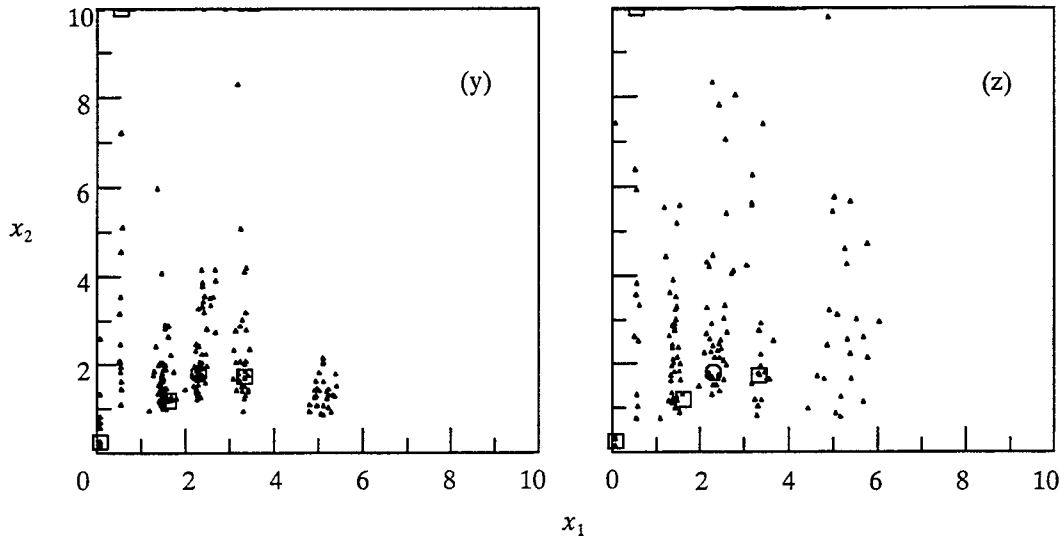

Figure A.4 (cont.) Noisy solutions for the five-measurement case (Case B) using different noisy data sets: (y) Case VI + ($\alpha = 0.20$); (z) Case VI + ($\alpha = 0.40$).

$\varepsilon = 10\%$ and $\varepsilon = 20\%$, respectively. Further, let each of the six simulated noisy data sets represent real data sets obtained from a modal testing of the structure. It is concluded that by applying the data perturbation scheme on a single noisy data set, one can actually simulate the sensitivity of the noise-free parameter estimation solutions to the measurement noise. The amplitude of the random perturbation should be selected as the same as the level of noise in the measured data. In addition, the data perturbation scheme shows better results when the parameter estimation problem has multiple solutions.

A.5 Summary

We have illustrated through a simple example that the data perturbation scheme can be used as a simulation tool for replicating the sensitivity of the noise-free parameter estimation solutions to the measurement noise. In the simulation environment, noisy measurements are simulated by adding random proportional errors with known amplitudes to the noise-free analytical response of a finite-element model of the structure. This concept was used as a basis for developing the error sensitivity analysis of solutions to the parameter estimation problem in Chapter 2. The error

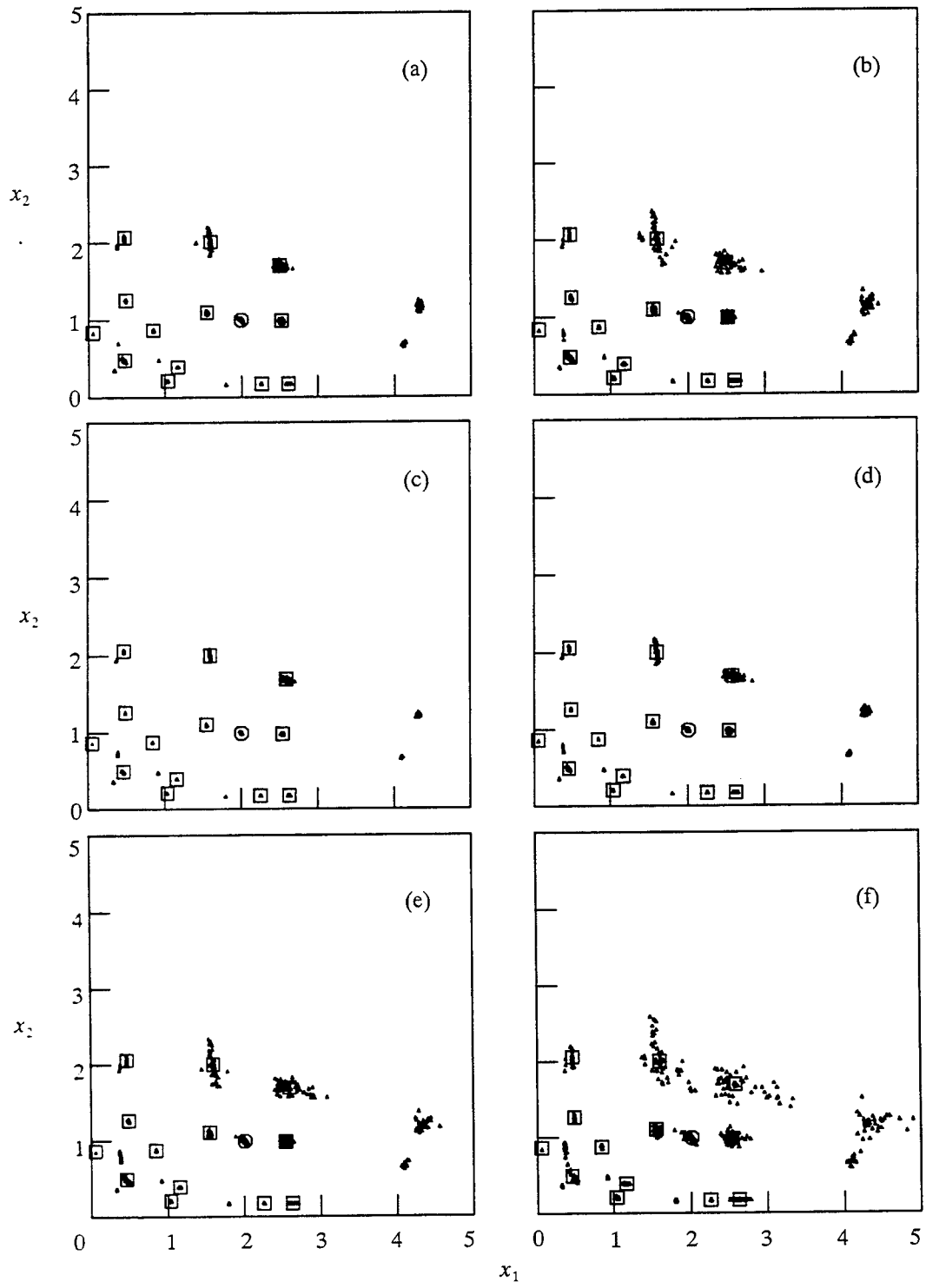

Figure A.5 Noisy solutions for the three-measurement case (Case C) using different noisy data sets: (a) Noise-free + ($\alpha = 0.10$); (b) Noise-free + ($\alpha = 0.20$); (c) Case I + ($\alpha = 0.05$); (d) Case I + ($\alpha = 0.10$); (e) Case I + ($\alpha = 0.20$); (f) Case I + ($\alpha = 0.40$).

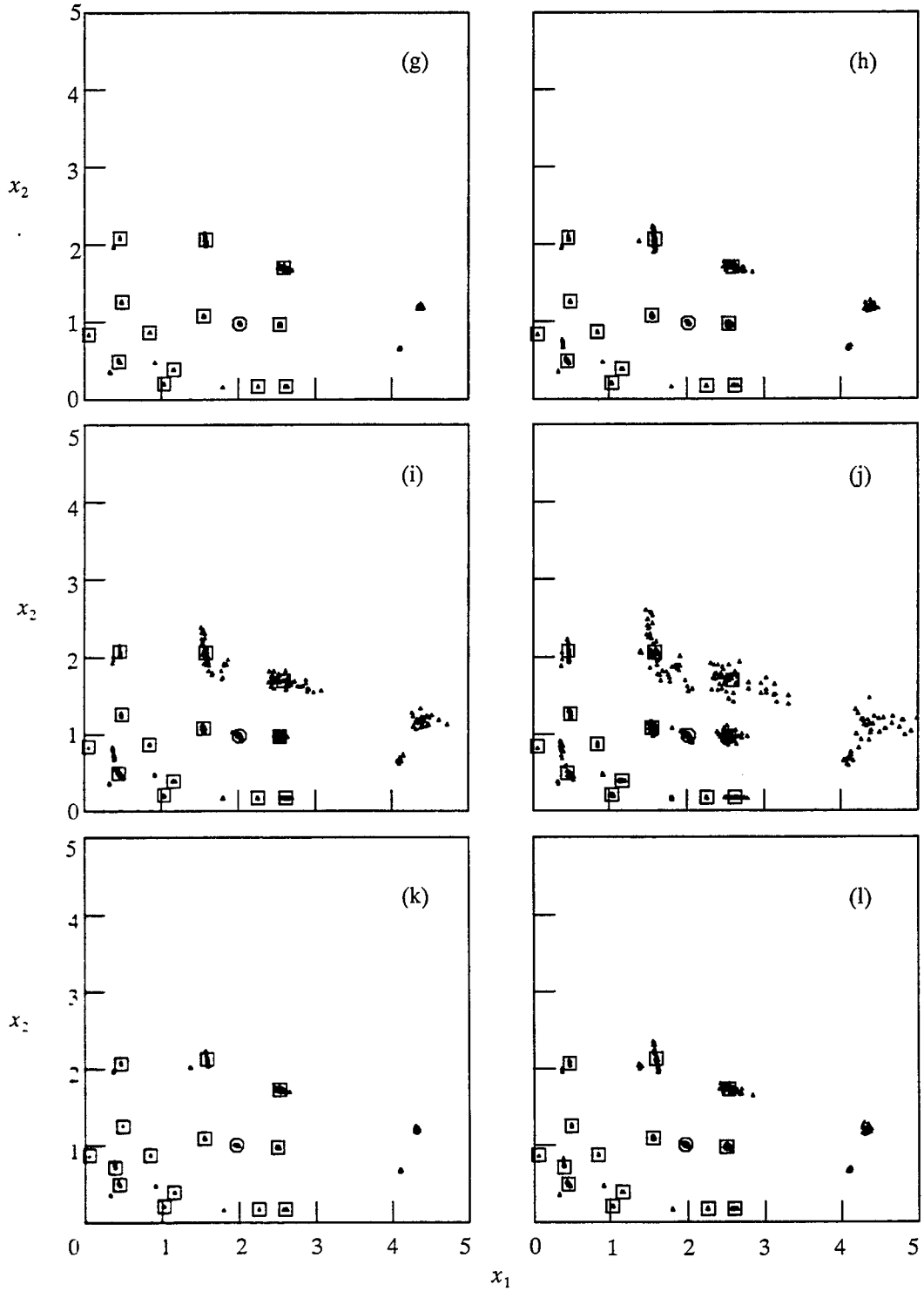

Figure A.5 (cont.) Noisy solutions for the three-measurement case (Case C) using different noisy data sets: (g) Case II + ($\alpha = 0.05$); (h) Case II + ($\alpha = 0.10$); (i) Case II + ($\alpha = 0.20$); (j) Case II + ($\alpha = 0.40$); (k) Case III + ($\alpha = 0.05$); (l) Case III + ($\alpha = 0.10$).

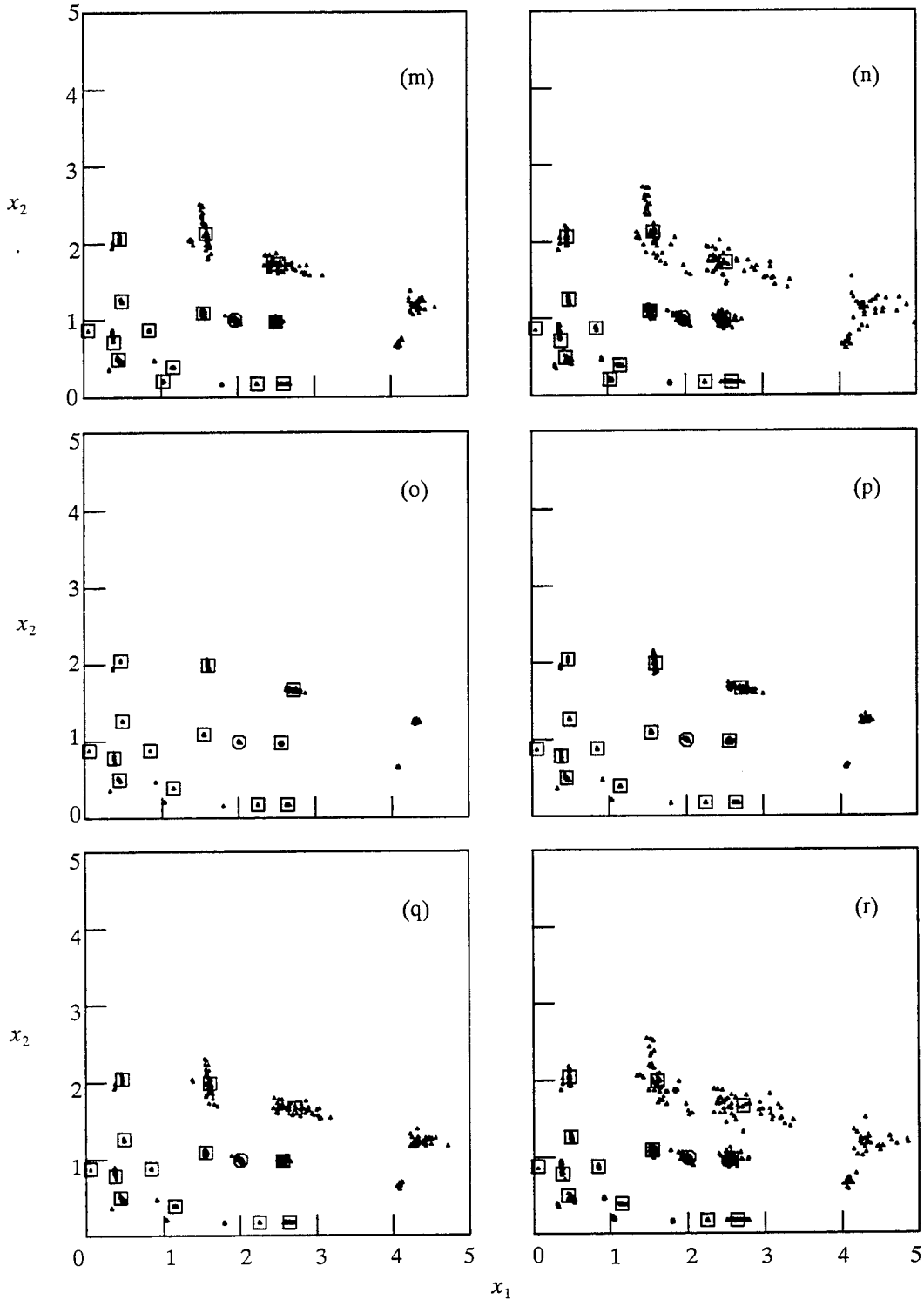

Figure A.5 (cont.) Noisy solutions for the three-measurement case (Case C) using different noisy data sets: (m) Case III + ($\alpha = 0.20$); (n) Case III + ($\alpha = 0.40$); (o) Case IV + ($\alpha = 0.05$); (p) Case IV + ($\alpha = 0.10$); (q) Case IV + ($\alpha = 0.20$); (r) Case IV + ($\alpha = 0.40$).

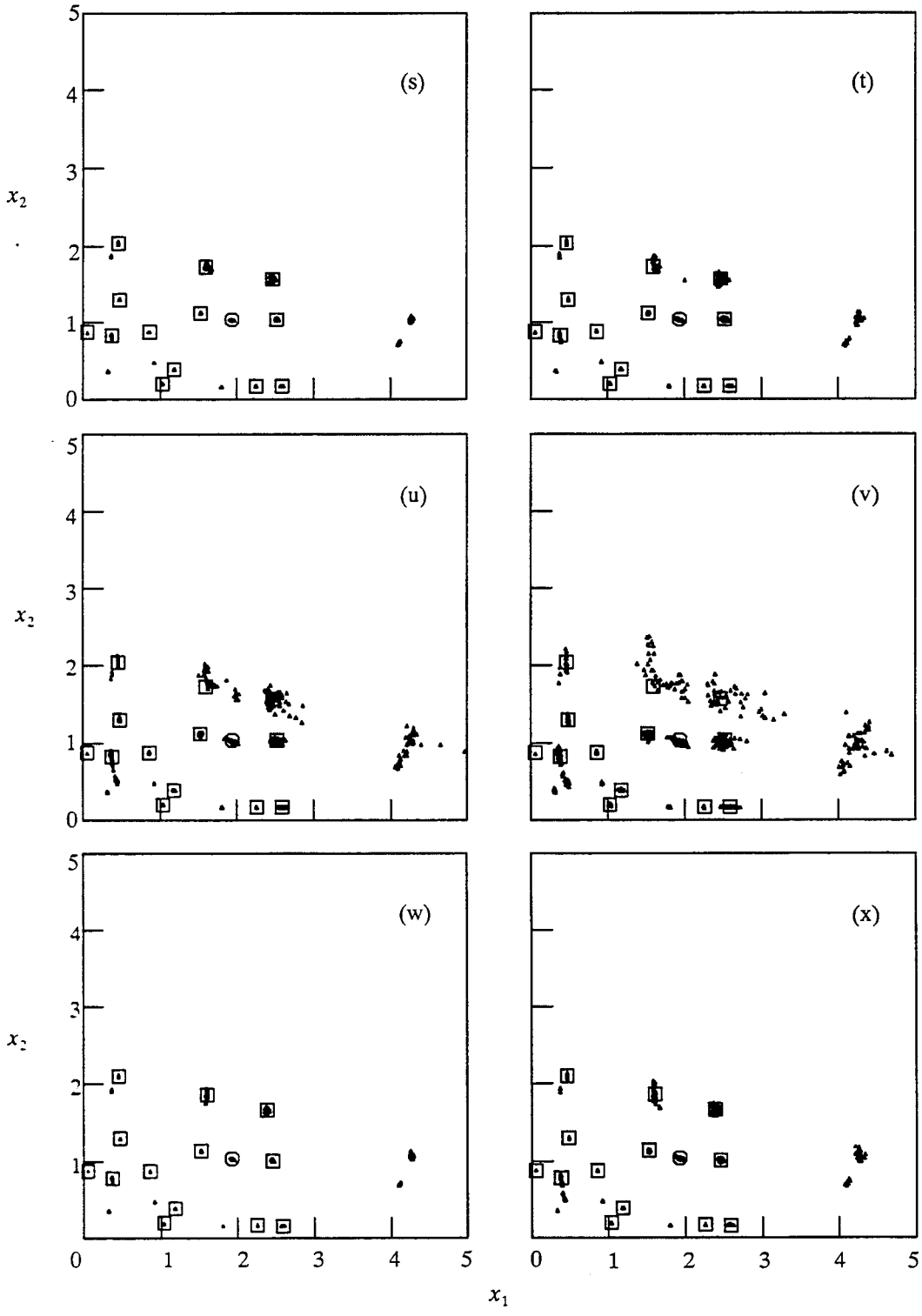

Figure A.5 (cont.) Noisy solutions for the three-measurement case (Case C) using different noisy data sets: (s) Case V + ($\alpha = 0.05$); (t) Case V + ($\alpha = 0.10$); (u) Case V + ($\alpha = 0.20$); (v) Case V + ($\alpha = 0.40$); (w) Case VI + ($\alpha = 0.05$); (x) Case VI + ($\alpha = 0.10$).

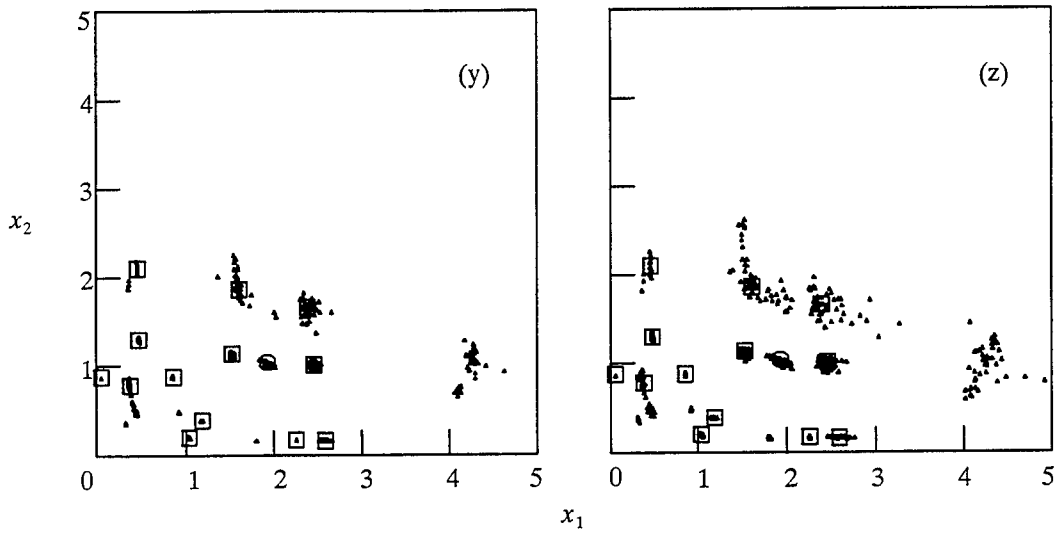

Figure A.5 (cont.) Noisy solutions for the three-measurement case (Case C) using different noisy data sets: (y) Case VI + ($\alpha = 0.20$); (z) Case VI + ($\alpha = 0.40$).

sensitivity analysis was subsequently incorporated into the global damage detection algorithm developed in Chapter 3.

REFERENCES

Adams, R. D., Cawley, P., Pye, C. J., and Stone, B. J. (1978). "A vibration technique for non-destructively assessing the integrity of structures." *J. Mech. Engrg. Science*, Vol. 20, 93–100.

Agbabian, M. S., Masri, S. F., Miller, R. K., and Caughey, T. K. (1991). "System identification approach to detection of structural changes." *J. Engrg. Mech.*, ASCE, 117(2), 370–390.

Araki, Y., and Hjelmstad, K. D. (2000). "Optimum sensitivity based statistical parameter estimation from modal response." *Submitted to AIAA J.*, February.

Banan, M.-R., and Hjelmstad, K. D. (1993). "Identification of structural systems from measured response." *Civ. Engrg. Studies*, SRS579, UILU-ENG-93-2002, University of Illinois at Urbana-Champaign, Ill.

Bathe, K.-J. (1996). *Finite Element Procedures*. Prentice-Hall. New Jersey.

Begg, R. D., Mackenzie, A. C., Dodds, C. J., and Loland, O. (1976). "Structural integrity monitoring using digital processing of vibration signals." *Proc. 8th Annual Offshore Technology Conference*, Houston, TX, 305–311.

Bray, D. E., and Stanley, R. K. (1989). *Nondestructive Evaluation: A Tool for Design, Manufacturing, and Service*. McGraw-Hill. New York, N. Y.

Cawley, P., and Adams R. D. (1979). "The locations of defects in structures from measurements of natural frequencies." *J. Strain Analysis*, 14(2), 49–57.

Chance, J., Tomlinson, G. R., and Worden, K. (1994). "A simplified approach to the numerical and experimental modeling of the dynamics of a cracked beam." *Proc. of the 12th International Modal Analysis Conference*, 778–785.

Chen, J., and Garba, J. A. (1988). "On-orbit damage assessment for large space structures." *AIAA J.*, 26(9), 1119–1126.

Cobb, R. G., and Liebst, B. S. (1997). "Sensor placement and structural damage identification from minimal sensor information." *AIAA J.*, 35(2), 369–374.

Doebling, S. W., Farrar, C. R., Prime, M. B., and Shevitz, D. W. (1996). "Damage identification and health monitoring of structural and mechanical systems from changes in their vibration characteristics: a literature review." *Los Alamos National Laboratory Report*, LA-13070-MS, Los Alamos National Laboratory, N. M.

Doebling, S. W. (1996). "Damage detection and model refinement using elemental stiffness perturbations with constrained connectivity." *Proc. of AIAA/ASME/AHS Adaptive Structures Forum*, 360–370.

Dong, C., Zhang, P. Q., Feng, W. Q., and Huang, T. C. (1994). "The sensitivity study of the modal parameters of a cracked beam." *Proc. of the 12th International Modal Analysis Conference*, 98–104.

Ewins, D. J. (1984). *Modal Testing: Theory and Practice*. John Wiley. New York, N. Y.

Ge, L., and Soong, T. T. (1998). "Damage identification through regularization method. I: Theory." *J. Engrg. Mech.*, ASCE, 124(1), 103–108.

Haftka, R. T., and Adelman, H. M. (1985). "Selection of actuator locations for static shape control of large space structures by heuristic integer programming." *Computers and Structures*, Vol. 20, 575–582.

Hajela, P., and Soeiro, F. J. (1990a). "Structural damage detection based on static and modal analysis." *AIAA J.*, 28(6), 1110–1115.

Hajela, P., and Soeiro, F. J. (1990b). "Recent developments in damage detection based on system identification methods." *Struct. Optimization*, Vol. 2, 1–10.

Hjelmstad, K. D., Wood, S. L., and Clark, S. J. (1992). "Mutual residual energy method for parameter estimation in linear structures." *J. Struct. Engrg.*, ASCE, 118(1), 223–242.

Hjelmstad, K. D., Banan, M. R., and Banan, M. R. (1995). "On building finite element models of structures from modal response." *Earthquake Engrg. Struct. Dynamics*, 24(1), 53–67.

Hjelmstad, K. D. (1996). "On the uniqueness of modal parameter estimation." *J. Sound Vibration*, 192(2), 581–598.

Hjelmstad, K. D., and Shin, S. (1996). "Crack identification in a cantilever beam from modal response." *J. Sound Vibration*, 198(5), 527–545.

Hjelmstad, K. D., and Shin, S. (1997). "Damage detection and assessment of structures from static response." *J. Engrg. Mech.*, ASCE, 123(6), 568–576.

Kammer, D. C. (1991). "Sensor placement for on-orbit modal identification and correlation of large space structures." *J. Guidance, Control, and Dynamics*, Vol. 14, 251–259.

Kim, H. M., and Bartkowicz, T. J. (1993). "Damage detection and health monitoring of large space structures." *The 34th AIAA/ASME/ASCE/AHS/ASC Structures, Structural Dynamics, and Material Conference*, 3527–3533.

Kosmatka, J. B., and Ricles, J. M. (1999). "Damage detection in structures by modal vibration characterization." *J. Struct. Engrg.*, ASCE, 125(12), 1384–1392.

Krawczuk, M., and Ostachowicz, W. M. (1992). "Parametric vibrations of a beam with crack." *Archive of Applied Mechanics*, Vol. 62, 463–473.

Kudva, J., Munir, N., and Tan, P. (1991). "Damage detection in smart structures using neural networks and finite element analysis." *Proc. of ADPA/AIAA/ASME/SPIE Conference on Active Materials and Adaptive Structures*, 559–562.

Law, S. S., Shi, Z. Y., and Zhang, L. M. (1998). "Structural damage detection from incomplete and noisy modal test data." *J. Engrg. Mech.*, ASCE, 124(11), 1280–1288.

Li, C., and Smith, S. W. (1995). "Hybrid approach for damage detection in flexible structures." *J. Guidance, Control, and Dynamics*, 18(3), 419–425.

Lifshitz, J. M., and Rotem, A. (1969). "Determination of reinforcement unbonding of composites by a vibration technique." *J. Composite Materials*, Vol. 3, 412–423.

Lim, T. W. (1990). "Submatrix approach to stiffness matrix correction using modal test data." *AIAA J.*, 28(6), 1123–1130.

Lin, R. M., and Ewins, D. J. (1990). "On the location of structural nonlinearity from modal testing–a feasibility study." *Proc. of the 8th International Modal Analysis Conference*, 358–364.

Liu, W. K., Belytschko, T., and Mani, A. (1986). "Probabilistic finite element for nonlinear structural dynamics." *Computer Methods in Applied Mechanics and Engineering*, Vol. 56, 61–81.

Manning, R. (1994). "Damage detection in adaptive structures using neural networks." *Proc. of 35th AIAA/ASME/ASCE/AHS/ASC Structures, Structural Dynamics, and Materials Conference*, 160–172.

Manson, G., Worden, K., and Tomlinson, G. R. (1993). "Pseudo-fault induction in engineering structures." *ASME Adaptive Structures and Materials Systems*, AD 35, 449–455.

Natke, H. G. (1989). "Identification approaches in damage detection and diagnosis." *DIAGNOSTIC'89*, Politechnike Pozuanska, 99–110.

Natke, H. G., and Cempel, C. (1991). "Fault detection and localization in structures: a discussion." *Math. Sys. and Signal Processing*, 5(5), 345–356.

Pandey, A. K., Biswas, M., and Samman, M. M. (1991). "Damage detection from changes in curvature mode shapes." *J. Sound Vibration*, 145(2), 321–332.

Papadimitriou, C., Beck, J. L., and Katafygiotis, L. S. (1997). "Asymptotic expansions for reliability and moments of uncertain systems." *J. Engrg. Mech.*, ASCE, 123(12), 1219–1229.

Papadopoulas, L., and Garcia, E. (1998). "Structural damage identification: a probabilistic approach." *AIAA J.*, 36(11), 2137–2145.

Sanayei, M., Onipede, O., and Babu, S. R. (1992). "Selection of noisy measurement locations for error reduction in static parameter identification." *AIAA J.*, 30(9), 2299–2309.

Sanayei, M., and Saletnik, M. J. (1996). "Parameter estimation of structures from static strain measurements. II: Error sensitivity analysis." *J. Struct. Engrg.*, ASCE, 122(5), 563–572.

Schwarz, B. J., McHargue, P. L., and Richardson, M. H. (1996). "Using SDM to train neural networks for solving modal sensitivity problems." *Proc. of the 14th International Modal Analysis Conference*, 1285–1291.

Shi, Z. Y., Law, S. S., and Zhang, L. M. (2000). "Optimum sensor placement for structural damage detection." *J. Engrg. Mech.*, ASCE, 126(11), 1173–1179.

Shin, S., and Hjelmstad, K. D. (1994). "Damage detection and assessment of structural systems from measured response." *Civ. Engrg. Studies*, SRS593, UILU-ENG-94-2013, University of Illinois at Urbana-Champaign, Ill.

Skelton, R. E., and Delorenzo, M. L. (1983). "Selection of noisy actuators and sensors in linear stochastic systems." *J. Large Scale Systems, Theory and Applications*, Vol. 4, 109–136.

Stubbs, N., Broome, T. H., and Osegueda, R. (1990). "Nondestructive construction error detection in large space structures." *AIAA J.*, 28(1), 146–152.

Stubbs, N., and Osegueda, R. (1990a). "Global non-destructive damage evaluation in solids." *Modal Analysis: The International Journal of Analytical and Experimental Modal Analysis*, 5(2), 67–79.

Stubbs, N., and Osegueda, R. (1990b). "Global damage detection in solids-experimental verification." *Modal Analysis: The International Journal of Analytical and Experimental Modal Analysis*, 5(2), 81–97.

Stubbs, N., Kim, J.-T., and Topole, K. (1992). "An efficient and robust algorithm for damage localization in offshore platforms." *Proc. ASCE 10th Structures Congress*, 543–546.

Vandiver, J. K. (1975). "Detection of structural failure on fixed platforms by measurement of dynamic response." *J. Petroleum Technology*, March, 305–310.

West, W. M. (1984). "Illustration of the use of modal assurance criterion to detect structural changes in an orbiter test specimen." *Proc. Air Force Conference on Aircraft Structural Integrity*, 1–6.

Wojnarowski, M. E., Stiansen, S. G., and Reddy, N. E. (1977). "Structural integrity evaluation of a fixed platform using vibration criteria." *Proc. 9th Annual Offshore Tech. Conf.*, 247–256.

Wu, X., Ghaboussi, J., and Garrett, J. H. (1992). "Use of neural networks in detection of structural damage." *Computers and Structures*, 42(4), 649–659.

Yao, G. C., Chang, K. C., and Lee, G. C. (1992). "Damage diagnosis of steel frames using vibrational signature analysis." *J. Engrg. Mech.*, ASCE, 118(9), 1949–1961.

Yeo, I., Shin, S., Lee, H. S., and Chang, S.-P. (2000). "Statistical damage assessment of framed structures from static responses." *J. Engrg. Mech.*, ASCE, 126(4), 414–421.

Yuen, M. M. F. (1985). "A numerical study of the eigenparameters of a damaged cantilever." *J. Sound Vibration*, Vol. 103, 301–310.

Zimmerman, D. C., and Kaouk, M. (1992). "Eigenstructure assignment approach for structural damage detection." *AIAA J.*, 30(7), 1848–1855.